AN INVESTIGATION OF INELASTIC SEISMIC DEMAND

by

Tarık Tufan

B.S., Civil Engineering, Boğaziçi University, 2005

Submitted to the Institute for Graduate Studies in

Science and Engineering in partial fulfillment of

The requirements for the degree of

Master of Science

Graduate Programs in Civil Engineering

Boğaziçi University

2008

AN INVESTIGATION OF INELASTIC SEISMIC DEMAND

APPROVED BY:

Assistant Prof. Dr. Hilmi LUŞ (Thesis Supervisor)	……
Assistant Prof. Dr. Kutay ORAKÇAL	……
Prof. Dr. Uğur ERSOY	……

DATE OF APPROVAL: 18.09.2008

ACKNOWLEDGEMENTS

First and foremost, I would like to give my thanks to my thesis advisor, Assistant Prof. Dr. Hilmi LUŞ, for his support, guidance and also for giving me valuable insight and encouragement throughout my study. Furthermore, I would like to thank my thesis examining committee Prof. Dr. Uğur ERSOY and Assistant Prof. Dr. Kutay ORAKÇAL for their valuable comments and recommendations.

The completion of this study is a result of the dedicated courage of my friends Edison, Serkan, İbrahim, Erdal. I am also grateful to all the friends who have provided a very pleasant diversion from my academic activities.

Finally, I would like to express my deep thanks to my mother, my brothers Faruk and Fatih and my sister Feyza for their love, support and encouragement that made everything possible. And I want to dedicate this dissertation to them.

ABSTRACT

AN INVESTIGATION OF INELASTIC SEISMIC DEMAND

In Turkish Earthquake Code (TEC), ratio between inelastic and elastic systems with same initial stiffness and damping is defined as spectral displacement ratios (also known as inelastic displacement ratios). The main aim of this study is to detect the correctness of the formulation about spectral displacement ratio given in TEC Annex-7c. Inelastic displacement ratios are affected by earthquake magnitude, soil conditions, critical damping ratio, yielding strength reduction factors, the material used in construction and resistance strain relation of the hysteresis. To analyze these parameters, total 555 records of Earthquakes occurred at Türkiye and Taiwan is selected and 21 groups and 6 stacks are formed. In the analysis of parameters, 3 to 6 values are investigated while all other parameters kept constant. It is concluded that distance to source has negligible effect due to its fluctuation between maximum and the minimum for each element. Earthquake magnitude, yield strength reduction factors have effects on inelastic displacement ratios in all constant regions. Soil conditions, damping coefficient, post-yield stiffness have moderate effect on inelastic displacement ratios in constant acceleration region. As critical damping increases, increase in inelastic displacement ratios decreases. Difference between trends of 5 and 20% critical damping in constant acceleration region is between 10-20%, and in other regions lower than 5%. Furthermore, detailed investigation on soil shear wave velocities in same NEHRP classification is done. Effects of different soil shear wave velocities in same NEHRP classification show great difference. For every period of vibration, maximum and minimum of mean inelastic displacement ratios of groups is recorded to construct inelastic displacement ratio boundaries which is dependent on yield strength reduction factors. According to this boundary, TEC (2007) formulation is checked. For low yield strength reduction factors like 2 good matches with boundaries, for higher yield strength reduction factor such as 4, 7 formulation underestimates inelastic displacement ratios and reasons for this are discussed. A formulation related with inelastic displacement ratio is presented at the end of paper.

ÖZET

ELASTİK ÖTESİ SİSMİK TALEP ÜZERİNE BİR İNCELEME

Türk Deprem Yönetmeliğinde (TDY), aynı ilk rijitlik ve sönüm oranına sahip tek serbest dereceli elastik ve elastik ötesi yer değiştirmelerin oranlarını ifade eden spektral yer değiştirme oranı (elastik ötesi yer değiştirme oranı olarak da bilinir) üzerine yapılmış bir çalışmadır. Çalışmanın amacı, TDY Ek-7c maddesinde verilen bu oranla ilgili formülün irdelenmesidir. Elastik ötesi yerdeğiştirme oranı; deprem şiddetine, binanın inşa edildiği toprak türüne, sistemin kritik sönüm oranına, taşıyıcı sistem davranış katsayısına, yapıda kullanılan malzemenin özelliğine ve kuvvet yer değiştirme ilişkisine bağlıdır. Bu parametreleri inceleyebilmek için Turkiyede ve Tayvan depremlerine ait toplam 555 kayıt seçilmiş ve bu kayıtları içeren 21 grup ve 6 küme oluşturulmuştur. İncelenen parametre dışındaki parametre değerleri sabit tutulmuş incelenen parametre için farklı değerler göz önüne alınarak spektral yer değiştirme üzerine olan etki araştırılmıştır. Yapılan çalışmada depreme olan uzaklık etkisinin her periyot değeri için çok farklılık gösterdiği, belli periyotlarda azami belli periyotlarda asgari değer aldığı, bu sebeple etkisinin (minimum sınıra göre) sabit bir değer alınması gerektiği düşünülmüştür. Deprem şiddetini, toprak türü ve bina davranış katsayısı etkisinin spektral yer değiştirme oranı üzerinde etkili olduğu bulunmuştur. Sönüm oranında %5 sönümden sonra spektral yer değiştirme oranını çok etkilemediği anlaşılmıştır. Ayrıca daha önce yapılan çalışmalardan farklı olarak NEHRP toprak tipi C-D sınıfları arasında yapılan analizde toprak tipi içinde spektral yer değiştirme oranının çok farklılık gösterdiği görülmüştür. Her periyot için grup bazındaki ortalama elastik ötesi yer değiştirme oranlarının azami ve asgari değerleri spektral yer değiştirme oranı sınırları olarak tanımlanmıştır ve bu sınır taşıyıcı sistem davranış katsayısına göre değişmektedir. Bu sınırlara göre yapılan kontrolde Türk Deprem Yönetmeliğinde yer alan formülün düşük bina davranış katsayısı (=2) için yer değiştirme oranının sınırları içerisinde kaldığı tespit edilmiş fakat daha yüksek bina davranış katsayısı için asgari spektral yer değiştirme oran sınırından çok daha az hesap ettiği görülmüştür ve bunun nedenleri tartışılmıştır. Son olarak yukarıda etkili olduğu belirtilen parametreler kullanılarak bir formül üretilmiştir.

TABLE OF CONTENTS

ACKNOWLEDGEMENTS iii

ABSTRACT iv

ÖZET v

TABLE OF CONTENTS vi

LIST OF FIGURES viii

LIST OF TABLES xiv

LIST OF SYMBOLS / ABBREVIATIONS xvi

1. INTRODUCTION 1

1.1. Problem Definition 1

1.2. Inelastic Displacement Ratios 3

1.2.1. Definition of Inelastic Displacement Ratios 3

1.2.2. Parameters Affecting Inelastic Displacement Ratio 4

1.3. Base Shear 4

1.4. Design Spectra 6

1.4.1. Elastic Design Spectra 7

1.4.1.1. Newmark-Hall Elastic Design Spectrum 7

1.4.1.2. FEMA 356 Elastic Design Spectrum 9

1.4.2. Newmark-Hall Inelastic Design Spectrum 12

1.5. Performance Based Design 13

1.5.1. Definition 13

1.5.2. Performance/Damage Limits of Cross-Sections 14

1.5.3. Cross-sections Damage Regions 15

1.6. Literature Review 16

1.7. Scope, Objectives and Goals 21

2. METHODOLOGY 22

2.1. Newmark-Beta Methods 22
2.2. Structural Models 24
2.3. Ground Motion Selection 26
2.4. Conversions for Soil Types 30
2.5. Period Range Selection 31
3. STATISTICAL RESULTS 33
3.1. Effect of Site Conditions 34
3.2. Effect of Magnitude 40
3.3. Effect of Distance-to-Source on Inelastic Displacement Ratios 44
3.4. Effect Post Yield Stiffness 50
3.5. Effects of Critical Damping Ratio 52
4. FORMULATIONS FOR INELASTIC DISPLACEMENT RATIOS 55
4.1. Formulations from Previous Studies 55
4.2. Turkish Earthquake Code Formulation 60
4.3. Formulation Proposed 64
5. CONCLUSIONS AND RECOMMENDATIONS 70
5.1. Conclusions Related with Inelastic Displacement Ratios 70
5.2. Other Conclusions 72
APPENDIX A: RELATED TABLES 73
REFERENCES 92

LIST OF FIGURES

Figure 1.1. Elastic horizontal design spectrum according to Newmark and Hall. (Bozorgnia and Bertero, 2004) 8

Figure 1.2. FEMA-356 Elastic Design Spectrum 10

Figure 1.3. Inelastic Design Spectrum According to Newmark-Hall (1982) 13

Figure 1.4. Cross-section Damage / Performance Limits and Cross-section Damage Regions on Capacity Curve (Akgül, 2007) 15

Figure 2.1. Bilinear Model: Resistance-deformation relation. 24

Figure 2.2. GMDS1 records, epidistance versus magnitude plot 28

Figure 2.3. Main S3 and Control S3 stacks, Average Soil Wave Shear Velocity at 30 m depth versus Distance to source 29

Figure 2.4. Main S1-2 and Control S1-2 stacks, Average Soil Wave Shear Velocity at 30 m depth versus Distance to source 29

Figure 2.5. Variations in local soil classes defined in Turkish Earthquake Code 2007 in Gölcük (Laue et al, 2003). 30

Figure 2.6. Variations in NEHRP soil classes in Gölcük (Laue et al, 2003). 31

Figure 3.1. Effect of soil condition(NEHRP firm site classes B,C,D) on mean inelastic displacement ratios for Magnitude 6.75 Earthquakes, Average Distance to source 39 km and R_y =2 34

Figure 3.2. Effect of soil condition(NEHRP firm site classes B,C,D) on mean inelastic displacement ratios for Magnitude 6.75 Earthquakes, Average Distance to source 39 km and R_y =7 35

Figure 3.3. Effect of soil condition (NEHRP firm site classes C,D) on mean inelastic displacement ratios for Magnitude 7.6 Earthquakes, Average Distance to source 43 km and R_y=2..... 35

Figure 3.4. Effect of soil condition (NEHRP firm site classes C,D) on mean inelastic displacement ratios for Magnitude 7.6 Earthquakes, Average Distance to source 43 km and R_y=7..... 36

Figure 3.5. Effect of soil condition (NEHRP site classes B,C,D) on ratio of mean inelastic displacement ratios to their average for Magnitude 6.75 Earthquakes, Average Distance to source 39 km and R_y=2,4..... 37

Figure 3.6. Effect of soil condition(NEHRP site classes B,C,D) on ratio of mean inelastic displacement ratios to their average for Magnitude 6.75 Earthquakes, Average Distance to source 39 km and R_y=7..... 38

Figure 3.7. Effect of soil conditions on ratio of mean inelastic displacement ratios to minimum of all for every sampled period for Magnitude 7.6 Earthquakes, Average Distance to source 43 km and R_y=2,7..... 39

Figure 3.8. Effect of soil conditions on the maximum ratio distributed over soil shear wave velocity range for constant acceleration region, different level of periods and R_y=4..... 40

Figure 3.9. Effect of earthquake magnitude on mean inelastic displacement ratios for distance to source 43 km, average $Vs30$ 500 m/sec and R_y=2,4,7 42

Figure 3.10. Effect of earthquake magnitude on mean inelastic displacement ratios for distance to source 102 km, Average $Vs30$ 500 m/sec and R_y=2,4,7 ... 42

Figure 3.11. Effect of earthquake magnitude on maximum ratio, maximum of mean inelastic displacement ratios over their minimum for distance to source (a) 43, (b) 102 km, Average Vs_{30} =500 m/sec and R_y =2,4,7..... 43

Figure 3.12. Effect of distance to source on mean inelastic displacement ratios for magnitude 6.2 earthquakes, average $Vs30$ =500 m/sec and R_y =2, 7..... 45

Figure 3.13. Effect of distance to source on mean inelastic displacement ratios for magnitude 7.6 earthquake, average Vs_{30} 500 m/sec and R_y =2, 7..... 46

Figure 3.14. Effect of distance to source on maximum ratio for Magnitude 6.2 Earthquakes, Average $Vs30$ 500 m/sec and R_y =2, 4, 7..... 47

Figure 3.15. Effect of distance to source on maximum ratio for Magnitude 7.6 Earthquakes, Average $Vs30$ 500 m/sec and R_y =2, 4, 7..... 49

Figure 3.16. Effect of stiffness on inelastic displacement ratio for R_y =4 (for 7079 records)..... 50

Figure 3.17. Maximum ratio for post-yield stiffness with ζ =5% and R_y =4..... 51

Figure 3.18. Ratio of mean inelastic displacement ratios for α =2, 5, 10 per cent over α =0 per cent for Ry =4 and ζ =5 per cent 51

Figure 3.19. Effect of critical damping on inelastic displacement ratio (GMDS1) for R_y =4 53

Figure 3.20. Maximum ratio for critical damping with α =3% and R_y =4..... 54

Figure 4.1. Krawinkler and Nassar's (1992) equation versus limiting mean inelastic displacement ratios derived from analysis for R_y =2..... 56

Figure 4.2. Krawinkler and Nassar's (1992) equation versus limiting mean inelastic displacement ratios derived from analysis for R_y=7 56

Figure 4.3. García and Miranda's (2003) equation versus limiting mean inelastic displacement ratios derived from analysis for R_y=2 57

Figure 4.4. García and Miranda's (2003) equation versus limiting mean inelastic displacement ratios derived from analysis for R_y=7 58

Figure 4.5. Chopra and Chintanapakdee (2004) equation versus limiting mean inelastic displacement ratios derived from analysis for R_y=2..... 59

Figure 4.6. Chopra and Chintanapakdee (2004) equation versus limiting mean inelastic displacement ratios derived from analysis for R_y=7..... 59

Figure 4.7. TEC (2007) equation versus limiting mean inelastic displacement ratios derived from analysis for R_y=2 60

Figure 4.8. TEC (2007) equation versus limiting mean inelastic displacement ratios derived from analysis for R_y=7 61

Figure 4.9. TEC (2007) equation versus mean of 7079 records for different post-yield stiffness values for R_y=2 61

Figure 4.10. TEC (2007) equation versus mean of 7079 records for different post-yield stiffness values for R_y=4 62

Figure 4.11. TEC (2007) equation versus mean of 7079 records for different post-yield stiffness values for R_y=8 62

Figure 4.12. TEC (2007) equation versus mean of inelastic displacement ratio of NEHRP-D (3685 records) and NEHRP-B(160 records) soil for different post-yield stiffness values for R_y =2 63

Figure 4.13. TEC (2007) equation versus mean of inelastic displacement ratio of NEHRP-D (3685 records) and NEHRP-B (160 records) soil for different post-yield stiffness values for R_y =8 63

Figure 4.14. Boundary Comparison, group mean maximum and minimum, 7079 records average for post-yield stiffness 0 and 10 per cent, NEHRP-B and NEHRP-D type soils with systems 0 and 10 per cent post-yield stiffness 64

Figure 4.15. Comparison between Inelastic displacement boundaries and formulation proposed (FP) for R_y =2 for 5.9 Earthquake Magnitude 65

Figure 4.16. Comparison between Inelastic displacement boundaries and formulation proposed (FP) for R_y =4 for 5.9 Earthquake Magnitude 66

Figure 4.17. Comparison between Inelastic displacement boundaries and formulation proposed (FP) for R_y =7 for 5.9 Earthquake Magnitude 66

Figure 4.18. Comparison between Magnitude 5.9 earthquake main stack with formulation proposed (T_B =0.4) 67

Figure 4.19. Comparison between magnitude 6.2 earthquake main stack with formulation proposed (T_B =0.4) 67

Figure 4.20. Comparison between magnitude 7.6 earthquake main stack with formulation proposed (T_B =0.4) 68

Figure 4.21. Comparison between magnitude 7.6 earthquake main stack with formulation proposed (R_y =2) 68

Figure 4.22. Comparison between magnitude 7.6 earthquake main stack with formulation proposed (R_y =7) 69

LIST OF TABLES

Table 1.1. Spectrum Characteristic Periods (T_A , T_B) 6

Table 1.2. Design spectrum modification factors 11

Table 2.1. Newmark Method Coefficients 24

Table 2.2. Groups Abbreviations and their corresponding properties 26

Table 2.3. Average Values for Magnitude, Epicenter and Soil Wave Velocity 27

Table 2.4. Stack names, groups inside stacks 28

Table 3.1. Point of intersections of all R_y levels 41

Table 4.1. Post-yield stiffness dependent coefficients to be used in Krawinkler and Nassar(1992) equation. 55

Table 4.2. Site Dependent coefficients to be used in García and Miranda (2003) equation. 57

Table 4.3. Coefficients used in Chopra and Chintanapakdee (2004) Equation. 58

Table A.1. Structural Behavior Factors (R_y) 73

Table A.2. List of ground motions in GMDS1 ensemble 74

Table A.3. List of ground motions in M1D1S5 ensemble (28 records) 75

Table A.4. List of ground motions in M1D2S5 ensemble (28 records) 76

Table A.5. List of ground motions in M1D3S5 ensemble (28 records) 77

Table A.6. List of ground motions in M1D4S5 ensemble (28 records) 78

Table A.7. List of ground motions in M1D5S5 ensemble (28 records) 79

Table A.8. List of ground motions in M1D6S5 ensemble (28 records) 80

Table A.9. List of ground motions in M2D1S5 ensemble (18 records) 81

Table A.10. List of ground motions in M2D2S5 ensemble (28 records) 82

Table A.11. List of ground motions in M2D3S5 ensemble (28 records) 83

Table A.12. List of ground motions in M2D4S5 ensemble (28 records) 84

Table A.13. List of ground motions in M2D5S5 ensemble (28 records) 85

Table A.14. List of ground motions in M3D2S5 ensemble (28 records) 86

Table A.15. List of ground motions in M3D5S5 ensemble (28 records) 87

Table A.16. List of ground motions in M2D2S1 ensemble (24 records) 88

Table A.17. List of ground motions in M2D2S2 ensemble (12 records) 89

Table A.18. List of ground motions in M2D2S3 ensemble (24 records) 89

Table A.19. List of ground motions in M2D2S4 ensemble (12 records) 90

Table A.20. List of ground motions in M4D2SD ensemble (22 records)..... 90

Table A.21. List of ground motions in M4D2SC ensemble (22 records)..... 91

Table A.22. List of ground motions in M4D2SB ensemble (12 records)..... 91

LIST OF SYMBOLS / ABBREVIATIONS

A	Dynamic amplification factors for *PGA*
a	Parameter in empirical formula for C_R , C_μ , or R_y
$A(T)$	spectral acceleration coefficient
A_0	effective ground acceleration
b	Parameter in empirical formula for C_R , C_μ , or R_y
B_1	damping coefficients used in FEMA-356 elastic design spectra
B_S	damping coefficients used in FEMA-356 elastic design spectra
C_R	Ratio of peak deformations of inelastic and corresponding elastic single degree of freedom systems for systems with known yield-strength reduction factor
C_μ	Ratio of peak deformations of inelastic and corresponding elastic single degree of freedom systems for systems with known ductility factor
C_t	constant related to the framing system of structure
c	Parameter in empirical formula for C_R , C_μ , or R_y
D	dynamic amplification factors for *PGD*
d	Parameter in empirical formula for C_R , C_μ
e	Strength ratio ($1/R_y$)
F_a	Site coefficient used in FEMA-356 design spectrum
F_v	Site coefficient used in FEMA-356 design spectrum
f_m	Peak resisting force of inelastic system
f_0	Peak resisting force of elastic system
f_s	Resisting force of system
f_y	Yield strength of inelastic system
H_n	height (in feet)
I	Building Importance Factor
k	Elastic (initial) stiffness of system
L_R	Deformation ratio C_R for zero-period system
L_μ	Deformation ratio C_μ for zero-period system
M	Earthquake magnitude
m	Mass of system
M_R	maximum ratio
PGA	Peak Ground Acceleration
PGD	Peak Ground Displacement
PGV	Peak Ground Velocity
$R_a(t)$	seismic load reduction factor
R_y	Yield-strength reduction factor
$S(T)$	spectrum coefficient

S_1	the response acceleration parameter
S_S	Response acceleration parameters
S_{X1}	Design response acceleration parameter at a one-second period,
S_{XS}	Design short-period spectral response acceleration parameter
T_a	Period defined in Newmark–Hall smooth design spectrum
T_b	Period defined in Newmark–Hall smooth design spectrum
T_c	Period separating acceleration- and velocity-sensitive regions
T_d	Period separating velocity- and displacement-sensitive regions
T_e	Period defined in Newmark–Hall smooth design spectrum
T_f	Period defined in Newmark–Hall smooth design spectrum
T_n	Elastic natural vibration period
T_s	Characteristic period in empirical formula by Miranda
T_0	Period separating extreme short period and short period ranges
T_S	Period separating constant acceleration and velocity regions
u^t	Total displacement of mass of system
$u(t)$	Deformation of single-degree-of-freedom system
$\ddot{u_g}(t)$	Earthquake ground acceleration
u_m	Peak deformations of inelastic single-degree of-freedom systems;
u_o	Peak deformations of corresponding elastic single-degree-of-freedom systems;
u_y	Yield deformation;
V	Dynamic amplification factors for *PGV*
V_t	total equivalent seismic load(base shear)
W	total building weight
α	Ratio of post yield and initial stiffness;
β	constant related to the framing system
ξ	Damping ratio;

1. INTRODUCTION

1.1. Problem Definition

After the 1999 Kocaeli earthquake, social and political awareness increased in two areas: To construct earthquake resistant buildings and to make existing buildings earthquake resistant. Works done by the government in Zeytinburnu to estimate seismic safety, the change in the name of the design code from "disaster areas" to "earthquake regions", various predictions about the awaiting big Marmara earthquake, the establishment of building audit firms, appending the design code to cover the seismic retrofitting of existing buildings, and social preferences in buying or renting houses from places with rock-type soils all imply the social and political consciousness about this subject.

Researches show that buildings designed according to the "Specification for Structures to be built in Disaster Areas" (1998) or Turkish Earthquake Code (2007) performs well in predetermined performance levels (Akgül, 2007). In this case, at least constructing buildings according to the code is sufficient. Expecting full compliance from the contractors to the code is not a very well enforced concept in Turkey. For this reason, building audit firms were introduced. Building audit firms control structures from the design phase to acquisition of the dwelling license given by local municipality.

The second concept is related to existing buildings. According to various studies and estimates of the awaiting Big Marmara Earthquake, thousands of people would die if no precautions are taken for earthquake mitigation. Two methods are possible for earthquake mitigation. One is to demolish the houses and reconstruct them according to the earthquake design codes under the guidance of building audit firms. Because many buildings have obtained their building construction certificates with the housing amnesty, reconstruction may either not be possible or it would be possible only with low number of stories, in which case contractors would not find the project feasible. The second alternative is to rehabilitate the structure.

One of the new concepts in the Turkish Earthquake Code 2007 (TEC), when compared with Specification for Structures to be built in Disaster Areas, is retrofitting and evaluation of existing buildings. Performance based engineering methods are used for this purpose.

Performance based engineering uses displacements rather than forces in the evaluation and rehabilitation of buildings, and performance levels are determined according to displacements. For the existing buildings subjected to the Maximum Credible Earthquake, which has two per cent probability of occurrence in 50 years, it is not reasonable to expect a structure not to be damaged structurally or non-structurally. On the contrary, thousands of buildings are expected to be heavily damaged (even to the point of collapse). Accepting some level of damage on structure without life loss or collapse prevention can be achieved by retrofitting existing structures. To accomplish these performance levels, compressive understanding of the nonlinear behavior of structures is required.

For elastic behavior a good accumulated knowledge exists. Researches want to benefit from such treasure in the understanding of inelastic behavior of structures. To make use of elastic behavior knowledge into inelastic behavior, two concepts are to be related: forces and displacements. Force due to earthquake motion can be calculated using base shear. Base shear is a function of elastic design spectrum which is basically spectral acceleration over maximum ground acceleration versus period plot. In the inelastic behavior stiffness is limited to a value due to resistance strain relationship of the material; this also lowers spectral acceleration acting on the system, so the design spectrum is lowered in inelastic behavior. As far as displacements are concerned, due to resistance strain relationship of material, it is expected that inelastic systems should displace larger than in elastic systems. To understand difference between displacements of inelastic and elastic systems; their ratio is investigated. This ratio is called inelastic displacement ratio.

Seismic loads acting on structures decrease with increasing yield strength reduction factors. Elastic design spectrum is used to understand elastic behavior of buildings and inelastic design spectra can be calculated from elastic design spectra. Inelastic

displacement ratio can be related using displacement modification methods. Such relations will be discussed in the following sections.

1.2. Inelastic Displacement Ratios

1.2.1. Definition of Inelastic Displacement Ratios

Inelastic displacement ratio is the ratio between the maximum inelastic displacement demands of non-linear SDOF systems and the maximum elastic displacement demands of linear SDOF systems. In FEMA standards a simplified expression is given for this ratio. Using this simplified expression one can convert elastic displacement demand to inelastic displacement demand of a system. Relating inelastic and elastic displacement demands with one expression is called modification factor method in the literature. To be able to use modification factor method, elastic and inelastic systems must have same initial stiffness and critical damping ratio.

Calculation methods used for inelastic displacement ratio are different for designing of new buildings and retrofitting for the existing buildings. Because parameters accepted as conservative, are different. In the design project, designing according to ductility gives more conservative results than designing according to quality and the quantities of the building, reverse is valid for existing buildings. Ductility is defined as the maximum displacement over yield displacement of the system. The maximum displacement of the inelastic system over target ductility ratio gives yield displacement of the system. Because change in yield displacement point and changes maximum inelastic displacement of system, It is an iterative process; and also there is no unique solution more than one yield displacement and maximum inelastic displacement may give same ductility. Minimum of all maximum inelastic displacements satisfying the target ductility is chosen. When maximum inelastic displacement demand is determined by ductility, the ratio between inelastic and elastic displacement is called constant ductility inelastic displacement ratio.

However in rehabilitation of existing structures, inelastic displacement ratio is determined from yield strength reduction factor. Spectral displacement of elastic systems is

divided by yield strength reduction factor. The resultant is yield displacement of inelastic system. For the yield displacement calculated, nonlinear dynamic analysis or push over analysis is done to calculate maximum inelastic displacement demand. The inelastic displacement ratio calculated using this method is called constant relative strength inelastic displacement ratios. In this thesis constant ductility inelastic displacement ratios are not considered.

In the Turkish Earthquake Code (2007), the constant relative strength inelastic displacement ratio is named as spectral displacement ratio and is denoted by the same nomenclature as NEHRP publications FEMA 273.

1.2.2. Parameters Affecting Inelastic Displacement Ratio

In order to formulate inelastic displacement ratio correctly, the parameters affecting inelastic displacement ratios have to be determined. Forces due to earthquakes and displacements are related. Thus, the parameters affecting base shear force are expected to change the displacements of the structure. Base shear force is a function of design spectrum ordinates and design spectrum is functions of earthquake magnitude, soil conditions and critical damping ratio. Furthermore, inelastic design spectrum used for inelastic behavior of structures is dependent on all parameters in elastic design spectrum and the yield strength reduction factor. It is also related with properties of materials used in the structure and force displacement relation of the members. All these parameters are expected to change inelastic and elastic displacements, and also inelastic displacement ratios.

1.3. Base Shear

In the evaluation of existing structures, the main interest is to determine the global and local deformations that a structure with known lateral strength may undergo when subjected to earthquakes (García and Miranda, 2003). Existing buildings may not meet current requirements for ductility. However, quantities and quality of construction with conserved margins (shape, size, dimension, strength, materials, and color) can be measured

or tested and thus they are known for existing buildings (Hom and Poland, 2006). Thus, using a yield strength reduction factor rather than ductility gives better estimates for existing structures in determination of global and local deformations. Yield strength reduction factor is defined as the lateral strength required to maintain the system elastic over the lateral yielding strength of the system.

Global and local deformations that a structure with known lateral strength may undergo when subjected to earthquakes can be calculated from base shear which is function of elastic design spectra and yield strength reduction factors. Calculation of base shear V_t is given in Turkish Earthquake Code (2007) as follows:

$$V_t = \frac{WA(T_1)}{R_a(T_1)} \geq 0.10 A_0 IW \tag{1.1}$$

where V_t denotes total equivalent seismic load (base shear), T_1 denotes building period of vibration, W denotes total building weight, R_a denotes seismic load reduction factor (given in equation (1.4)), and A denotes the spectral acceleration coefficient defined as

$$A(T) = A_0 IS(T) \tag{1.2}$$

where A_0 denotes effective ground acceleration and I denotes building importance factor, S denotes the spectrum coefficient which is evaluated via

$$\begin{aligned} S(T) &= 1 + 1.5\frac{T}{T_A} && (0 \leq T \leq T_A) \\ S(T) &= 2.5 && (T_A \leq T \leq T_B) \\ S(T) &= 2.5\left(\frac{T_B}{T_A}\right)^{0.8} && (T_B \leq T) \end{aligned} \tag{1.3}$$

where T_A and T_B denote the spectrum characteristic periods specified in Table 1.1. T_B separates the constant acceleration region from the constant velocity region,

Table 1.1. Spectrum Characteristic Periods (T_A, T_B)

Local Site Class	T_A (seconds)	T_B (seconds)
Z1	0.10	0.30
Z2	0.15	0.40
Z3	0.15	0.60
Z4	0.20	0.90

$$\begin{aligned} R_a(T) &= 1.5 + (R_y - 1.5)\frac{T}{T_A} && (0 \le T \le T_A) \\ R_a(T) &= R_y && (T_A < T) \end{aligned} \tag{1.4}$$

where R_y denotes structural behavior factors specified in Table A.1 (in Appendix A section), and T_A is the spectrum characteristic period.

In TEC 2007, $S(T)$ is the elastic design spectrum appearing in Equation (1.3) and $R_a(T_1)$ is the reduction factor used to construct the inelastic design spectrum from $S(T)$. To understand their relationship better, design spectra will be discussed below.

1.4. Design Spectra

For design purposes using a design spectrum is more appropriate rather than using response spectrums. A design spectrum is based on a statistical analysis of a collection of numerous spectra of different recorded ground motions in different earthquakes with possible modifications based on engineering practice. Two elastic and one inelastic design spectra will be discussed below.

1.4.1. Elastic Design Spectra

1.4.1.1. **Newmark-Hall Elastic Design Spectrum**

The design spectrum proposed by Newmark and Hall (1982) is plotted in the format of a tripartite logarithmic plot, showing spectral velocity on the vertical axis and the period of vibration on the horizontal axis; spectral acceleration is plotted along 135 degrees with the horizontal and spectral displacement along 45 degrees with the horizontal. Construction procedure for *Newmark-Hall Elastic Design Spectrum* is as follows:

Estimate peak ground acceleration (PGA), peak ground Velocity (PGV) and peak ground displacement (PGD). In practice, PGD may be difficult to estimate. Newmark and Hall (1982) suggested approximate rules in estimation of PGV and PGD for a given value of PGA. Based on an analysis of several strong-motion records, they suggested that the ratio of PGV and PGA may be taken as 1.22 and 0.91 meters/sec/g for competent soil and rock, respectively; and the relation between PGD, PGV and PGA is given by a dimensionless ratio

$$\frac{PGA * PGD}{PGV^2} \simeq 6 \tag{1.5}$$

where PGA in not in g but in same dimensional units with PGV and PGD (e.g. PGA in cm/sec^2, PGV in cm/sec and PGD in cm) (Bozorgnia and Bertero, 2004).

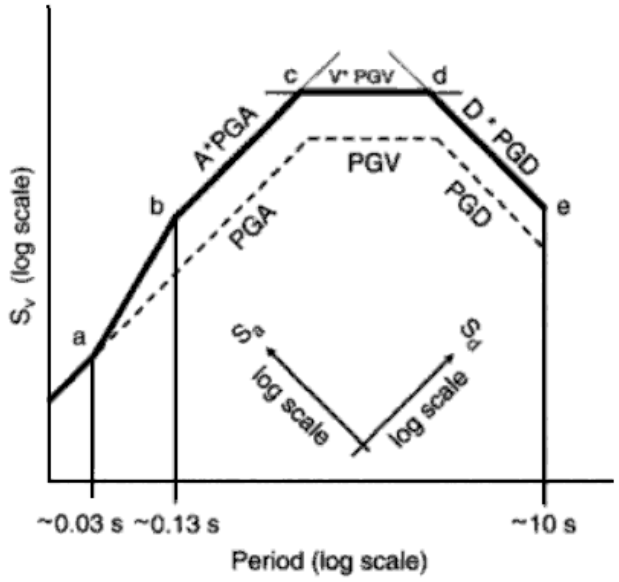

Figure 1.1. Elastic horizontal design spectrum according to Newmark and Hall.(Bozorgnia and Bertero, 2004)

Draw PGA, PGV and PGD lines on a tripartite logarithmic plot. Parallel to the PGA, where A, V and D are dynamic amplification factors for the acceleration, velocity and displacement, respectively appearing in equation (1.6) and (1.7). Values of A, V and D for use in developing a median design spectrum (50 per cent probability of nonexceedance of the spectral ordinates), are given in equation (1.6) and those proposed for use in developing a median plus one standard deviation spectrum (84.1 per cent probability of nonexceedance) are given in equation (1.7):

$$A = 3.21 - 0.68\ln\zeta; \quad V = 2.31 - 0.41\ln\zeta \quad D = 1.82 - 0.27\ln\zeta \tag{1.6}$$

$$A = 4.38 - 1.04\ln\zeta; \quad V = 3.38 - 0.67\ln\zeta \quad D = 2.73 - 0.45\ln\zeta \tag{1.7}$$

where ζ is damping ratio in percent.

In general, a is approximately 0.03, and b is close to 0.13, and e is almost 10 seconds. Points c and d fall in ranges of approximately 0.5-0.7 and 1.5-4 seconds

respectively (see Figure 1.1). For periods shorter than about 0.03 seconds, the design spectrum follows the constant PGA line.

1.4.1.2. **FEMA 356 Elastic Design Spectrum**

According to performance levels, two ground motions are considered in FEMA 356 Elastic Design Spectrum and performance levels defined as BSE-1 and BSE-2. The ground motion used in BSE-2 is more severe than in BSE-1. Construction procedure for the elastic design spectrum is as follows:

For BSE-2 ground motion level, the spectral accelerations S_S (at period of 0.2 sec) and S_1 (at period of 1 seconds) are obtained using the approved contour maps for Maximum Considered Earthquake (MCE). S_S and S_1 for the BSE-2 ground motion level are adjusted for local site conditions. These adjusted spectral accelerations S_{XS} and S_{X1} are calculated as following:

$$S_{XS} = F_a S_S \tag{1.8}$$

where S_{XS} denotes the design short-period spectral response acceleration parameter, F_a denotes site coefficient, S_S denotes response acceleration parameters. In addition,

$$S_{X1} = F_v S_1 \tag{1.9}$$

where S_{X1} denotes the design short-period spectral response acceleration parameter, F_v denotes the site coefficient, and S_1 denotes the response acceleration parameter. (Values for F_a and F_v are given in FEMA-356 document (see tables 1-4 and 1-5 in FEMA 356))

For the BSE-1 ground motion level, the spectral accelerations S_S and S_1 are taken as described below:

- The values of S_S and S_1 taken from approved contour maps of spectral accelerations for 10 per cent probability of exceedance in 50 years (BSE-1)
- Or 2/3 of the values taken from BSE-2 ground motion level

Using equations (1.8) and (1.9) to calculate S_{XS} and S_{X1} from the minimum of S_S and S_1 values defined above.

Given spectral accelerations S_{XS} and S_{X1}, the elastic horizontal spectra for BSE-2 and BSE-1 ground motion levels are constructed according to Figure 1.2. In this figure, B_S and B_1 are damping modification factors to modify S_{XS} and S_{X1}, respectively, for damping values other than five per cent.

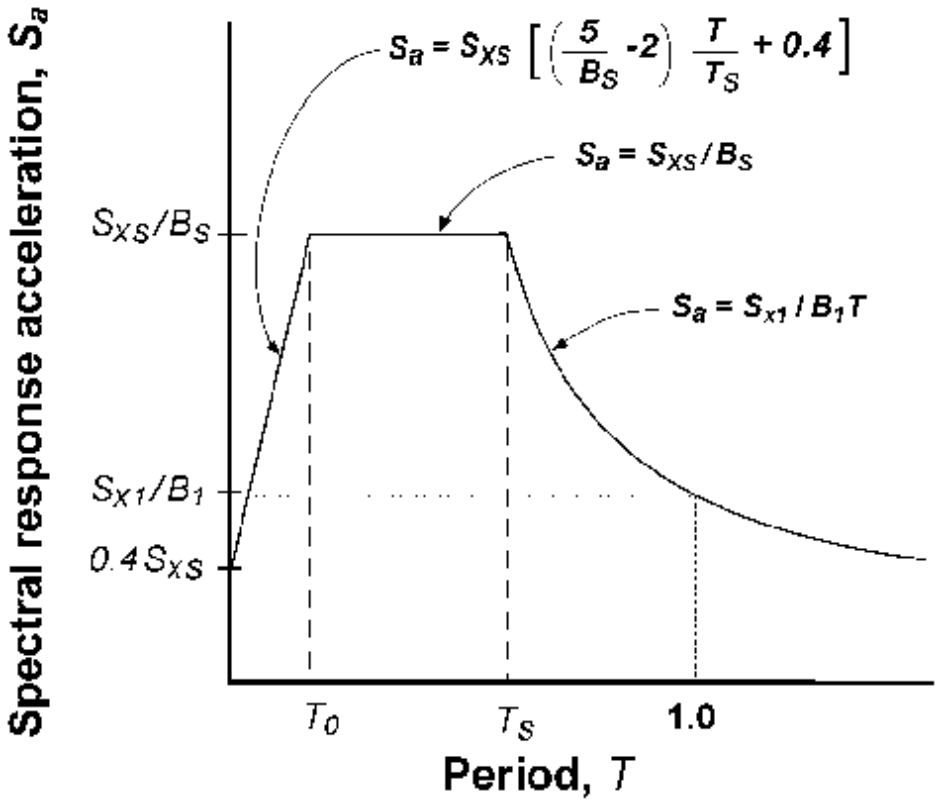

Figure 1.2. FEMA-356 Elastic Design Spectrum

The recommended values of B_S and B_1 (damping coefficients as a function of critical damping) are given in Table 1.2. For given S_{XS}, S_{X1}, B_S and B_1, one can determine the corner periods T_S and T_0 as

$$T_0 = 0.2T_S$$
$$T_S = \frac{S_{X1}B_S}{S_{XS}B_1} \tag{1.10}$$

where T_S denotes period separating constant acceleration and velocity regions, T_0 denotes period separating the short period range and the extreme short period range, B_S and B_1 denotes damping coefficients.

The design spectrum can be constructed as indicated in Figure 1.2. For five per cent damping, B_S and B_1 are 1, and the peak of the design spectrum over the zero period (T =0) acceleration is 2.5 (Bozorgnia and Bertero, 2004).

Table 1.2. Design spectrum modification factors

	Newmark-Hall(1982)			FEMA-356(2000)	
Damping	Acceleration	Velocity	Displacement	B_S	B_1
2	0.77	0.81	0.85	0.80	0.80
5	1.00	1.00	1.00	1.00	1.00
10	1.29	1.21	1.12	1.30	1.20
20	1.80	1.53	1.37	1.80	1.50
30	2.36	1.80	1.54	2.30	1.70
40	3.02	2.07	1.68	2.70	1.90
50	3.85	2.34	1.81	3.00	2.00

1.4.2. Newmark-Hall Inelastic Design Spectrum

Inelastic design spectrum is basically a reduced form of elastic design spectrum. The transition from the elastic to the inelastic spectrum can be made by using the ductility factor μ. The ductility factor is defined as (Bozorgnia and Bertero, 2004)

$$\mu = \frac{u_m}{u_y} \tag{1.11}$$

where u_m denotes maximum deformation of the inelastic system and u_y denotes yield deformation of the same system. Ductility is also given by

$$\mu = C_R R_y \tag{1.12}$$

where C_R denotes the inelastic displacement ratio defined as

$$C_R = \frac{\mu}{R_y} = \frac{u_m}{u_0} \tag{1.13}$$

where R_y denotes yield strength reduction and where u_0 denotes the maximum deformation of the elastic system. The yield strength reduction factor can be evaluated as

$$R_y = \frac{u_0}{u_y} \tag{1.14}$$

The inelastic design spectra can be constructed by dividing the *Newmark-Hall Elastic Design Spectrum* by $\sqrt{2\mu - 1}$ in short period range and by μ in long period range (constant velocity region) for elasto-plastic systems. The point c' is obtained as the intersection of flat and decaying parts of the inelastic design spectrum. An inelastic design spectrum is shown schematically in Figure 1.3.

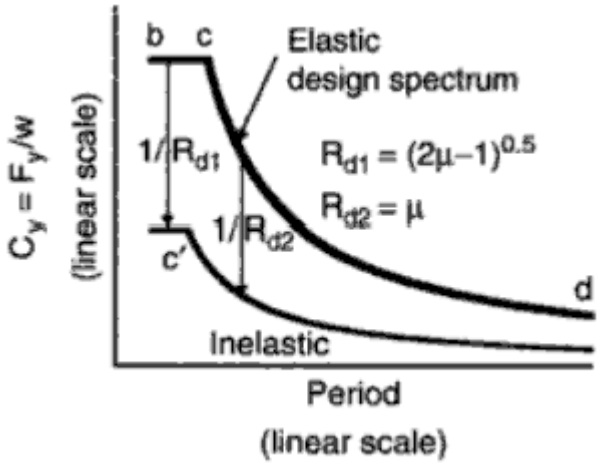

Figure 1.3. Inelastic Design Spectrum According to Newmark-Hall (1982)

1.5. Performance Based Design

1.5.1. Definition

In traditional practice, earthquake design has been explicitly performed for only a single design event level, at which a level of performance generally termed "life safety" has been targeted. On contrary in performance based design, multiple performance levels such as operation and immediate occupancy are introduced.

In early years of performance based earthquake engineering, performance and performance based design is defined, respectively, as follows: “Performance is measured in terms of the amount of damage sustained by a building, when affected by earthquake ground motion, and the impacts of this damage on post-earthquake disposition of the building,” and “performance-based design is the definition of multiple target performance (damage) levels which are expected to be achieved, or at least not exceeded, when the structure is subjected to an earthquake ground motion of specified intensity.” (Hamburger, 1997)

In the following years, economical and political objectives are also included into the definition. One of the best definitions is given by Krawinkler and Miranda (2004): "Performance-based earthquake engineering (PBEE) implies design, evaluation,

construction, and monitoring the function and maintenance of engineered facilities whose performance under common and extreme loads responds to the diverse needs and objectives of owners-users and society. It is based on the premise that performance can be predicted and evaluated with quantifiable confidence to make, together with the client, intelligent and informed trade-offs based on life-cycle considerations rather than construction costs alone."

One brief description is as follows: "Factors to determine the performance objectives are seismic risk, hazard tolerance, economic background, social acceptance of damage, technical development, and construction practice. Minimum levels may be established by a society, but the performance level of an individual building should be selected by the owner." (Otani, 2004)

As it can be understood, it is the choice of the owner to make. Owners cannot choose a performance level lower than given by the codes in order to gain more. But they can choose safer structures to live in relief. If the property in the structure is too valuable and must be protected, the owner may prefer (by paying more) a very though earthquake resistant structure that could experience high magnitude earthquakes with negligible damage. But to lower the cost of the building, an owner may choose a lower performance level such that the building would not collapse and there would be no life loss in a high magnitude earthquake, but the structure would probably be unusable after such an earthquake without retrofitting or reconstructing.

1.5.2. Performance/Damage Limits of Cross-Sections

In TEC 2007, three limits about ductile components are defined based on observed behavior on their cross-sections. The limits are called Minimum Performance Limit (MPL), Margin of Safety (MS) and Collapse Limit (CL). Minimum Performance Limit implies commence of yielding on the cross-section, Margin of Safety implies that the cross-section assures sufficient strength in inelastic limit, Collapse Limit defines the limit of the cross-section just before its failure. The classification may not be valid for cross-sections showing brittle type of failure.

1.5.3. Cross-sections Damage Regions

Performance of Critical cross-section of members:

- doesn't reach MPL; is in Minimum Damage/Performance region
- is in between MPL and MS region; is in Prominent/Visible Damage region
- is in between MS and CL region; is in Significant Damage region
- exceeds CL; is in Collapse region.(see Figure 1.4.)

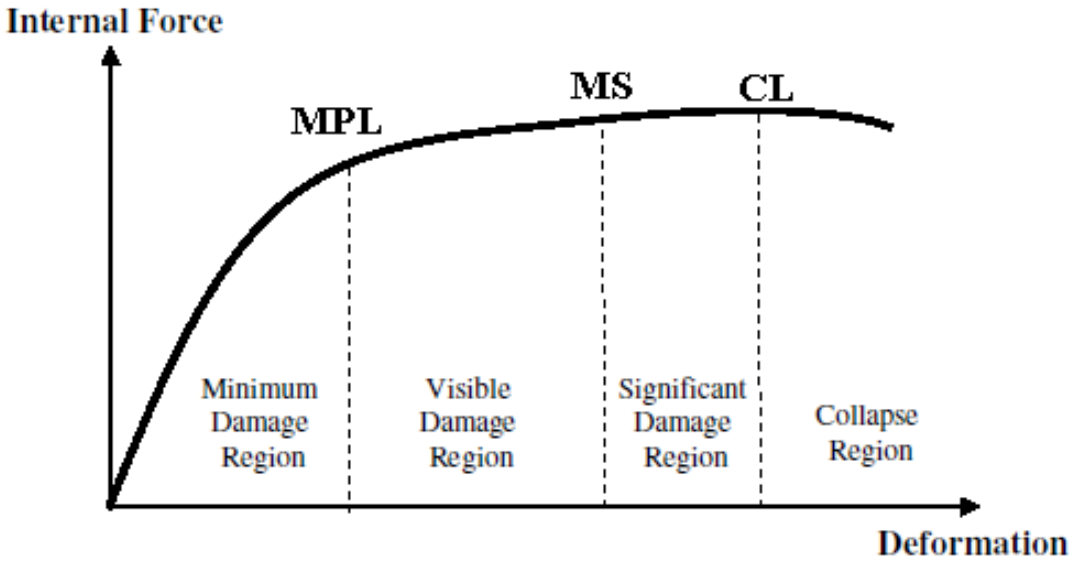

Figure 1.4. Cross-Section Damage/Performance Limits and Cross-section Damage Regions on Capacity Curve (Akgül, 2007)

1.6. Literature Review

It is appropriate to start the review with the most referred to paper in this subject, namely "Effect of inelastic behavior on the response of simple systems to earthquake motions" by Veletsos and Newmark (1960). They started investigating this subject after the really hazardous El Centro earthquake. They found out that a building designed for an average magnitude earthquake performed successfully under such disastrous earthquakes. It showed to the researchers that they were neglecting a crucial property of materials, namely ductility, in the design, evaluation and rehabilitation of buildings. Veletsos and Newmark noted that "For most structural materials, including steel or reinforced concrete, plastic deformations of the order of three times the elastic limit deformation, or total deformation corresponding to μ=4, involve no serious distortions or undue amounts of damage." Furthermore, they formulated the so called equal displacement rule, which means that for the same initial stiffness and critical damping ratio and for long periods and low critical damping values (e.g. two per cent to five per cent), the displacement of an inelastic system is roughly equal to its elastic counterpart. For higher critical damping ratios such as 10 per cent or 20 per cent, equating strain energy for elastic and inelastic systems leads to the following expression:

$$\frac{u_m}{u_0} = \frac{\mu}{\sqrt{2\mu - 1}} \tag{1.15}$$

They also describe the procedure for constructing a tripartite type graph (four way log graph) showing spectral displacement, velocity, acceleration and period. Thanks to tripartite plots, the natural period axis can be divided into three period ranges in the form of constant acceleration, velocity and displacement regions.

After the publication of the study by Newmark and Veletsos (1960), many studies were conducted to investigate the equal displacement rule to determine when it is valid and under what conditions the inelastic displacement exceeds its elastic counterpart. Shimazaki and Sozen (1984) studied five different models whose damping ratios is a function of stiffness (equivalent linearization method), used the Newmark-β method to integrate the

equations of motion defining β as 0.167, and inspected two periods (0.3 and 1 seconds) for three ground motion records of the El Centro Earthquake. Strength ratio e, which is the strength required to keep structure elastic over yield strength of the system (inverse of yield-strength reduction factor R_y), and the period ratio TR, which is defined as the ratio of the period of vibration to the recording site's characteristic period separating constant acceleration and constant velocity regions, are introduced. According to the analyses done using 0.33, 1, 2 as TR values and 0.250, 0.200, 0.166, 0.142, 0.125 as e values, if $TR+e$ is greater than 1.00, equal displacement rule is valid except (period independently) for e values lower than 0.200. For $TR+e$ less than 1.00, the inelastic displacement ratio exceeds one and it is dependent on the hysteresis shape of model used in the analysis. Current studies also suggest that when e is less than 0.2 and the period of vibration is less than or equal to 1 second, inelastic displacement ratio exceeds unity. But for longer periods, the inelastic displacement may be equal to or be even less than its elastic counterpart. As period increases, for all e values, the inelastic displacement ratio eventually reaches 1.

Linear and nonlinear procedures for the design and rehabilitation of buildings have been developed in resource documents FEMA 273 and FEMA 356 (FEMA 1997, FEMA 2000). In both documents, the article entitled "Nonlinear Static Procedures" says that the target displacement δ_t of an inelastic system can be calculated using a simplified method called the coefficient method. The relation between the base shear force and the lateral displacement of the control node is established for control node displacements ranging between zero and 150% of the target displacement δ_t. The formula recommended is

$$\delta_t = \frac{C_0 C_1 C_2 C_3 S_a T_e^2}{4\pi^2} \tag{1.16}$$

where C_0 and C_1 relate the spectral displacement to the displacements calculated for linear elastic response, C_2 helps to incorporate stiffness degradation, strength deterioration and pinching effects and it takes values between one and one half, C_3 helps to incorporate increased displacements due to dynamic $P-\Delta$ effects, T_e is the effective fundamental period of the building, and S_a is the function of elastic response spectrum acceleration at T_e.

Three methods to calculate the period of vibration of a building are also given. In this study, the second method (FEMA 356, article 3.3.1.2.2) that relates height to the period is used to select the periods used in the analyses.

A study supporting the findings of Shimazaki and Sozen in the light of FEMA 273 resource document is presented by Whittaker et al (1998). In this study, 20 horizontal component records of 10 large magnitude earthquakes are analyzed using the nonlinear static procedure of FEMA 273 (push-over analysis) with elasto-plastic and Bouc-Wen models. Recording sites have 10 – 20 kilometers epidistance to earthquakes and their NEHRP soil profile types were C or D. Although the authors declare it an incorrect assumption, critical damping ratio used in the design is a function of period of vibration, spectral displacement, and spectral acceleration. Two post-yield stiffness values (5 and 25 per cent of initial stiffness), five strength ratios (e =0.10, 0.15, 0.20, 0.30, 0.50 (R_y = 2, 3.33, 5, 6.67,10)) and four periods of vibration, T_0, (0.1, 0.3, 0.5 and 1) are used. The conclusions are in supporting manner and agree with the conclusions of the former study by Shimazaki and Sozen. Some additional conclusions are drawn: Dispersion in the displacement demand around mean value is significant, the inelastic displacement ratio exceeds unity when T_0 is greater than T_g, mean plus one standard deviation satisfies 1.5 times the target displacement criteria of FEMA 273 in the constant velocity and displacement regions, for low and medium-rise construction the strength ratio e is generally greater than 0.20, and the relation between elastic and mean inelastic displacement can be used confidently.

Researchers generally refer to two different approximate categories, namely equivalent linearization methods and displacement modification factor methods, to calculate inelastic displacement demands of structures from maximum displacements of linear elastic systems. Miranda and García (2002) evaluated four proposals of equivalent linearization and two proposals of displacement modification methods. In equivalent linearization methods inelastic deformation is calculated from elastic systems having lower stiffness and higher damping coefficients, and damping ratio is a function of ductility and post-yield stiffness. In displacement modification methods, same stiffness and damping ratio is used for both elastic and inelastic systems. It is concluded that displacement modification methods are much easier to use in practical situations for intermediate and

long period spectral regions due to the equal displacement rule, since the displacement demand of the elastic system can be directly used in the estimation of the maximum inelastic displacement demand. Furthermore, according to a comparison of the particular methods in these categories, Miranda's (Miranda, 2000) equation yields better estimates than the Newmark-Hall method (Newmark and Hall, 1982). One conclusion supporting one of the findings of Whittaker et al. (1998) is about the dispersion in the maximum inelastic displacement, and it is said that for an individual earthquake record the approximate methods may lead to significant errors.

Effects of earthquake and recording site parameters on inelastic displacement ratios are also investigated by various researchers. The effects of soil properties were discussed by Miranda (1991). For the structures built on soft soils, when TR equals approximately to one, the inelastic displacement ratio is 0.6-0.7. When TR less than 1, the inelastic displacement ratio exceeds 1 for rock and stiff soil sites, for short periods it is a function of ductility, and for the transition period the equal displacement rule is valid. In the analyses of this study, post-yield stiffness equals to three per cent of initial stiffness, critical damping ratio is five per cent. A total of 124 ground motions recorded in California are used to analyze systems having 50 different periods and five levels of ductility ranging from one to six.

Effects of earthquake magnitude, distance to source and site conditions are studied by García and Miranda (García and Miranda, 2003). 216 records of 12 earthquakes, with magnitudes varying between 5.8 and 7.7, NEHRP B, C, D type soils, six levels of yield-strength reduction factor R_y, five per cent critical damping, and 50 different periods of vibration between 0.05 and 3, are investigated in the analyses. Their conclusions indicate that distances greater than 10 kilometers to source has negligible effect. In the constant velocity region and for moderate strength reduction factors, ratios between inelastic displacement ratios calculated using records from high magnitude (7.2-7.8) records and inelastic displacement ratios calculated from low magnitude (5.8-6.1) records reach two. Shear wave velocity of soil is shown to have moderate effects on inelastic displacement ratios. Dispersion of the inelastic displacement ratio is also investigated through the coefficient of variation COV, which is the ratio of the standard deviation to the average. In

the constant acceleration region COV is as high as 1.2 for all R_y values, and for periods of vibration between 1 and 3 seconds with R_y values greater than 4, the COV is approximately equal to 0.4. An empirical equation is given at the end of the study which is a function of the period of vibration, the yield-strength reduction factor, and the NEHRP soil classification. In this paper, Mutual effect of distance to source and magnitude is not investigated

Chopra and Chintanapakdee (2004) grouped records used in the analysis according to magnitude and distance to source parameters, and to NEHRP soil classes. According to their study, four groups containing large magnitude and small distance (LMSR), large magnitude and large distance (LMLR), small magnitude and large distance (SMLR), small magnitude and small distance (SMSR) records, and three ensembles categorized by NEHRP site classes B, C, or D, all seven ensembles of far-fault ground motion of records have similar inelastic displacement ratio versus period plots. Maximum differences were observed for a period of 0.25 sec with almost 50 per cent variations between SMLR and LMSR; in the constant displacement region, this ratio is seen to be around 10 per cent. To calculate limiting values of the inelastic displacement ratio, period of vibration is taken to be zero (assuming mass is fixed to the ground) which results in the maximum ground acceleration being equal to the spectral acceleration, and the value of the inelastic deformation ratio calculated from the yield-strength reduction factor for elasto-plastic systems going to infinity. The other limiting case is when the period of vibration goes to infinity; in this case, the spectral displacement equals to the maximum ground displacement, leading to equal displacement rule. All seven ensembles have similar inelastic displacement ratio versus period relations, in which the inelastic displacement ratio exceeds unity at the constant acceleration region, is almost equal to one at the constant velocity region, is a bit lower than one (minimum 0.8) in the constant displacement region up to a period of 10 seconds, and is equal to one after 10 seconds. Dispersion in the inelastic displacement ratios is also investigated. It is concluded that the dispersion isn't affected by an increase in the post-yield stiffness, but it increases by increasing yield-strength reduction factor. A simplified equation for inelastic displacement ratio is proposed also. In their discussion of prior formulations for the inelastic displacement ratio, the authors find the results satisfactory and note that for bilinear

systems, the relation developed by Krawinkler and Nassar (1992) gives better results than the relations developed by García and Miranda (2003) and Newmark and Hall (1982). The authors concluded that all the formulations given are overestimating the inelastic displacement ratio in the constant acceleration region.

More recently, Mehanny and Ayoup (2007) used the Monte Carlo method by randomly choosing records and system parameters in a huge data set to choose the system parameters and compared record to record variability. According to this study, record to record variability contributed most to the dispersion in the inelastic displacement ratios, while degrading, normalized yield strength, critical damping and hysteresis shape effects contributed relatively less.

1.7. Scope, Objectives and Goals

In this study, single degree of freedom systems (SDOF) having bilinear force-deformation relations with non-negative post-yield stiffness and non-degrading material models are used. No near fault earthquake records are considered in the analyses. In calculations, same initial stiffness and critical damping values are used in inelastic and elastic systems. The main aim this thesis is to investigate the spectral displacement ratio formulation given in Annex 7-C of the Turkish Earthquake Code (2007). Secondary aims are establishing a simplified expression for this ratio and comparing it with the prior formulations.

2. METHODOLOGY

In this study, inelastic and elastic seismic demands of structures are determined using nonlinear and linear time history analyses. The procedure is defined in the Turkish Earthquake Code (2007) as follows:

"The aim of nonlinear time history analysis is to take the nonlinear behavior of structural components into consideration, and integrating the equation of motion step by step. During the analysis, in every time step of integration; displacements, inelastic deformations, internal forces and their spectral values corresponding to seismic demand are calculated."

Newmark integration methods used in the integration of the equation of motion and it will be discussed in the next section.

2.1. Newmark-Beta Methods

The Newmark-beta method is a method of numerical integration used to solve differential equations. It is used in finite element analysis to model dynamic systems. For linear and nonlinear Simple Degree of Freedom (SDOF) systems, equation of motion appearing to be integrated step by step is given by

$$m\ddot{q} + c\dot{q} + f_x = m\ddot{q}_g \tag{2.1}$$

where m denotes the mass, c denotes damping, q denotes displacement, $\dot{q}$ denotes velocity, $\ddot{q}$ denotes acceleration of system, $\ddot{q}_g$ denotes the ground acceleration and f_x denotes spring force which is a function of k (linear stiffness) and q for elastic systems and u_y (yielding displacement), k (initial stiffness) and α (post yield stiffness) and q for bilinear systems.

Integration is very a complex process and solving integral equation may not be always possible. However using discrete mathematical models gives very accurate results and with the use of computers with high processors negligible errors can be attained in very short time. Discrete model can be obtained from the continuous model by dividing time into small intervals. In discrete model instead of using time values (t), corresponding interval numbers (n^{th} step) are used.

For the initial time step ($t = 0$) of the Newmark integration method, if there is no initial displacement or velocity, the calculation of acceleration is as follows:

$$\ddot{q}(0) = \frac{1}{m}(F(0) - c\dot{q}(0) - F_k(0)) \tag{2.2}$$

where F_k is the force in the spring due to displacement, $F(0)$ is the force acting on mass at time zero.

Newmark integration methods use equations (2.3) and (2.4) to calculate displacement, velocity and acceleration at n^{th} step:

$$\dot{q}[n] = \dot{q}[n-1] + \Delta t(1-\gamma)\ddot{q}[n-1] + \Delta t\gamma\ddot{q}[n] \tag{2.3}$$

$$q[n] = q[n-1] + \Delta t\dot{q}[n-1] + (\Delta t)^2\ddot{q}[n-1]\left(\frac{1}{2} - \beta\right) + (\Delta t)^2(\beta)\ddot{q}[n] \tag{2.4}$$

where γ and β denote coefficients, Δt denotes the time separating two consecutive steps, and n is the step number.

Values for β and γ coefficients are given in Table 2.1.

Table 2.1. Newmark Method Coefficients

Method	β	γ
Constant Acceleration Method	0.25	0.00
Average Acceleration Method	0.25	0.50
Linear Acceleration Method	0.17	0.50

In the analysis, linear acceleration method is used.

2.2. Structural Models

Single Degree of Freedom (SDOF) systems with 5% critical damping ratio and bilinear (both zero (elasto-plastic) and three per cent post-yield stiffness ratio) force-deformation characteristics are considered. The bilinear force-deformation relation is shown below:

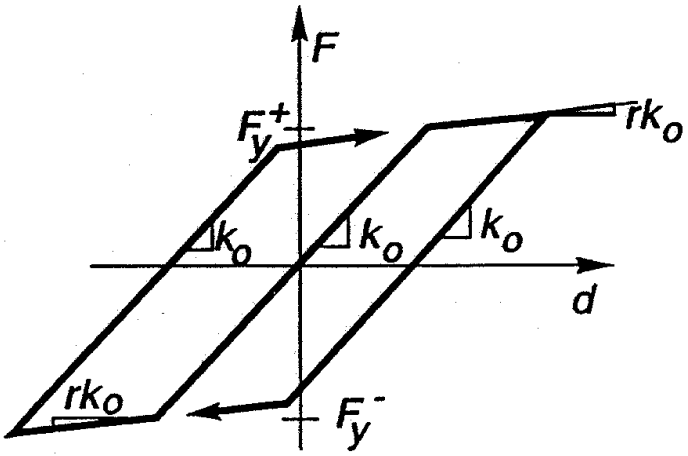

Figure 2.1. Bilinear Model: Resistance-deformation relation.

In the calculation of constant relative strength inelastic displacement ratio, inputs are initial stiffness of system, period of the system, yield strength reduction factor and critical damping of system. Yielding strength, mass and damping coefficient of the system is calculated as follows:

Yielding force of the system is determined from maximum displacement of corresponding elastic system (same initial stiffness and critical damping) and the yield strength reduction factor.

$$F_y = k\frac{u_0}{R_y} \tag{2.5}$$

where k is initial stiffness of the system, u_0 is the maximum displacement of the elastic system, R_y is the yield strength reduction factor.

Mass of the system is calculated from initial stiffness and period of the system as follows:

$$m = \frac{kT_N{}^2}{4\pi^2} \tag{2.6}$$

where m denotes mass, k denotes initial stiffness, T_N is the period of the system.

In the equation of motion, damping coefficient, c, is calculated from critical damping ratio as follows:

$$c = 2\zeta\sqrt{km} \tag{2.7}$$

where ζ denotes critical damping, k denotes initial stiffness, m denotes mass of the system.

2.3. Ground Motion Selection

In the selection of ground motion individual and mutual effects of earthquake magnitude, soil conditions and distance-to-source relation on inelastic displacement ratio are considered. First aim was to analyze mutual and triple effects of earthquake magnitude, soil condition and distance-to-source parameters. To accomplish this, records are grouped according to high and low values of these parameters. Since, investigating only two regions (high and low) of these parameters is not sufficient enough to analyze overall effect of each parameter on inelastic displacement ratio; records and groups used in the research is altered even though all analysis's were completed. This led the research to have a better opinion of grouping records according to individual parameters' effects on inelastic displacement ratio. The parameter is analyzed for 3-6 values by keeping other parameters constant, and effects of the each parameter are investigated. 555 records used in the analyses are assembled into 21 different groups. The first group GMDS1 is used to investigate effect of critical damping and post-yield stiffness. Other groups are assembled into six stacks. Three main stacks and three control stacks are used to determine effects of distance-to-source, soil conditions and earthquake magnitude. Abbreviations used in the group names and their corresponding property are given in Table 2.2. In Table 2.3. group list is given with average values of magnitude, distance to source (epidistance), and soil shear wave velocity (average at 30m depth).

Table 2.2. Groups Abbreviations and their corresponding properties

Abbr.	Min	Max	Avg	Unit
M1	6.2	6.2	6.2	Richter
M2	7.6	7.6	7.6	Richter
M3	5.9	5.9	5.9	Richter
M4	6.6	6.9	6.7	Richter
D1	10	30	23	km
D2	31	50	43	km
D3	51	70	60	km
D4	71	90	79	km
D5	91	110	103	km

Abbr.	Min	Max	Avg	Unit
D6	111	150	124	km
S1	180	240	222	m/sec
S2	270	280	273	m/sec
S3	360	480	454	m/sec
S4	481	720	561	m/sec
S5	360	760	500	m/sec
SD	180	360	296	m/sec
SC	360	760	428	m/sec
SB	760	1500	935	m/sec

Table 2.3. Average Values for Magnitude, Epicenter and Soil Wave Velocity

Group Name	Magn	EpiD	Vs_{30}
GMDS1	7.3	71	418
M1D1S5	6.2	23	500
M1D2S5	6.2	43	502
M1D3S5	6.2	61	498
M1D4S5	6.2	80	497
M1D5S5	6.2	102	501
M1D6S5	6.2	124	501
M2D1S5	7.6	22	499
M2D2S5	7.6	44	502
M2D3S5	7.6	59	502
M2D4S5	7.6	78	502

Group Name	Magn	EpiD	Vs_{30}
M2D5S5	7.6	103	501
M3D2S5	5.9	44	499
M3D5S5	5.9	103	501
M2D2S1	7.6	43	222
M2D2S2	7.6	42	273
M2D2S3	7.6	43	454
M2D2S4	7.6	42	561
M4D2SD	6.8	40	296
M4D2SC	6.7	40	428
M4D2SB	6.7	39	935

In FEMA 356, article 3.3.2.2.4 (Time History Method) paragraph two reads: “Response parameters shall be calculated for each time history analysis. If three or more time history analyses are performed, the maximum response of the parameter of interest shall be used for design. If seven or more consistent pairs of horizontal ground motion records are used for time history analysis, use of the average of all responses of the parameter of interest shall be permitted for design.” In some groups, records selected according to soil condition, epidistance and magnitude, as low as 12. Even in that case, the use of the average values of the response parameters are justified according to the excerpt above.

Main S1 stacks are used to control the effect of distance to source on inelastic displacement ratios and it is controlled by Control S1 stack. Main S2 stack is used to check the effect of magnitude on inelastic displacement ratios and their control stack is Control S2. Effect of the soil condition is investigated through Main S3 stack and controlled with Control S3 stack. (Table 2.4.)

Table 2.4. Stack names, groups inside stacks

Distance to Source		Earthquake Magnitude		Soil Shear Wave Velocity	
Main S1	**Control S1**	**Main S2**	**Control S2**	**Main S3**	**Control S3**
M1D1S5	M2D1S5	M1D2S5	M1D5S5	M4D2SD	M2D2S1
M1D2S5	M2D2S5	M2D2S5	M2D5S5	M4D2SC	M2D2S2
M1D3S5	M2D3S5	M3D2S5	M3D5S5	M4D2SB	M2D2S3
M1D4S5	M2D4S5				M2D2S4
M1D5S5	M2D5S5				M2D2S5
M1D6S5					

Magnitude versus Distance-to-Source plot is given for GMDS1 is as follows:

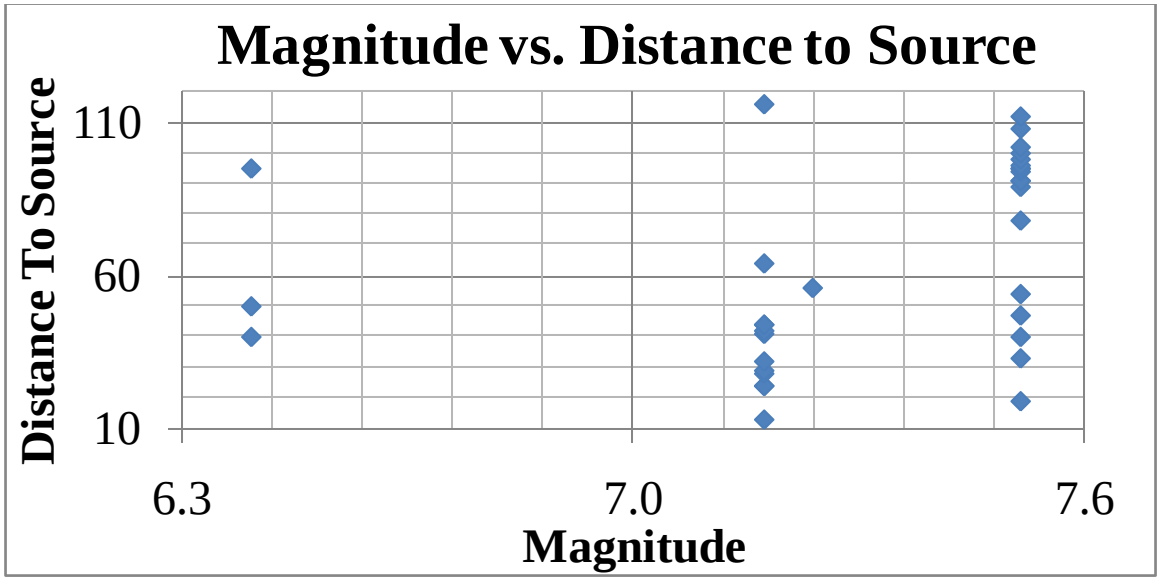

Figure 2.2. GMDS1 records, epidistance versus magnitude plot

Soil shear wave velocity versus distance to source plots for all stacks are shown in Figure 2.3 and Figure 2.4.

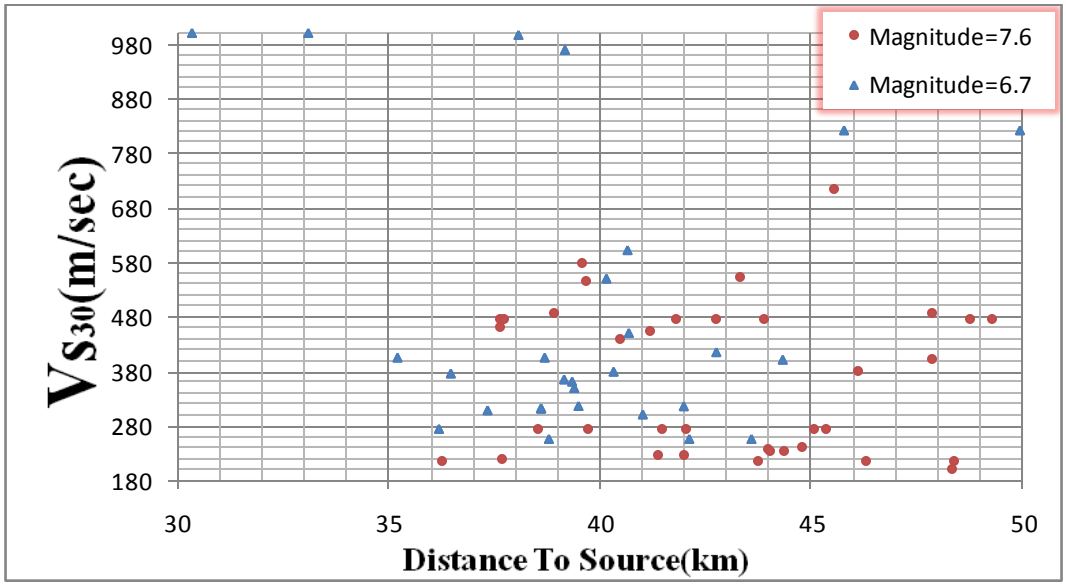

Figure 2.3. Main S3 and ControlS3 stacks, Average Soil Wave Shear Velocity at 30 m depth versus Distance to source

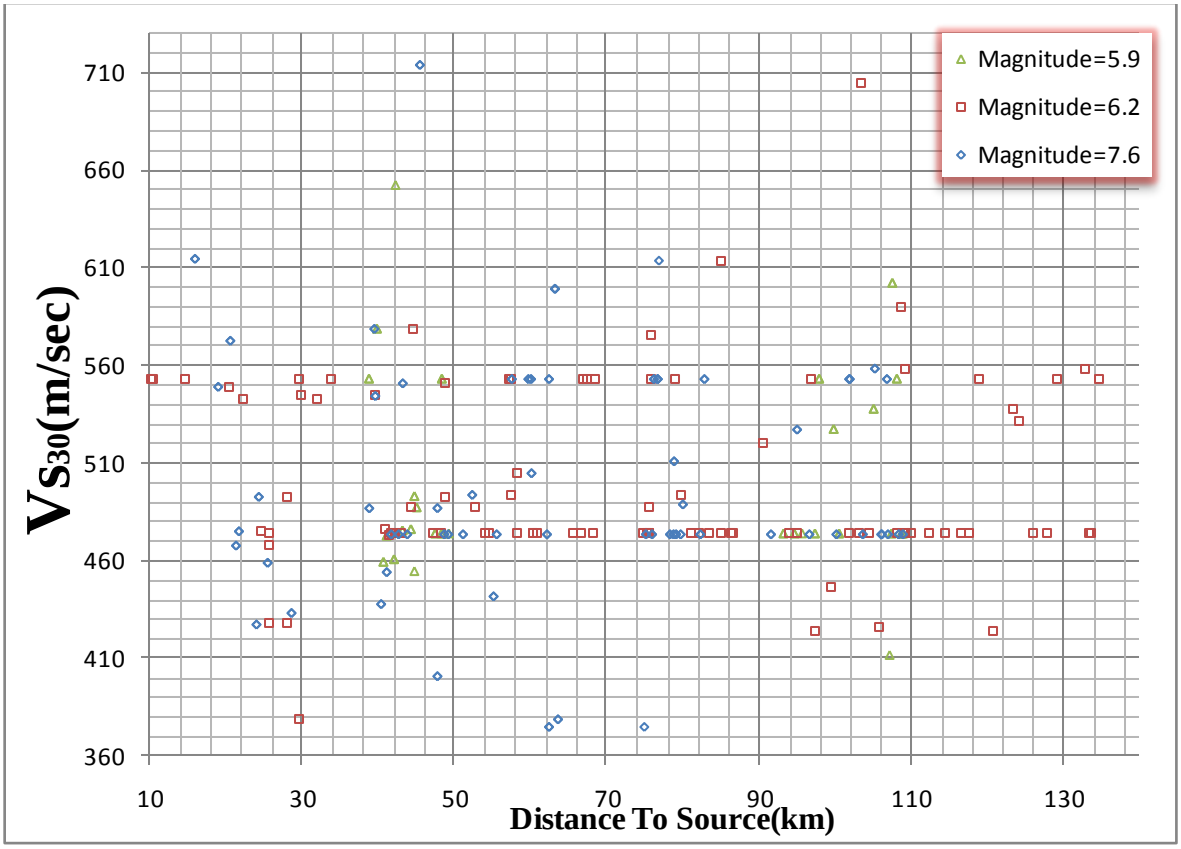

Figure 2.4. Main S1-2 and Control S1-2 stacks, Average Soil Wave Shear Velocity at 30 m depth versus Distance to source

All Ground motion records are given in Appendix A section.

2.4. Conversions for Soil Types

Although the NEHRP soil classifications of all earthquake stations in Turkey are available, no information about the Turkish local site classification of the recording sites is encountered in the investigations conducted. For a comparison between NEHRP and Turkish local soil classes, two maps are presented in Figure 2.5 and Figure 2.6 (Laue et al, 2003).

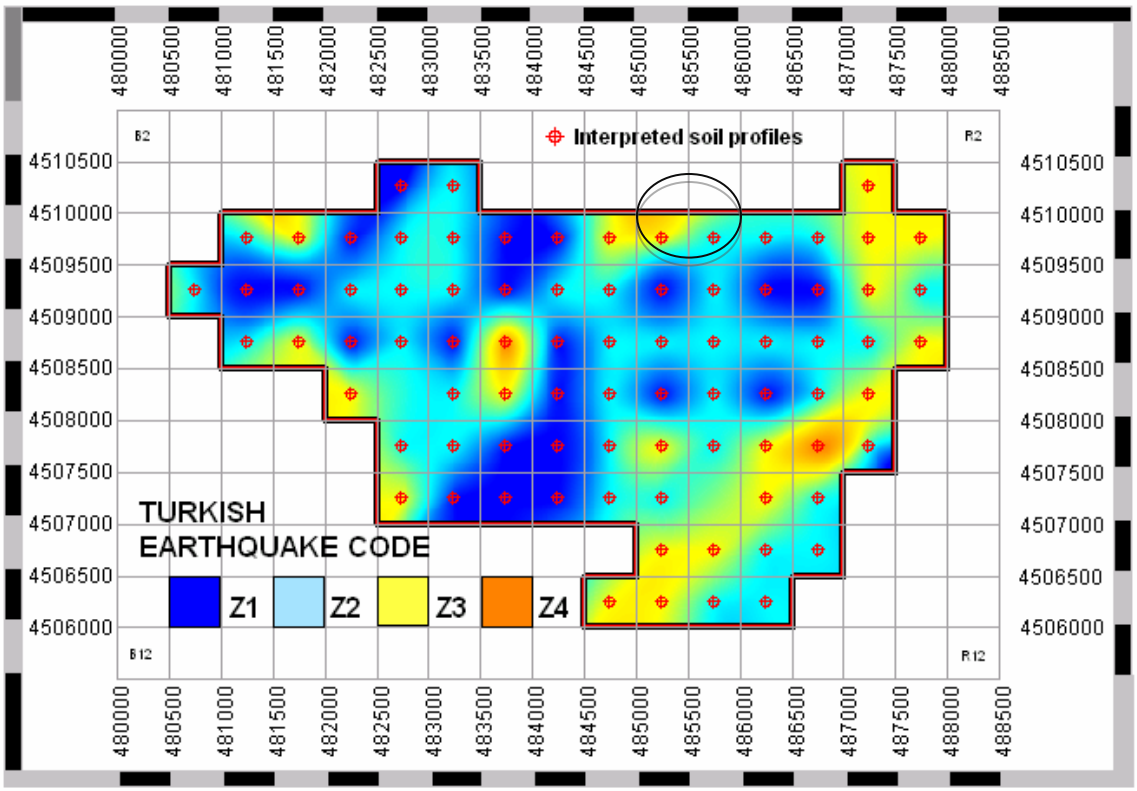

Figure 2.5. Variations in local soil classes defined in Turkish Earthquake Code 2007 in Gölcük (Laue et al, 2003).

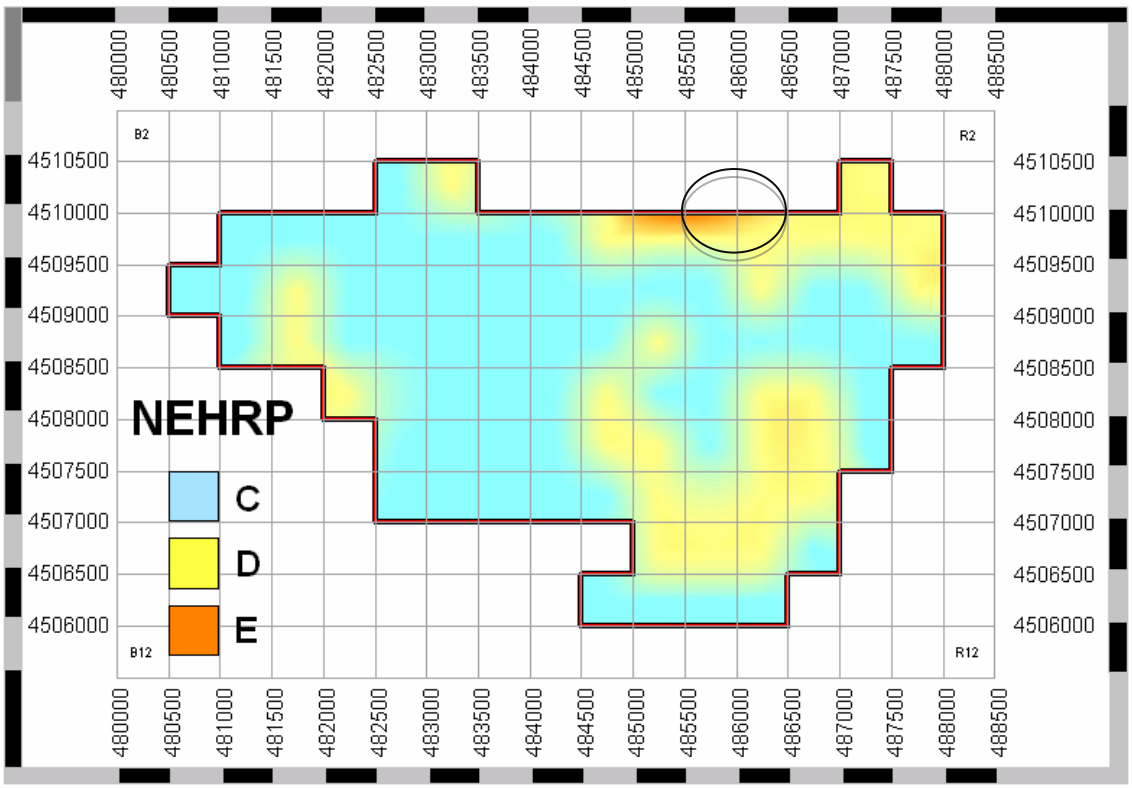

Figure 2.6. Variations in NEHRP soil classes in Gölcük (Laue et al, 2003).

NEHRP classification is dependent on only one number while Turkish local site conditions are dependent on two height value and two soil parameters. Because of this reason NEHRP-E type soil may correspond to Z2 type soil. (See the area inside oval shapes on Figure 2.5 and Figure 2.6)

Inspired from other researches, lack of information on Turkish soil classification may be cured by normalizing period of vibration by period separating constant acceleration and velocity regions.

2.5. Period Range Selection

In FEMA 356, three methods are given to calculate the period of vibration of a structure. The empirical second method, relating the base-to-roof level height with the period of vibration, is used here in period range selection. According to FEMA 356, this

formulation underestimates the period of vibration of the system. The formula to be used is:

$$T = C_t H_n^{\beta} \tag{2.8}$$

where T is the fundamental period (in seconds), C_t is a constant related to the framing system (its range is 0.018 to 0.06), H_n is height (in feet) above base to the roof level, and β is a constant related to the framing system (its range is 0.75 to 0.90).

Using this equation for structures with reinforced concrete framing system, period of one storey which is approximately 3.5 m in height is 0.16 seconds and period of 20 storey building is 2.1 seconds. Total 34 period values used in the analysis are in between 0.1 and 10 seconds.

3. STATISTICAL RESULTS

Elastic design spectrum used in TEC (2007) is dependent on site conditions (see Equation(1.3)) and magnitude (with 3 earthquake or performance level considerations, see TEC article 7.8.1 (2007)) and FEMA-356 elastic design spectrum is dependent on design earthquake magnitude (according to 2 performance levels), site conditions and critical damping ratio. Because of these, it is specifically important to investigate the effect of magnitude, soil conditions and critical damping ratio on inelastic displacement ratios (used in estimation of maximum inelastic displacement demand from corresponding elastic displacement demand.)

Three levels of yield strength reduction factors (2, 4, and 7) are analyzed and effects of the yield strength reduction factor discussed with effects of the magnitude, distance to source.

For all groups mean inelastic displacement ratio is calculated. To investigate the effect of each parameter better, for a period of vibration, mean inelastic displacement ratios of groups in one stack is normalized by the minimum of all mean inelastic displacement ratio of that group and this ratio expressed as “maximum ratio”. Maximum ratios are to be used in the formulation proposed. Maximum and minimum mean elastic displacement ratios of all groups are called inelastic displacement ratio boundaries or limits. Inside any stack, M_R is calculated as:

$$M_R(R_y, T_N) = \frac{\max(\overline{C}_R(R_y, T_N))}{\min(\overline{C}_R(R_y, T_N))} \tag{3.1}$$

where; M_R denotes maximum ratio defined above, R_y denotes yield strength reduction factor, T_N denotes period of vibration of system, $\overline{C}_R$ denotes mean inelastic displacement ratios.

The aim of use of M_R is to investigate effect of distance from rapture, earthquake magnitude and soil conditions on inelastic displacement ratios.

3.1. Effect of Site Conditions

To determine the effect of soil conditions, two stacks are defined. Main stack is to detect inelastic displacement ratio of same structures built on NEHRP-B, C and D respectively. In second stack, investigation inside NEHRP classes is aimed. As soil shear wave velocity increases, trend of inelastic displacement ratio is investigated.

For magnitude 6.75 earthquake, and average distance-to-source 39 km, the change in inelastic displacement ratio trend according to NEHRP firm soil types can be seen in Figure 3.2. Mean inelastic displacement ratios of structures built on NEHRP-D type soil has the highest value when $T_N < 0.5$. For buildings established on NEHRP-B and NEHRP-C shows almost same trend. However for structures built on NEHRP-B is always lower when $T_N < 0.3$ and afterwards one is higher is some period range and other is higher in other period range.

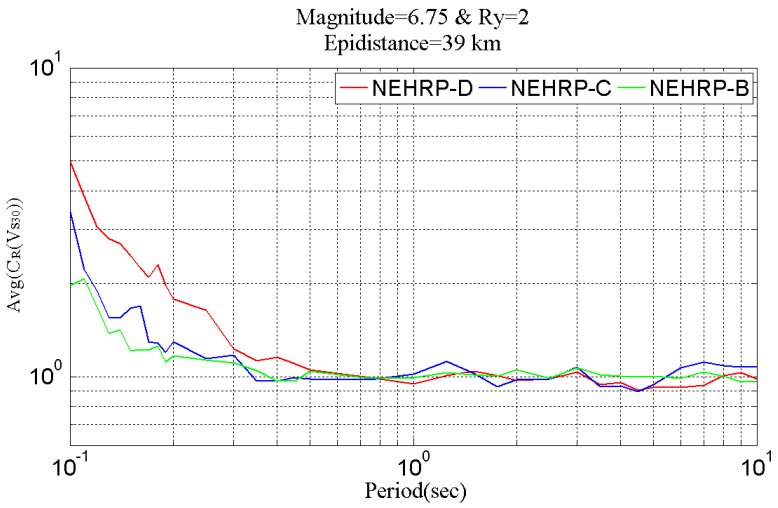

Figure 3.1. Effect of soil condition(NEHRP firm site classes B,C,D) on mean inelastic displacement ratios for Magnitude 6.75 Earthquakes, Average Distance to source 39 km and R_y=2

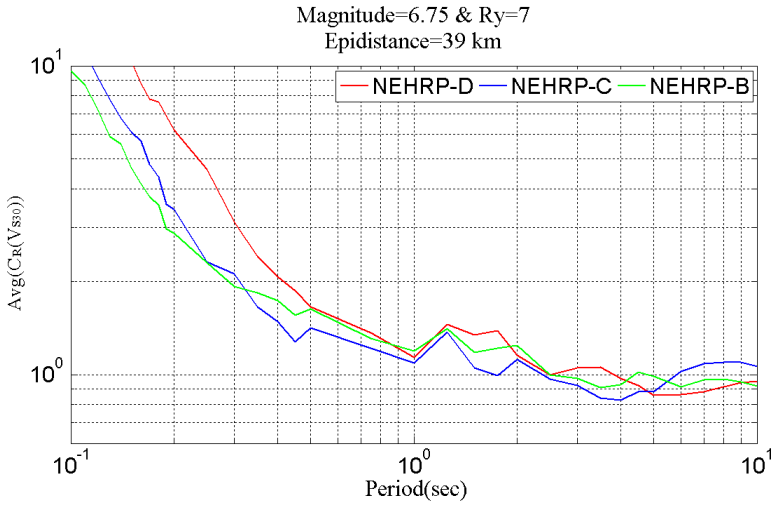

Figure 3.2. Effect of soil condition(NEHRP firm site classes B,C,D) on mean inelastic displacement ratios for Magnitude 6.75 Earthquakes, Average Distance to source 39 km and R_y=7

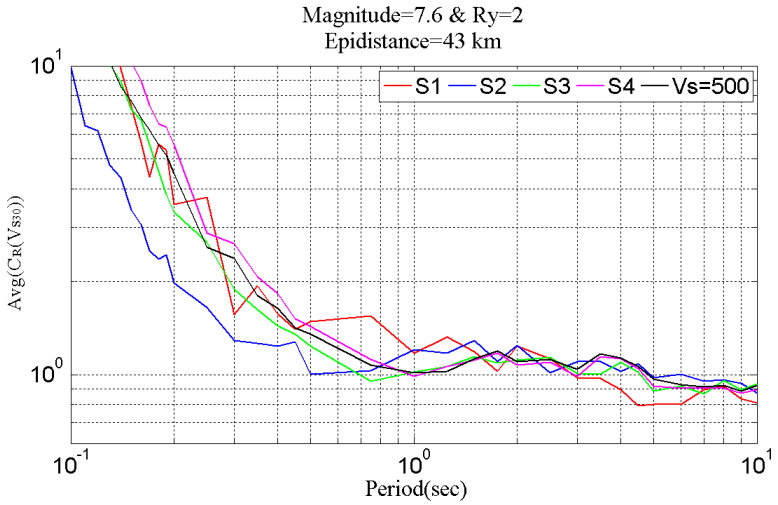

Figure 3.3. Effect of soil condition (NEHRP firm site classes C,D) on mean inelastic displacement ratios for Magnitude 7.6 Earthquakes, Average Distance to source 43 km and R_y=2

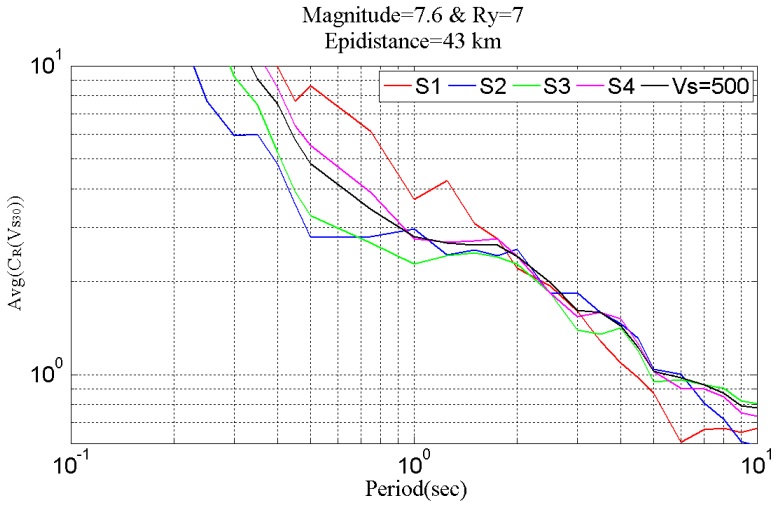

Figure 3.4. Effect of soil condition (NEHRP firm site classes C,D) on mean inelastic displacement ratios for Magnitude 7.6 Earthquakes, Average Distance to source 43 km and R_y=7

To spot the difference between the maximum and the minimum, ***maximum ratio*** which is, maximum of mean inelastic displacement ratios for NEHRP-B (296 m/sec), NEHRP-C (428 m/sec) and NEHRP-D (935 m/sec) normalized by minimum of three for each sampled period, is considered(Equation(3.1)). The maximum ratio between inelastic displacement ratios for structures built on NEHRP-B, NEHRP-C and NEHRP-D soil class is at 0.1 seconds 2.5, 3, 2.3 for R_y=2, 4, 7 respectively. These ratios drops to 1.2 at 0.3, 0.4 and 0.5 seconds for R_y=2, 4, 7 respectively. After this period, the maximum ratio changes between 1 and 1.2 for every yield strength reduction factor (Figure 3.5.)

Maximum ratio has highest value for R_y=4 the constant acceleration region, and for R_y=7 in constant velocity and displacement region.

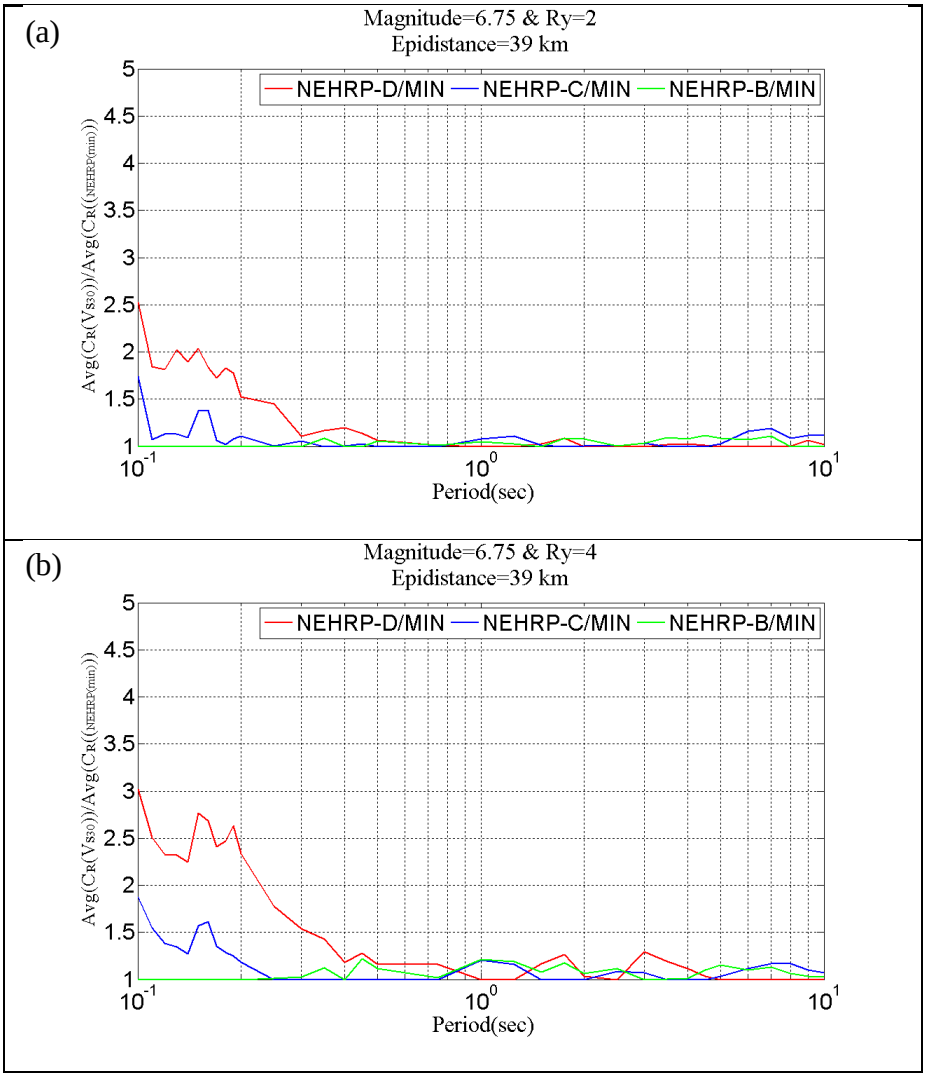

Figure 3.5. Effect of soil condition(NEHRP site classes B,C,D) on ratio of mean inelastic displacement ratios to their average for Magnitude 6.75 Earthquakes, Average Distance to source 39 km and R_y =2,4

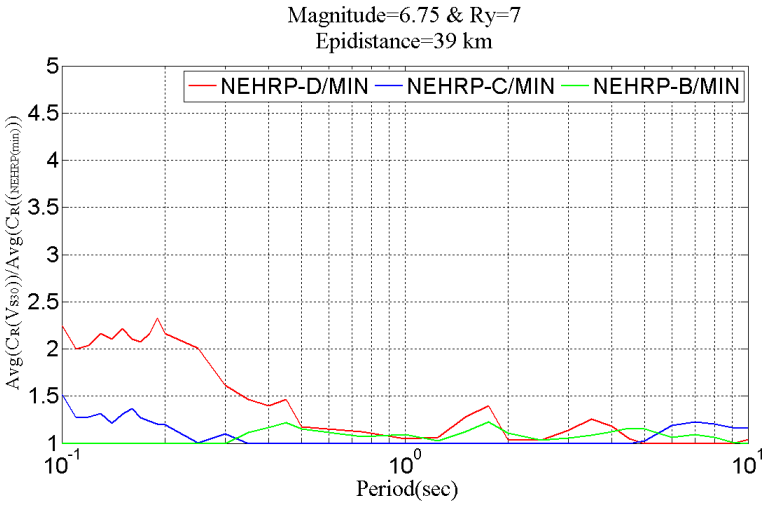

Figure 3.6. Effect of soil condition(NEHRP site classes B,C,D) on ratio of mean inelastic displacement ratios to their average for Magnitude 6.75 Earthquakes, Average Distance to source 39 km and R_y=7

To control the above findings, another detailed assemble containing NEHRP-C (3 groups), D (2 groups) soil types, for R_y=4, Magnitude 7.6 Earthquake and distance to source 43 km. It is expected that as soil shear wave velocity increases, inelastic displacement ratio decreases (linear relation). But in contrary to the expectation, soil wave velocity versus inelastic displacement ratio are showing sinusoidal trend in the constant acceleration region (Figure 3.7).

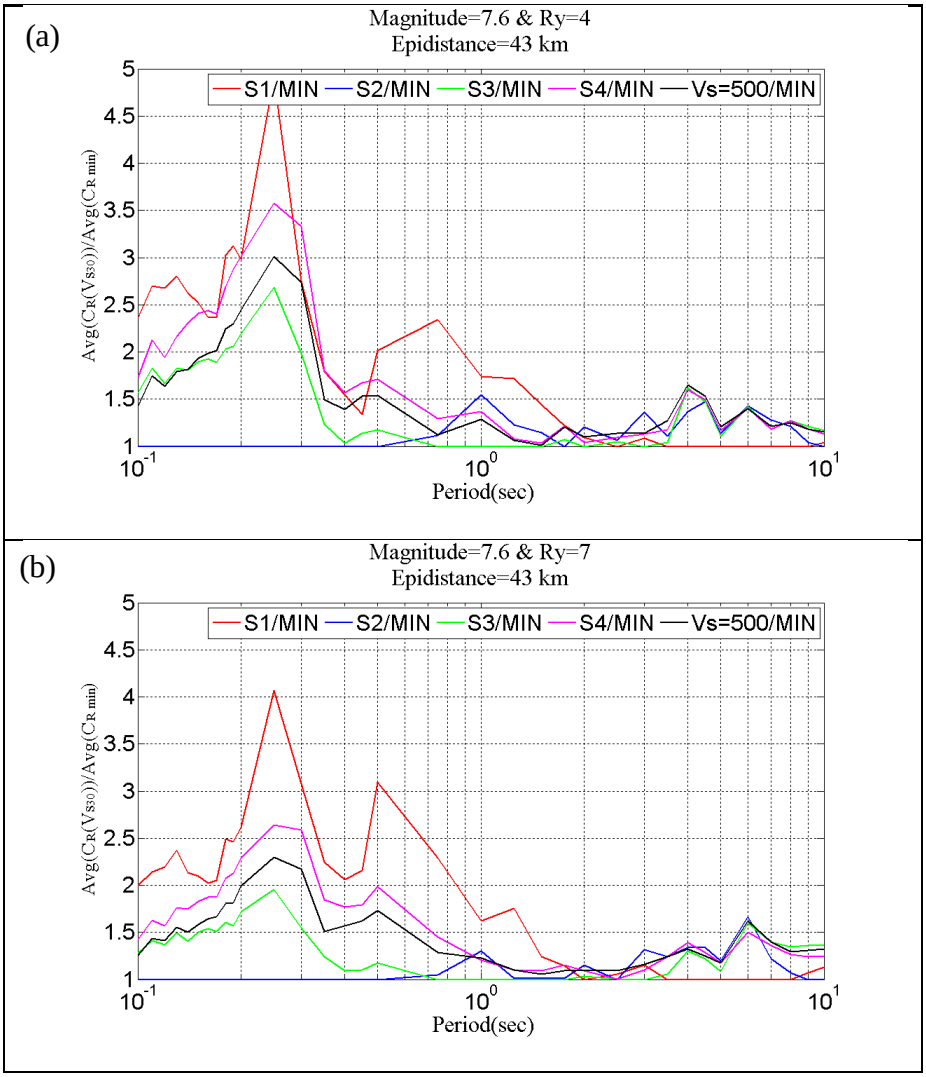

Figure 3.7. Effect of soil conditions on ratio of mean inelastic displacement ratios to minimum of all for every sampled period for Magnitude 7.6 Earthquakes, Average Distance to source 43 km and R_y =2,7

This trend can be seen well in Figure 3.8. Inelastic displacement ratio is highest in structures built on soil with average shear wave velocity 222 m/sec while with 273 m/sec takes lowest value and they are both in NEHRP-D type soil in the constant acceleration region. This is crucially important that just using NEHRP-B, C, D may lead to contradictory results in researches.

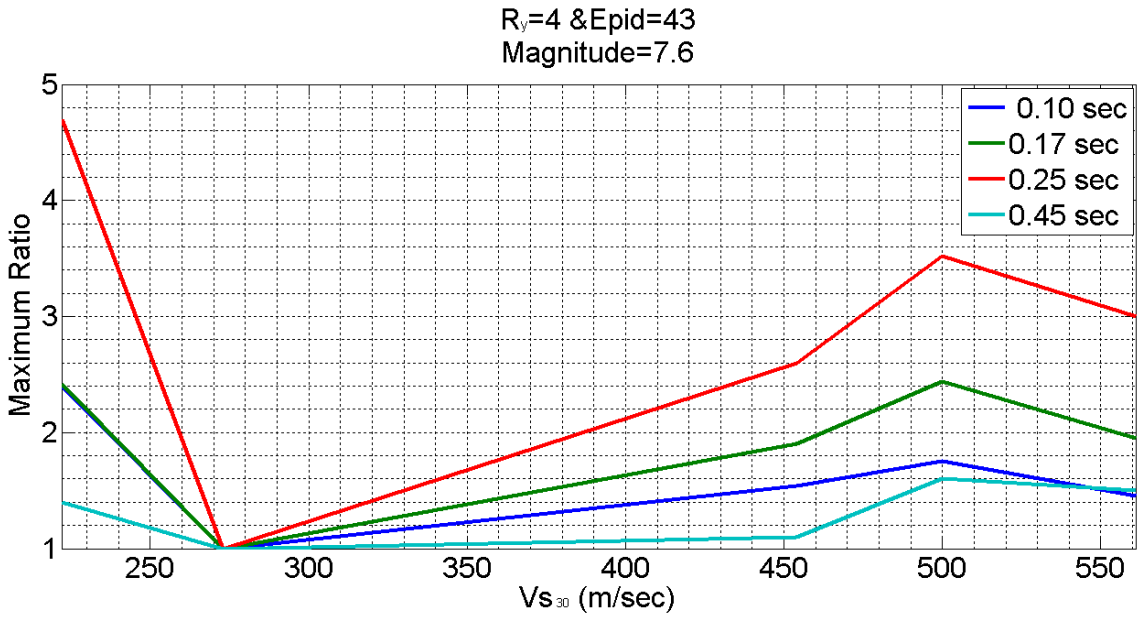

Figure 3.8. Effect of soil conditions on the maximum ratio distributed over soil shear wave velocity range for constant acceleration region, different level of periods and R_y=4

3.2. Effect of Magnitude

To investigate the effect of magnitude to inelastic displacement ratio, Chichi-1, 2, 3 earthquakes are considered. Main stack and control stack is differed by distance-to-source parameter. Groups with average 43 km and 102 km distance-to-source and 500 m/sec average soil shear wave velocity are analyzed.

Effect of earthquake magnitude is distinctive. As magnitude increases the inelastic displacement ratios also increases in constant velocity and acceleration regions.

For Magnitude 5.9 Earthquake the trend of R_y=2, 4, 7 intersecting at 0.75 seconds, and for Magnitude 6.2 Earthquake they are intersecting at 1.25 seconds and for Magnitude 7.6 Earthquake they are crossing each other at 5 seconds. After these periods, their mean inelastic displacement ratio does not exceed 1.1 till 10 seconds (maximum period of vibration analyzed in this study). It can be said that equal displacement rule is valid. Point

of intersections of R_y is given according to distance to source values of 43 and 102 km and mean is given in Table 3.1.

Table 3.1. Point of intersections of all R_y levels

	M=5.9	**M=6.2**	**M=7.9**
For EpiD=43 & $\overline{C}_R = 1$	0.75	1.25	5
For EpiD=102 & $\overline{C}_R = 1$	0.75	1.25	5

In preparation of Table 3.1, some approximations are used. Due to sinusoidal trend of inelastic displacement ratios 10% difference is neglected (see Figure 3.9 and Figure 3.10). As it can be seen, the point of intersection of all levels of R_y may be related with the period, T_B separating constant acceleration region with constant velocity region ($0.3 < T_B < 0.9$ seconds for TEC (2007)) for magnitude 5.9 earthquake, but cannot be related for higher magnitude earthquakes like 6.2 or 7.6.

It is expected that R_y, acts as a modification factor for inelastic displacement ratios. Actually R_y acts as a power factor. For $R_y = 2$ when the inelastic displacement ratio is greater than 1, it is greater for $R_y = 7$. When inelastic displacement ratio is less than 1 for $R_y = 2$, it is lower for $R_y = 7$. (Figure 3.10) If it was a modification factor for any period of time and any values of $R_y = 2$, $R_y = 7$ should be always greater.

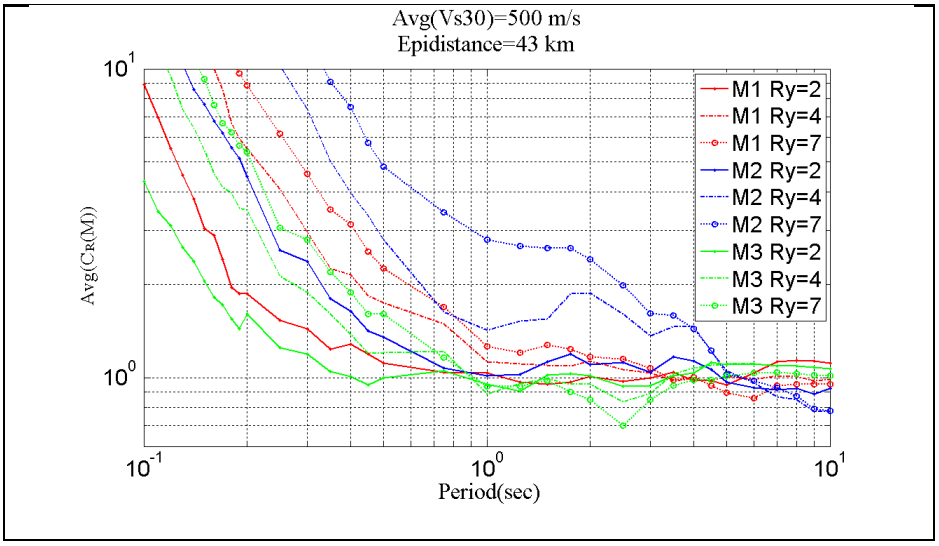

Figure 3.9. Effect of earthquake magnitude on mean inelastic displacement ratios for distance to source 43 km, average *Vs*30 500 m/sec and R_y =2,4,7

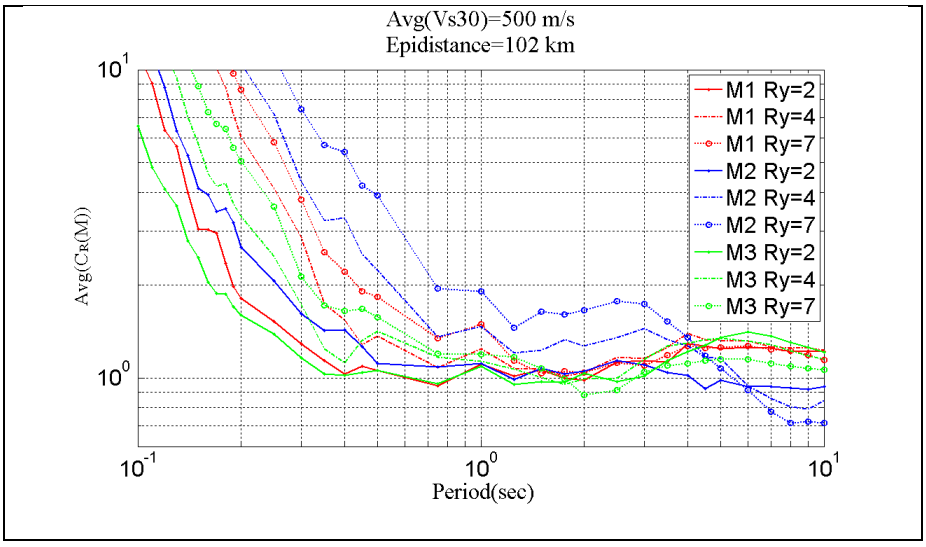

Figure 3.10. Effect of earthquake magnitude on mean inelastic displacement ratios for distance to source 102 km, Average *Vs*30 500 m/sec and R_y =2,4,7

As far as maximum ratio, M_R, is concerned, For R_y =7, it varies around 5.5 between 0.1 to 0.25 seconds and between 0.25-0.5 seconds it starts to fall from 5.5 to 3 and stays at 3 between 0.5 and 2.5 seconds, and it again starts to decrease to 1.2 between 2.5 to 5 seconds and afterwards stay at that value. The control stack (same properties except

distance to source is 102 km) shows almost same trend with exactly half values with same period ranges except last portion.

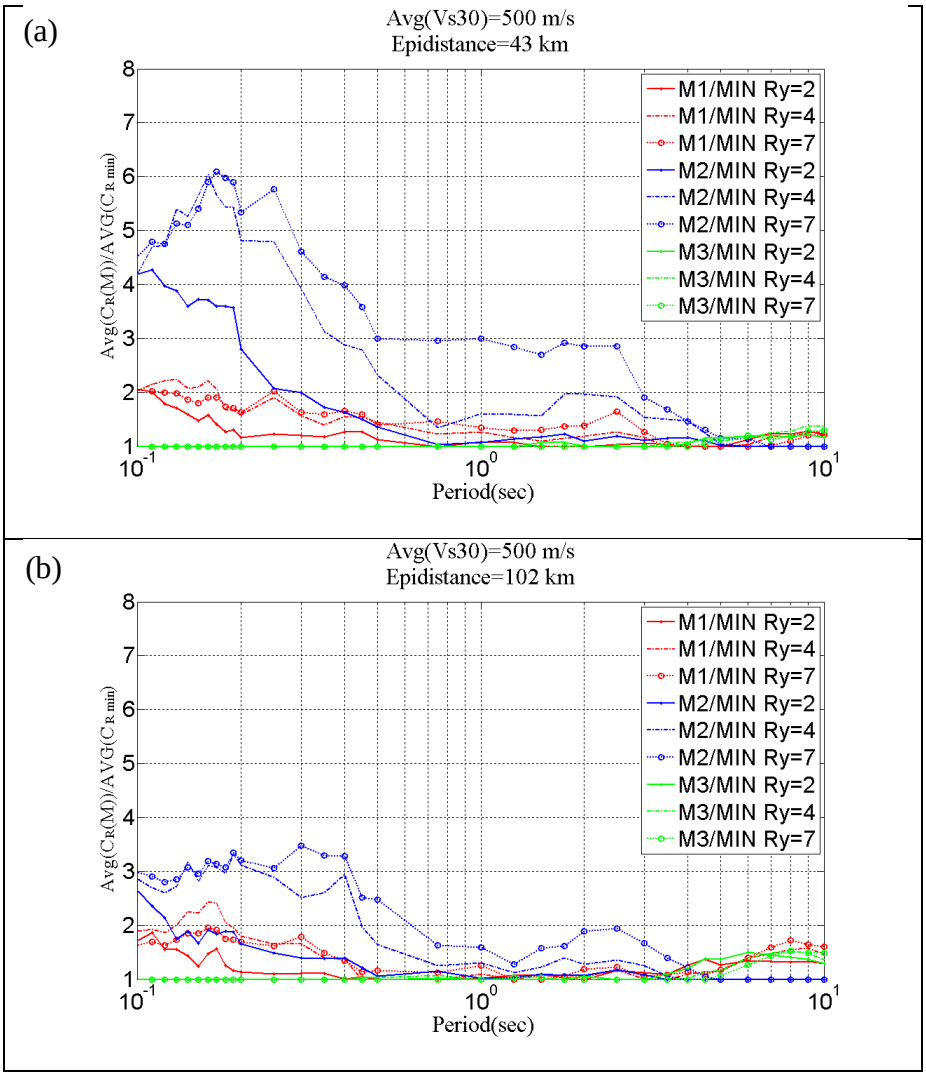

Figure 3.11. Effect of earthquake magnitude on maximum ratio, maximum of mean inelastic displacement ratios over their minimum for distance to source (a) 43, (b) 102 km, Average Vs_{30} =500 m/sec and R_y =2,4,7

Relation for earthquake magnitude going to be used in the proposed equation as follows:

$$M_{R,M} = 1 + \frac{5*(R_y - 1)(M - 5.9)}{T_N^{0.85}} \tag{3.2}$$

where; T_N denotes natural vibration of building, M denotes earthquake magnitude magnitudes in Richter, R_y denotes yield strength reduction factor.

3.3. Effect of Distance-to-Source on Inelastic Displacement Ratios

In order to investigate the effect of distance between recording site and epicenter of earthquake on inelastic displacement ratios, records were grouped into six in main stack and five for control stack. Station between 10 to 130 kilometers from epicenter with 20 kilometer intervals, with almost same average distance-to-source values with control stack is investigated. Groups are labeled with the abbreviations representing distance-to-source, site conditions and earthquake magnitudes. Magnitude in main stack is 6.2 while in control stack it is7.6 Richter. Average soil shear wave velocity is 500m/sec for all groups analyzed.

For main stack, inelastic displacement ratios are affected by almost equally for each distance to source in constant velocity and displacement regions. In constant acceleration region, structures with highest distance from source (D6=124km) have highest mean inelastic displacement ratio while the structures with lowest distance from source (D1=23km) have lowest inelastic displacement ratios. However for in between these two distances, mean inelastic displacement ratios showing random behavior. For example, for D4 (79 km), mean inelastic displacement is lower than for D2 (43km), and higher than for D3 (60 km). Through the period range, distance-to-source shows sinusoidal type of behavior with different phases.

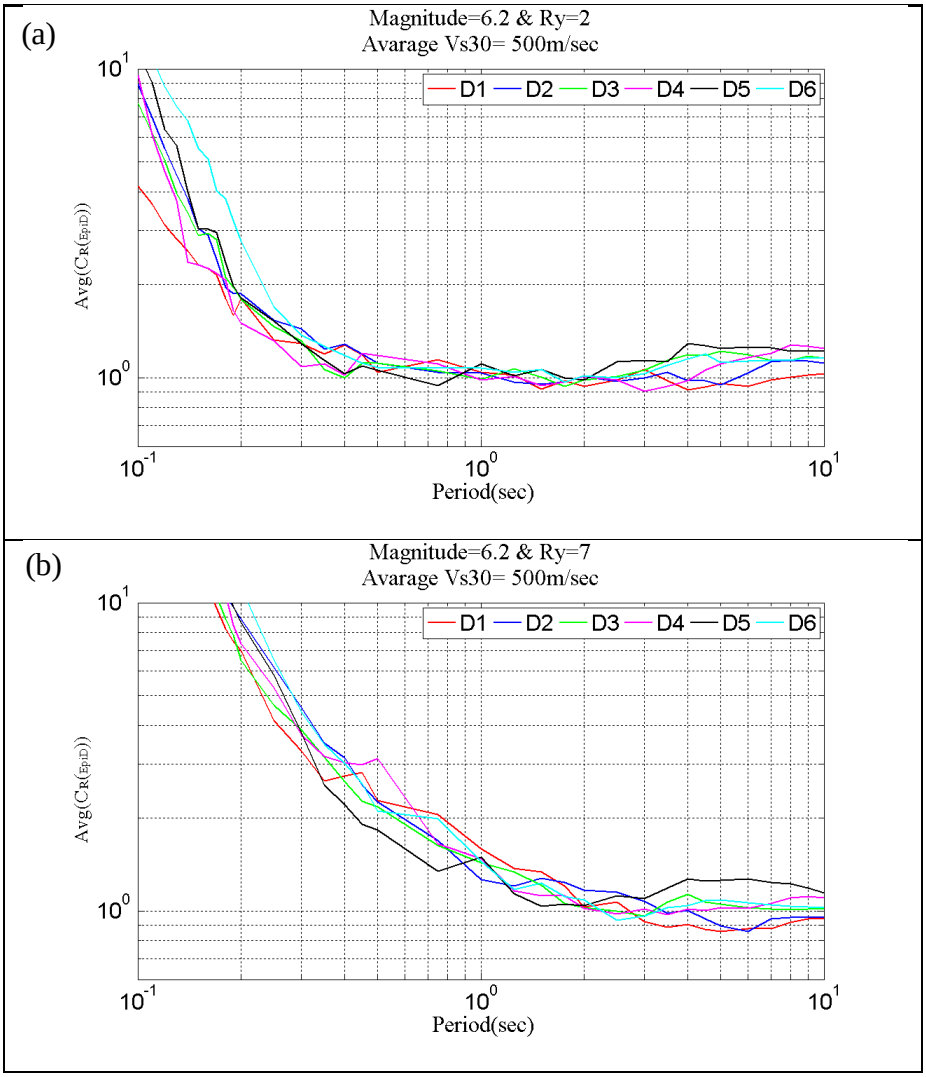

Figure 3.12. Effect of distance to source on mean inelastic displacement ratios for magnitude 6.2 earthquakes, average $Vs30$ =500 m/sec and R_y =2, 7

For magnitude 7.6 earthquake and NEHRP-C type soil with 500 m/sec average soil shear wave velocity (control stacks), D2 (43 km) has apparently the highest mean inelastic displacement ratio between periods 0.1 to 0.7, D4 (79 km) has the lowest value.

Comparing control and main groups intuitively leads to point that as magnitude increases, the distance to source which has the highest inelastic displacement ratio decreases.

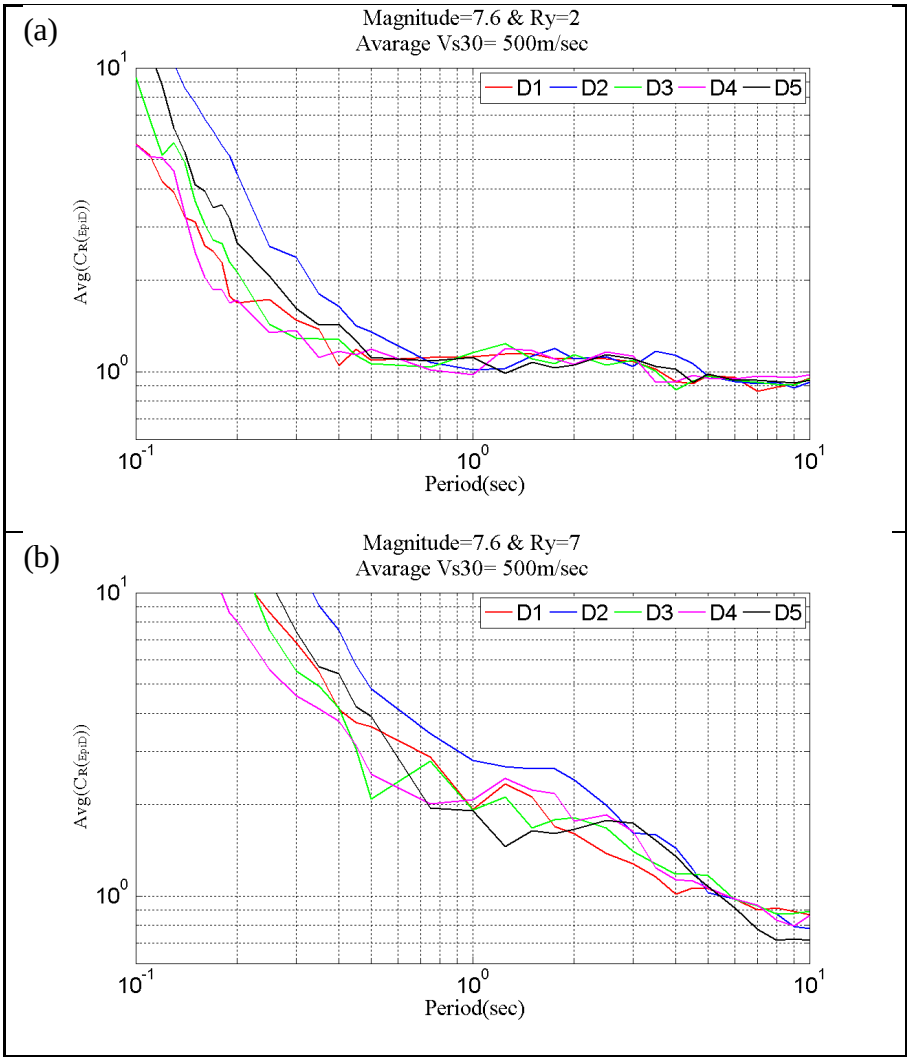

Figure 3.13. Effect of distance to source on mean inelastic displacement ratios for magnitude 7.6 earthquake, average Vs_{30} 500 m/sec and R_y =2, 7

As far as maximum ratio is concerned, for main stacks as R_y increases, maximum ratio decreases in constant acceleration region from 3.25 to 1.5 for period of vibration 0.1 seconds. For the constant velocity and displacement regions, as R_y increases, maximum ratio also increases. For R_y =4, peaks of almost all mean inelastic displacement ratios for different distance to source coincides and for R_y =7 peaks do not coincide anymore. This shows the yield strength reduction factor also act as phase shifter in the consideration of mean inelastic displacement ratios have sinusoidal trends (Figure 3.14).

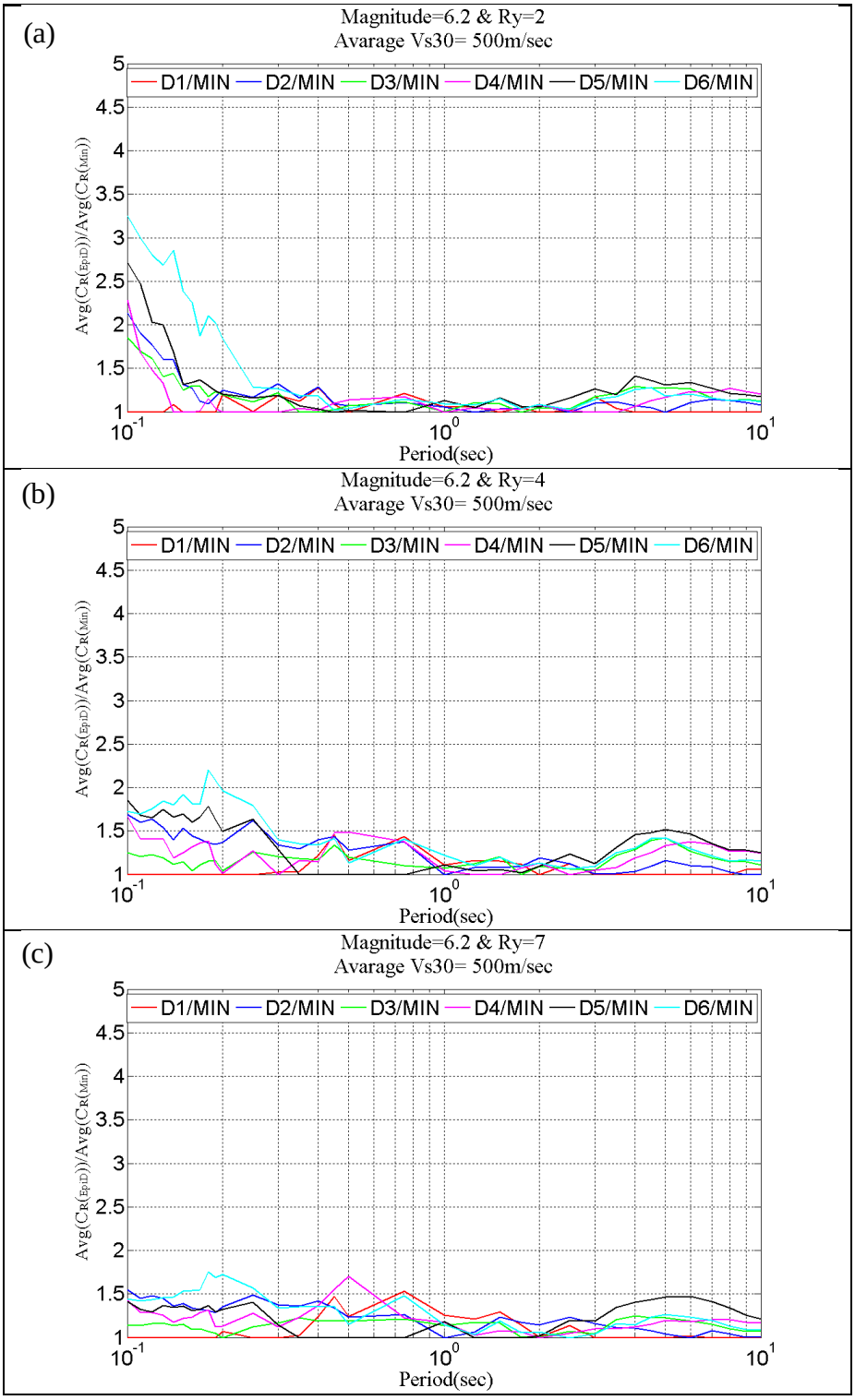

Figure 3.14. Effect of distance to source on maximum ratio for Magnitude 6.2 Earthquakes, Average $Vs30$ 500 m/sec and R_y =2, 4, 7

As far as the control stack is concerned, (Figure 3.15) For R_y=2, maximum ratio is approximately equal to 3 between 0.1 and 0.2 seconds, starts to decrease and from 3 to 1.25 between 0.2 and 0.45 seconds. Afterwards it stays at 1.25.

Same trend can be seen for R_y=4, between 0.1 and 0.25 seconds maximum ratio roughly equal to 3.4, between 0.25 to 0.7 seconds it decreases from 3.4 to 1.5, between 0.7 and 4 seconds it stays at 1.5 and between 5 and 10 seconds it is approximately 1.25.

For R_y=7, between 0.1 and 0.2 seconds maximum ratio is changing around 3.3, between 0.2 to 1 seconds decreases from 3.3 to 1.5, between 1 and 10 it also decreases from 1.5 to 1.25.

To sum up, effect of distance-to-source parameter is increasing with magnitude. For magnitude 6.2 earthquake, for large values of R_y, effect of distance-to-source on inelastic displacement ratios is negligible. But for magnitude 7.6 earthquake, distance-to-source parameter effect should be considered as important. However, for a design formulation, forces dependent on distance to source seems irrelevant, because the earthquake occurrence location on the fault cannot be predicted with confidence. Therefore, mutual effect of magnitude and distance-to-source effect should be considered, and maximum of two effects should be investigated.

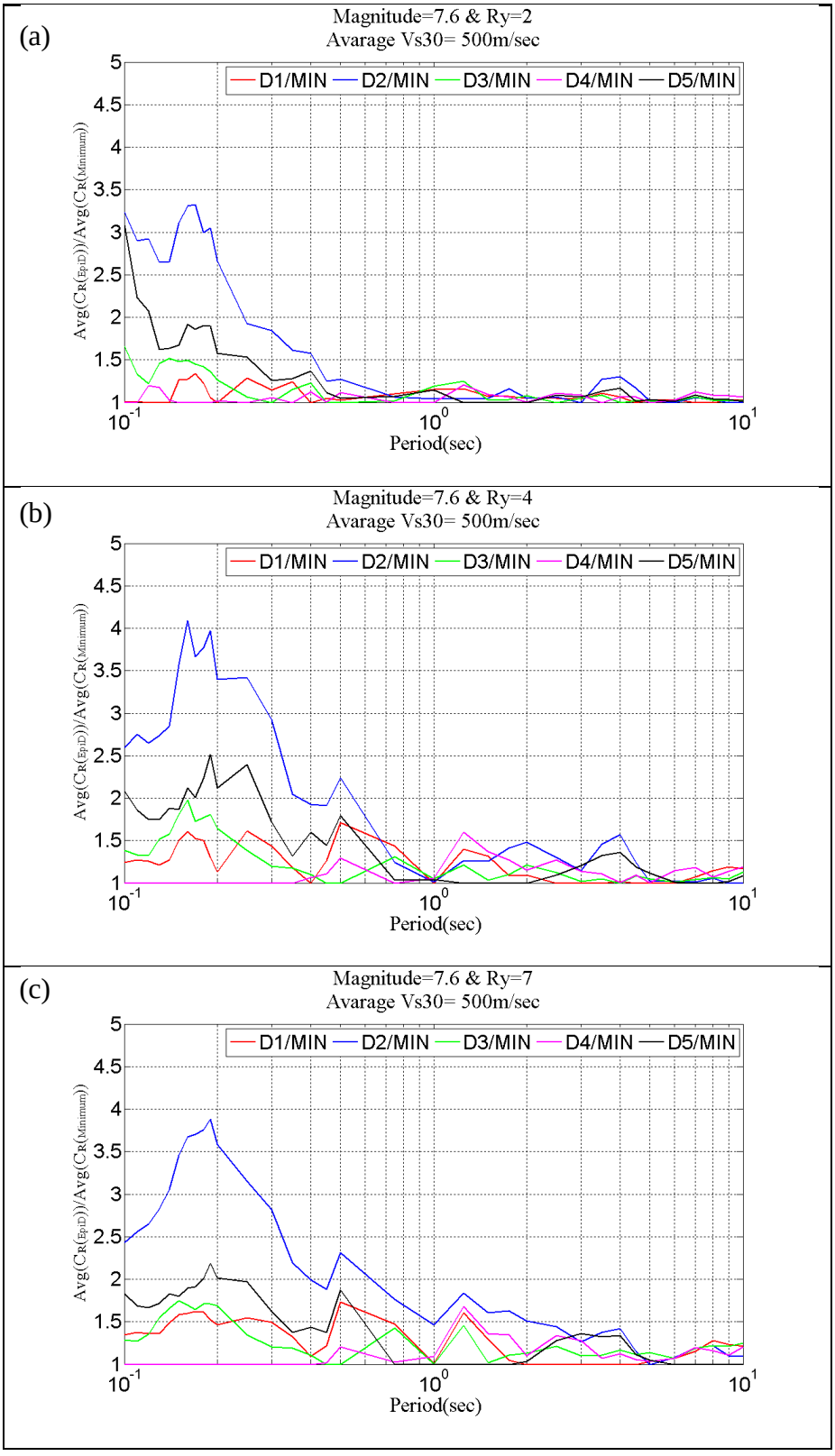

Figure 3.15. Effect of distance to source on maximum ratio for Magnitude 7.6 Earthquakes, Average $Vs30$ 500 m/sec and R_y =2, 4, 7

3.4. Effect Post Yield Stiffness

Using 7079 records (all horizontal ground acceleration components in Pacific Earthquake Engineering Research Center: NGA Database) to detect effect of post-yield stiffness on inelastic displacement ratios 8 different levels of post-yield stiffness which are 0, 3, 5, 10 is analyzed.

Increase in post-yield stiffness leads to decrease in inelastic displacement ratio. It is a phenomenon that no sinusoidal trend can be seen. All levels of post-yield stiffness do not intersect or cross each other.

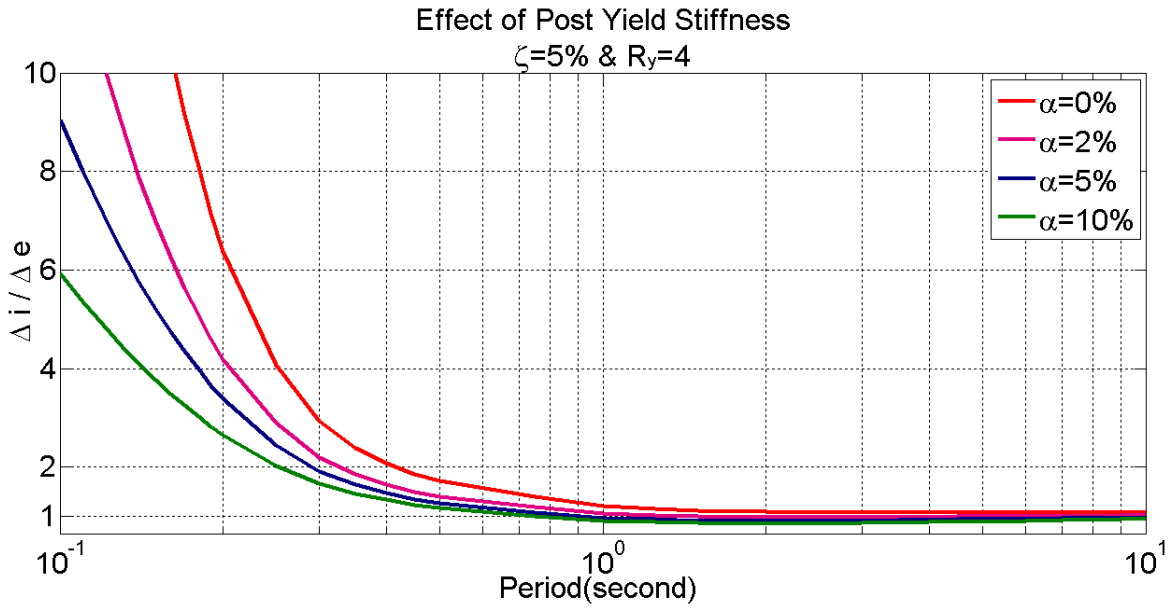

Figure 3.16. Effect of stiffness on inelastic displacement ratio for R_y=4 (for 7079 records)

Trend of maximum ratio (for this group, mean inelastic displacement ratio over mean inelastic displacement ratio of 10 per cent post-yield stiffness) can be approximated into 3 regions, between 0.1 and 0.2 seconds maximum ratio higher than 1.5, between 0.2 and 1.75 seconds maximum ratio dropping slowly and reaching 1.1, after 1.75 seconds maximum ratio is unity.

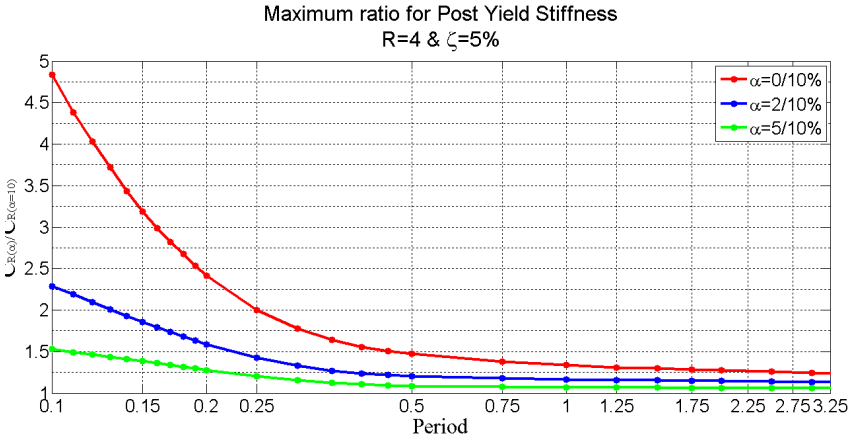

Figure 3.17. Maximum ratio for post-yield stiffness with ζ =5% and R_y =4

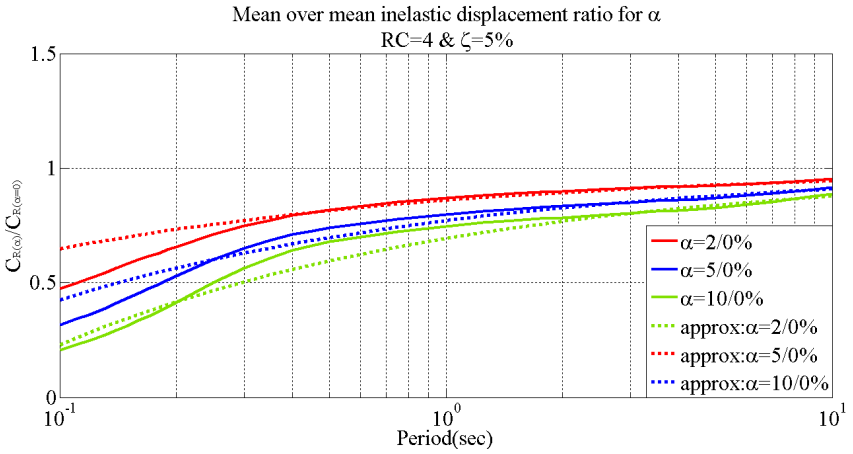

Figure 3.18. Ratio of mean inelastic displacement ratios for α =2, 5, 10 per cent over α =0 per cent for Ry =4 and ζ =5 per cent

Formulation for maximum ratio for post-yield stiffness is as follows:

$$M_{R,\alpha} = 1 - \frac{log_{10}(\sqrt{1+\alpha})}{1.7 * T_N^{\,0.4}} \tag{3.3}$$

where; α denotes post-yield stiffness in per cent and greater than one, T_N denotes natural period of the system. This factor is used to convert elasto-plastic systems to bilinear systems for period of vibration greater than 0.1 seconds.

3.5. Effects of Critical Damping Ratio

For 3 per cent post-yield stiffness, 5 different levels of critical damping ratio are analyzed. No control group for critical damping ratio is considered.

According to FEMA 356 document article 1.6.1.5.3 (Damping Ratios), "a 5% damped response spectrum shall be used for the rehabilitation design of all buildings and structural systems except structures without exterior cladding and structures with wood diaphragms and interior partitions and cross walls that interconnect the diaphragm levels at a maximum spacing of 40 feet on center transverse to the direction of motion and structures rehabilitated using seismic isolation technology or enhanced energy dissipation technology."

Even though recommended critical viscous damping is set to five per cent for almost all buildings, here the effects of various damping ratios on the inelastic displacement ratio are also investigated to clarify the role of damping. Other parameters such as post-yield stiffness and distance from rapture and for every parameter effect of strength reduction factor will be investigated.

As it can be seen in Figure 3.19, as critical damping increases inelastic displacement trend converges to shape of negative slope straight line in logarithmic versus logarithmic plot. Between 0.01 and 0.02 the order of inelastic displacement ratios higher to lower is 0, 2, 5, 10 and 20. After 0.2 seconds the order is exactly reverse. In between the two ranges, trend of inelastic displacement ratio is very sharp fall following a sinusoidal line for 0 per cent, other experience close trend with 0 per cent critical damping, mild drop following little downward slope line. After 2.25 seconds effect of critical damping can be neglected.

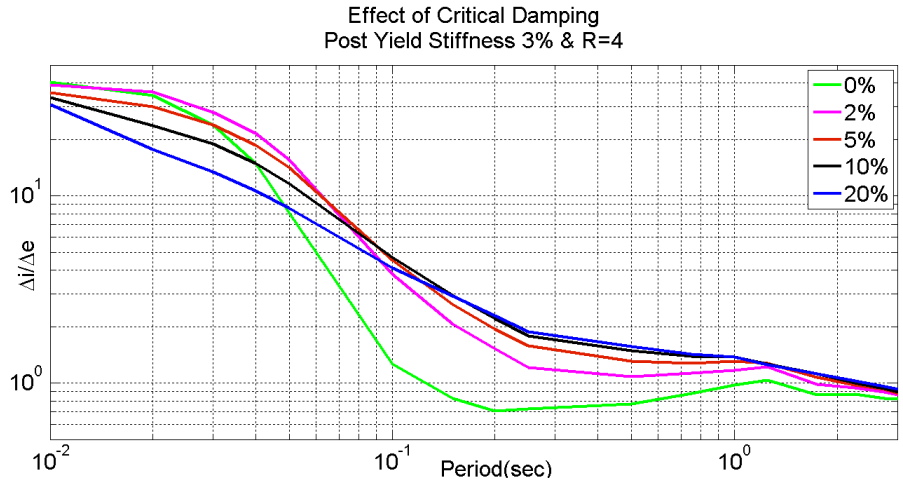

Figure 3.19. Effect of critical damping on inelastic displacement ratio (GMDS1) for R_y =4

Between 0.15 and 1.25 seconds, maximum ratio is dropping 3.5 to 1.25 with mild drop, afterwards it starts falling slowly and reaching 0.1 at 3.25 seconds. Because special interest in put on five per cent critical damping. Between 0.15 and 0.8 seconds ratio between mean inelastic displacement for 10 or 20 percent over 5 per cent critical damping ratio is in between 1.1 and 1.2. After 0.8 seconds, this ratio keeps below 1.1. Ratio between mean inelastic displacement ratios for 2 percent over 5 per cent critical damping is approximately 0.83 between 0.1 and 1.25 seconds. Afterwards this ratio starts to converge to 1. The ratio between mean inelastic displacement ratios for 2 per cent over 5 per cent critical damping is 0.3 at 0.1 seconds, 0.67 at 0.7, 1 at 3.25 seconds and it is increasing linearly.

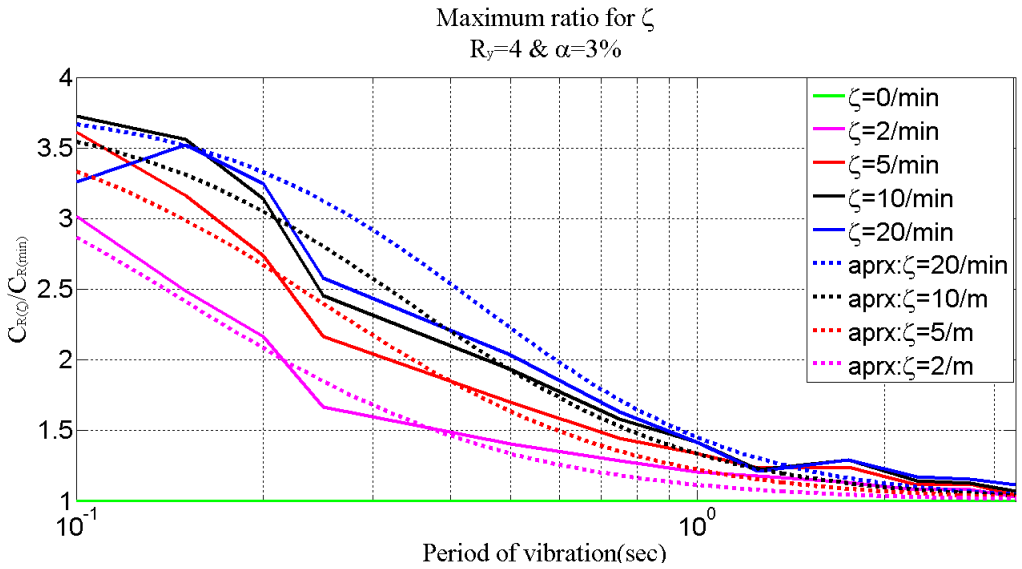

Figure 3.20. Maximum ratio for critical damping with α =3% and R_y =4

Approximate formulation of maximum ratios for critical damping ratio is defined as:

$$c = 1/\zeta$$
$$d = 1.5 + \sqrt{\zeta / 75} \qquad (3.4)$$
$$M_{R,\zeta} = 1 + 2.8*(1 + c*T_N{}^{d} *10^{d})^{-1}$$

where T_N denotes natural period, ζ denotes critical damping ratio, c and d denotes constants depend on ζ .

4. FORMULATIONS FOR INELASTIC DISPLACEMENT RATIOS

4.1. Formulations from Previous Studies

In order to estimate inelastic displacement demand from elastic displacement demands, many studies are done to estimate inelastic displacement ratios, some of them are given below:

Relation developed by Krawinkler and Nassar is as follows(1992):

$$C_R = \frac{1}{R_y}\left[1+\frac{1}{c}\left(R_y^c - 1\right)\right] \tag{4.1}$$

where; C_R denotes inelastic displacement ratios, R_y denotes yield strength reduction factor c denotes a constant which can be evaluated as

$$c = \frac{T_n^a}{1+T_n^a} + \frac{b}{T_n} \tag{4.2}$$

where; T_n period of vibration, a and b constants given in Table 4.1

Table 4.1. Post-yield stiffness dependent coefficients to be used in Krawinkler and Nassar(1992) equation.

Post Yield Stiffness	a	b
0 per cent	1	0.42
2 per cent	1	0.37
10 per cent	0.8	0.29

The relation is plotted with inelastic displacement ratio boundaries. As it can be seen in short period range, this relation underestimates the inelastic displacement ratios for large values of yield strength reduction factors.

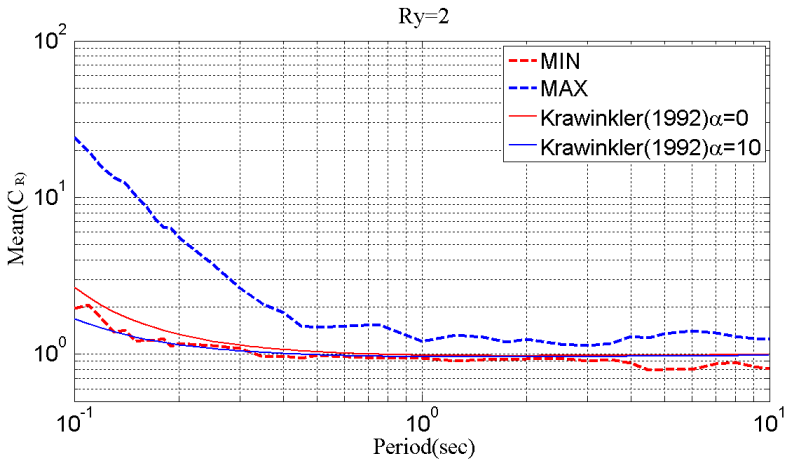

Figure 4.1. Krawinkler and Nassar's (1992) equation versus limiting mean inelastic displacement ratios derived from analysis for R_y=2

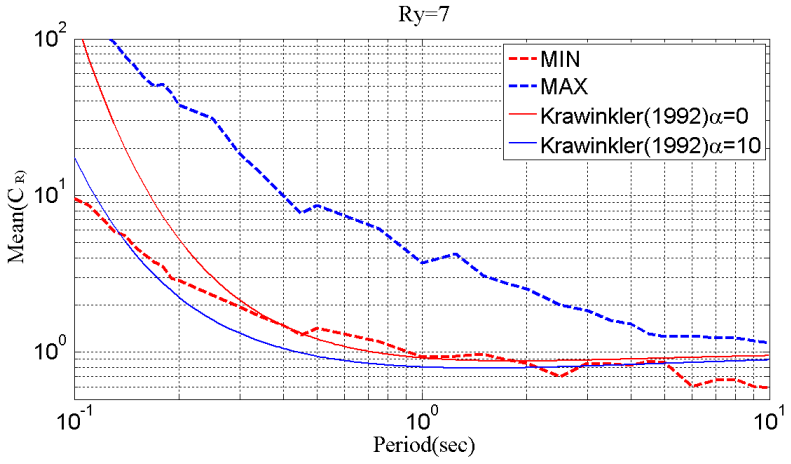

Figure 4.2. Krawinkler and Nassar's (1992) equation versus limiting mean inelastic displacement ratios derived from analysis for R_y=7

Another relation for constant relative strength inelastic displacement ratios is developed by García and Miranda (2003):

$$C_R = 1 + \left[\frac{1}{a\left(T / T_s\right)^b} + \frac{1}{c} \right] \left(R_y - 1 \right) \tag{4.3}$$

where; T_s denotes period separating constant acceleration and velocity regions, T denotes period of vibration R_y denotes yield strength reduction factors, a and b constants given in Table 4.2.

Table 4.2. Site Dependent coefficients to be used in García and Miranda (2003) equation.

Site Class	a	b	c	Ts(s)
NEHRP-B	42	1.6	45	0.75
NEHRP-C	48	1.8	50	0.85
NEHRP-D	57	1.85	60	1.05

The plot of the equation is as follows:

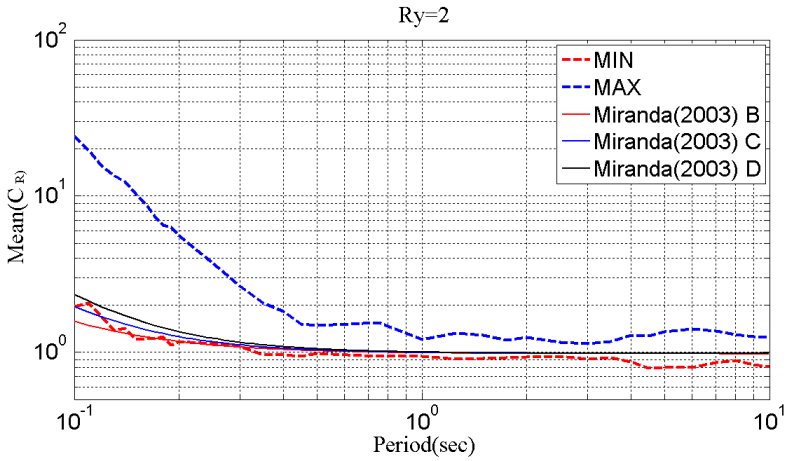

Figure 4.3. García and Miranda's (2003) equation versus limiting mean inelastic displacement ratios derived from analysis for R_y=2

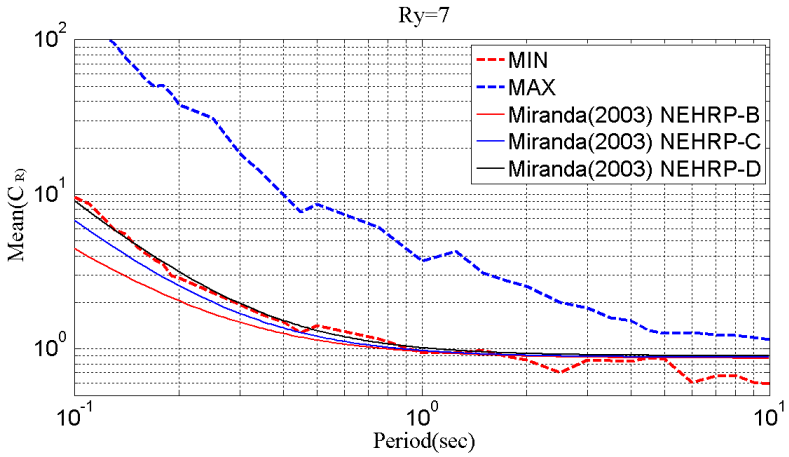

Figure 4.4. García and Miranda's (2003) equation versus limiting mean inelastic displacement ratios derived from analysis for R_y=7

Chopra and Chintanapakdee (2004) formulation is also investigated and compared with the inelastic displacement ratio boundaries, using period separating constant acceleration and velocity values of Turkish local site conditions.

$$C_R = 1 + \left[\left(L_R - 1 \right)^{-1} + \left(\frac{a}{R_y^b} + c \right) \left(\frac{T_n}{T_c} \right)^d \right]^{-1} \tag{4.4}$$

where; T_c denotes period separating constant acceleration and velocity regions T_n denotes natural period of vibration, L_R denotes constant relative strength inelastic displacement ratio limit which is infinity, a, b, c, d are given in Table 4.3.

Table 4.3. Coefficients used in Chopra and Chintanapakdee (2004) Equation.

Group	**a**	**b**	**c**	**d**	**Tc**
Large Magnitude Small Distance to source	63	2.30	1.70	2.30	0.43
Large Magnitude Large Distance to source	61	2.40	1.50	2.40	0.46
Small Magnitude Small Distance to source	61	2.40	1.50	2.40	0.41
Small Magnitude Large Distance to source	61	2.40	1.50	2.40	0.44
NEHRP B	61	2.40	1.50	2.40	0.32
NEHRP C	61	2.40	1.50	2.40	0.33
NEHRP D	61	2.40	1.50	2.40	0.40

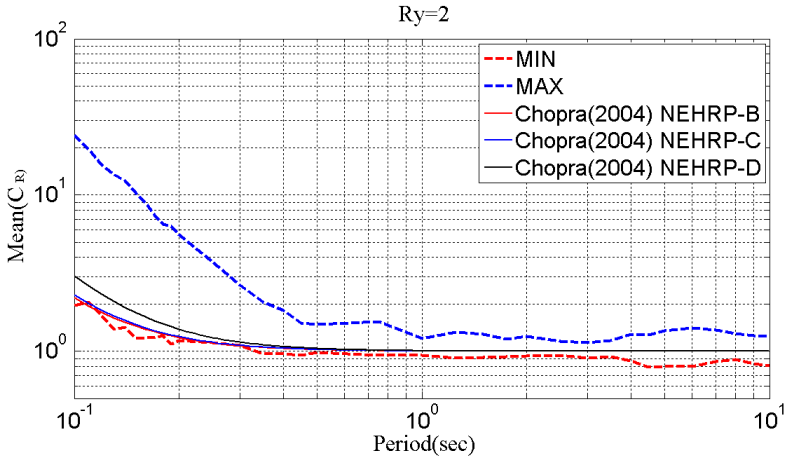

Figure 4.5. Chopra and Chintanapakdee (2004) equation versus limiting mean inelastic displacement ratios derived from analysis for R_y=2

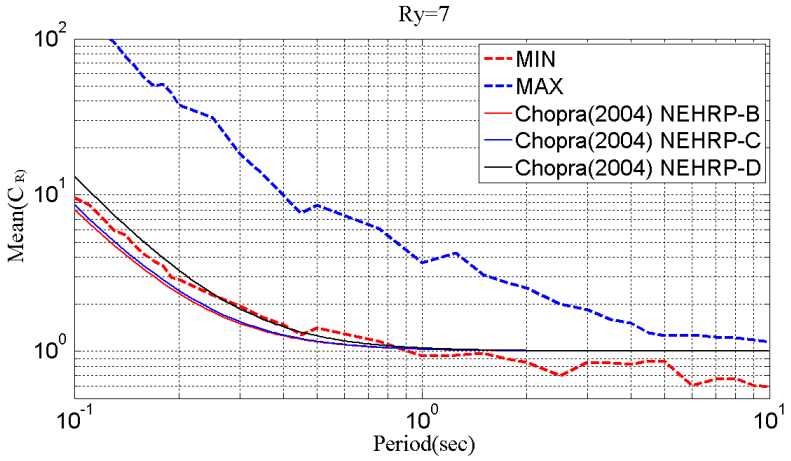

Figure 4.6. Chopra and Chintanapakdee (2004) equation versus limiting mean inelastic displacement ratios derived from analysis for R_y=7

Among the formulation given, the best match for mean inelastic displacement ratio boundaries, derived from analysis for every level of yield strength reduction factor and all regions, is Chopra and Chintanapakdee's (2004) formulation.

4.2. Turkish Earthquake Code Formulation

The formulation in the Turkish design code is investigated in this part and it is compared with the inelastic displacement ratio boundaries. Formulation in TEC annex 7c is as follows:

$$C_R = \frac{1+\left(R_y - 1\right)T_B / T_1}{R_y} \tag{4.5}$$

where; R_y denotes yield strength reduction factor T_B denotes period separating constant acceleration and velocity regions T denotes period of vibration.

Values for T_B are given Table 1.1

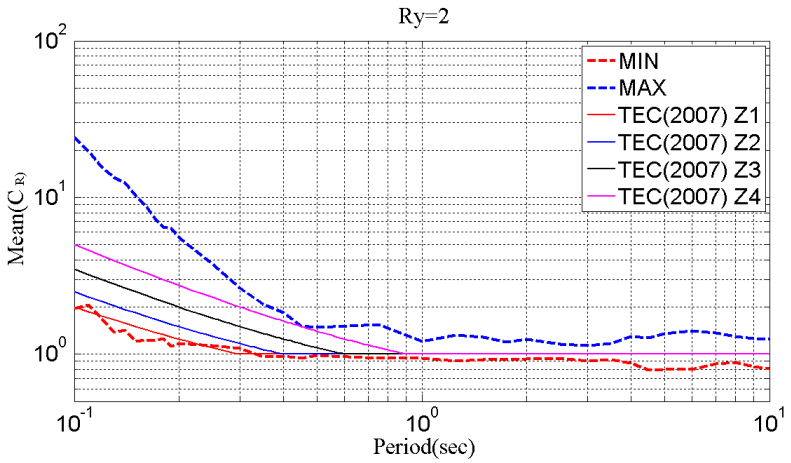

Figure 4.7. TEC (2007) equation versus limiting mean inelastic displacement ratios derived from analysis for R_y=2

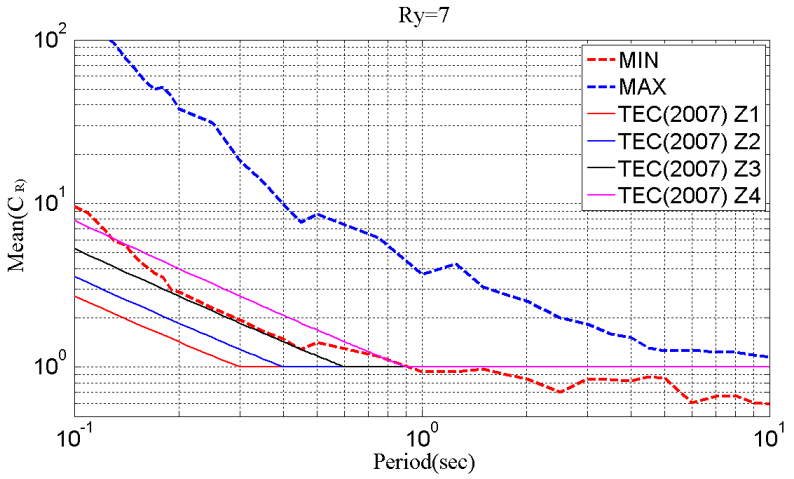

Figure 4.8. TEC (2007) equation versus limiting mean inelastic displacement ratios derived from analysis for R_y=7

TEC (2007) formulation is a good match for limiting mean inelastic displacement ratios derived from analysis for R_y=2. However, for higher R_y values such as 7, it underestimates the inelastic displacement ratio for periods lower than 1 second. Furthermore, for R_y=2 TEC formulation covers in between maximum and minimum boundaries, while other formulations trends follows minimum boundary. This shows TEC formulation overestimate the effect of soil conditions on inelastic displacement ratios.

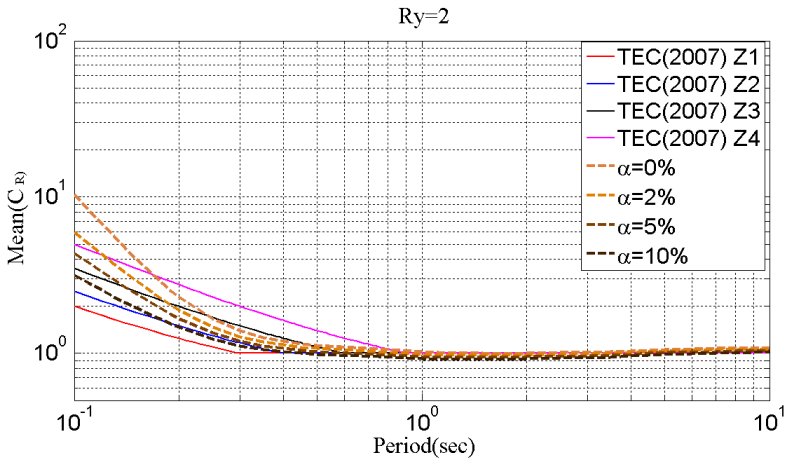

Figure 4.9. TEC (2007) equation versus mean of 7079 records for different post-yield stiffness values for R_y=2

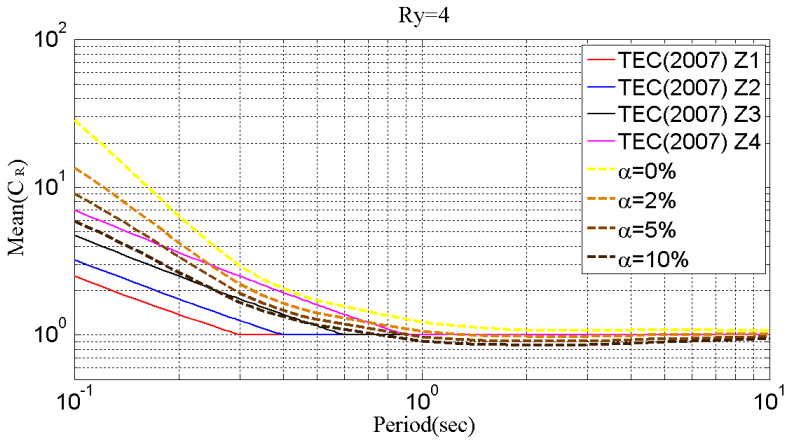

Figure 4.10. TEC (2007) equation versus mean of 7079 records for different post-yield stiffness values for R_y =4

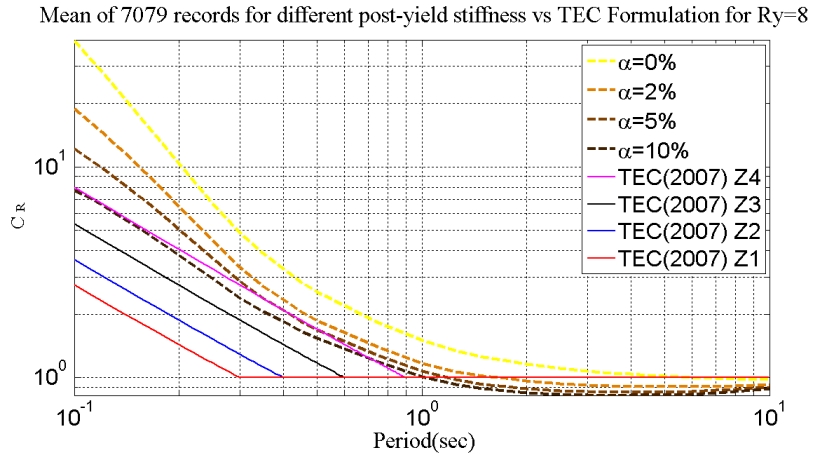

Figure 4.11. TEC (2007) equation versus mean of 7079 records for different post-yield stiffness values for R_y =8

For post-yield stiffness between 0 and 10, trend of mean inelastic displacement ratio of 7079 records lies in between inelastic displacement ratio trend for Z1 and Z4 type soil for R_y =2. For higher R_y values TEC formulation underestimates the inelastic displacement ratios according to this boundary.

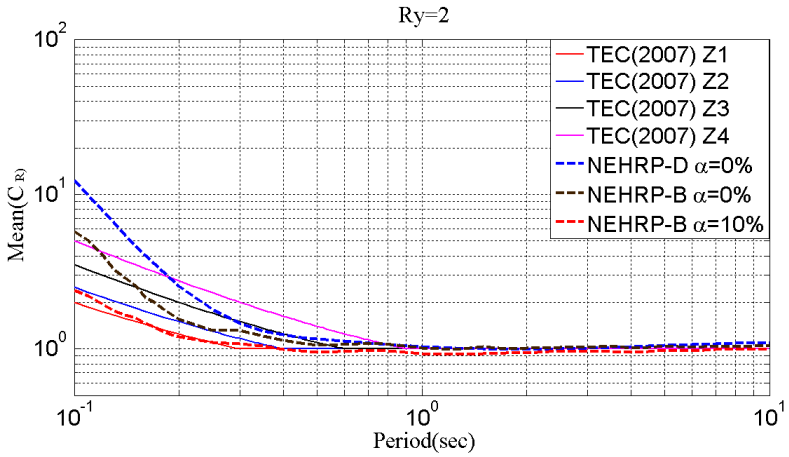

Figure 4.12. TEC (2007) equation versus mean of inelastic displacement ratio of NEHRP-D (3685 records) and NEHRP-B(160 records) soil for different post-yield stiffness values for R_y =2

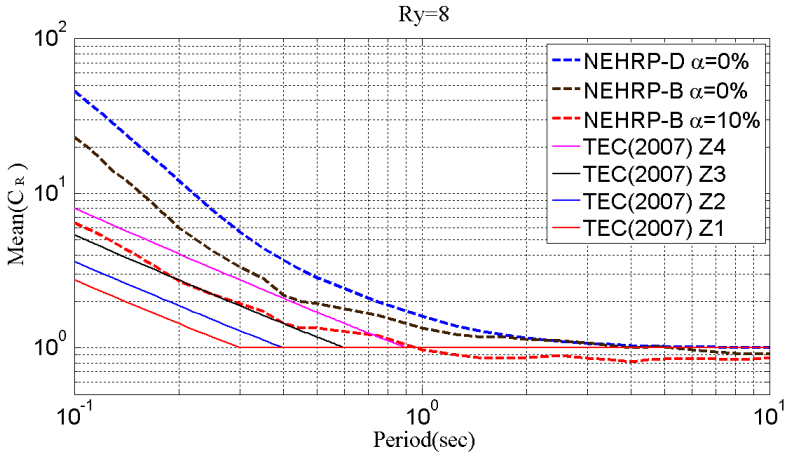

Figure 4.13. TEC (2007) equation versus mean of inelastic displacement ratio of NEHRP-D (3685 records) and NEHRP-B (160 records) soil for different post-yield stiffness values for R_y =8

For the last check, TEC (2007) formulation is compared with inelastic displacement ratio trend of NEHRP B(160 records)-D(3685 records) soils for different post-yield stiffness. As in the previous check, the TEC (2007) gives good results for the boundaries and for higher yield strength reduction factors it underestimates the displacements according to these boundaries.

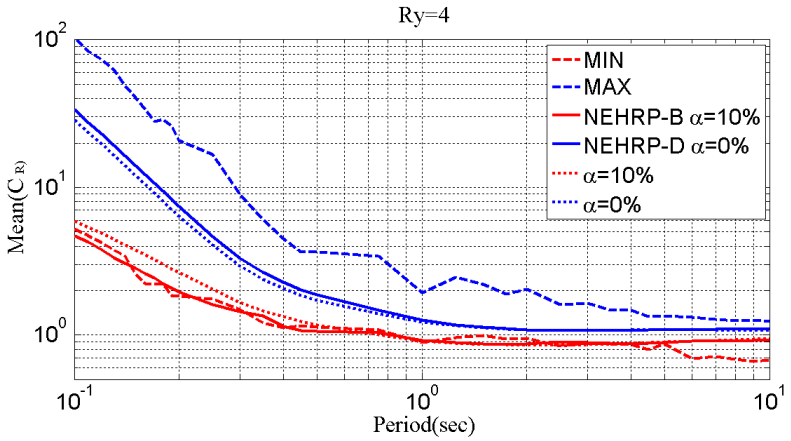

Figure 4.14. Boundary Comparison, group mean maximum and minimum, 7079 records average for post-yield stiffness 0 and 10 per cent, NEHRP-B and NEHRP-D type soils with systems 0 and 10 per cent post-yield stiffness

Figure 4.14 shows the boundaries used in the investigation of TEC (2007) formulation correctness. As it can be seen, minimums and maximum boundaries show very close trends.

4.3. Formulation Proposed

First, it is started with simple equation in curve relations. Curve fitting equations are used for all mean inelastic displacement ratios for all stacks (20), all periods (34) and all yield strength reduction factors (3). The aim is to derive a basis trend for inelastic displacement ratios according to minimum boundary of inelastic displacement ratio. The basis trend is function of period normalized by period separating constant acceleration and constant velocity regions, yield strength reduction factor as it is in former relations. After it is constructed appropriately, effect of magnitude, effect of post-yield stiffness and effect of damping coefficient will be added by multiplying the basis trend. Following equation is proposed as a result.

$$M_{R,M} = 1 + 5(R_y - 1)\left(\frac{M - 5.9}{T_N^{0.85}}\right)$$

$$C_R = \left(3.5 M_{R,M} \frac{T_B}{T_N}\right)^{\left(\frac{Ry^{0.22} - 1}{3 T_N^{0.7}}\right)} \quad (4.6)$$

where R_y denotes yield strength reduction factors, T_B period separating constant acceleration(values given in Table 1.1. and formulation only valid for these periods) and velocity regions, T_N denotes period of vibration, M denotes magnitude of earthquake, $M_{R,M}$ denotes maximum ratio for earthquake.

Following figures shows the match between inelastic displacement ratio boundaries with formulation proposed (Equation 4.6).

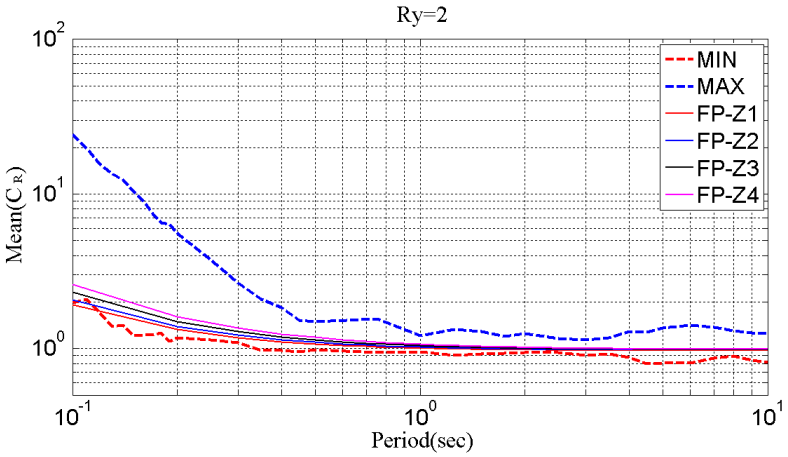

Figure 4.15. Comparison between Inelastic displacement boundaries and formulation proposed (FP) for R_y=2 for 5.9 Earthquake Magnitude

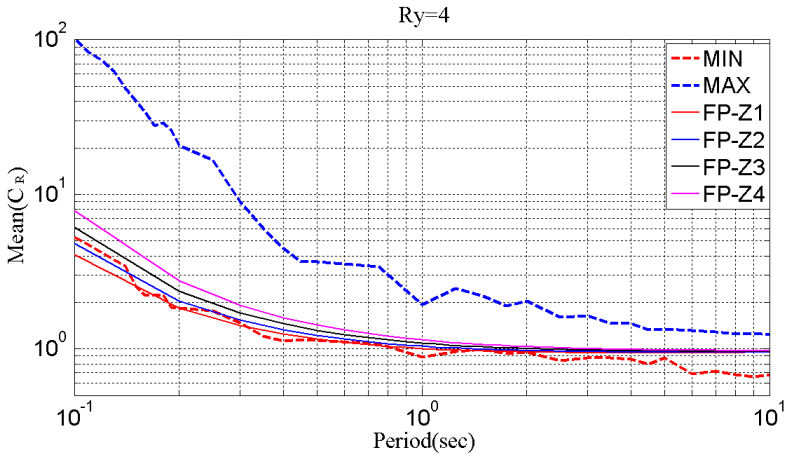

Figure 4.16. Comparison between Inelastic displacement boundaries and formulation proposed (FP) for R_y=4 for 5.9 Earthquake Magnitude

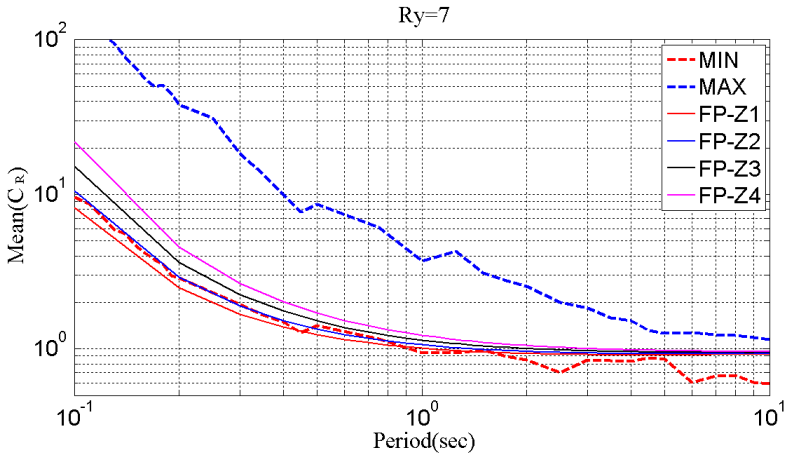

Figure 4.17. Comparison between Inelastic displacement boundaries and formulation proposed (FP) for R_y=7 for 5.9 Earthquake Magnitude

For Magnitude main stack, good match is attained.

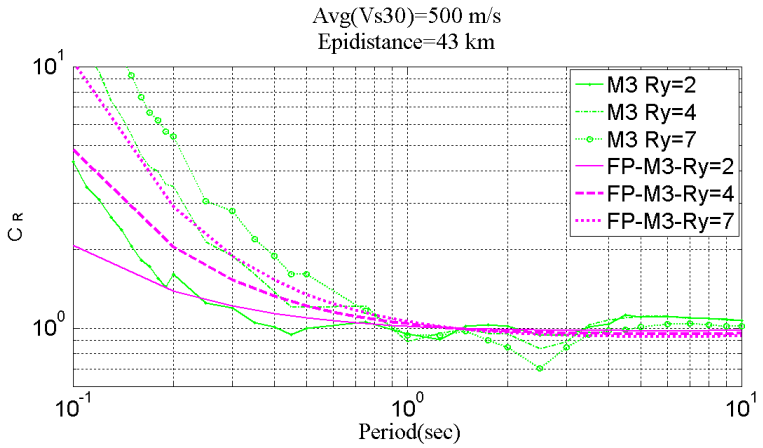

Figure 4.18. Comparison between Magnitude 5.9 earthquake main stack with formulation proposed (T_B =0.4)

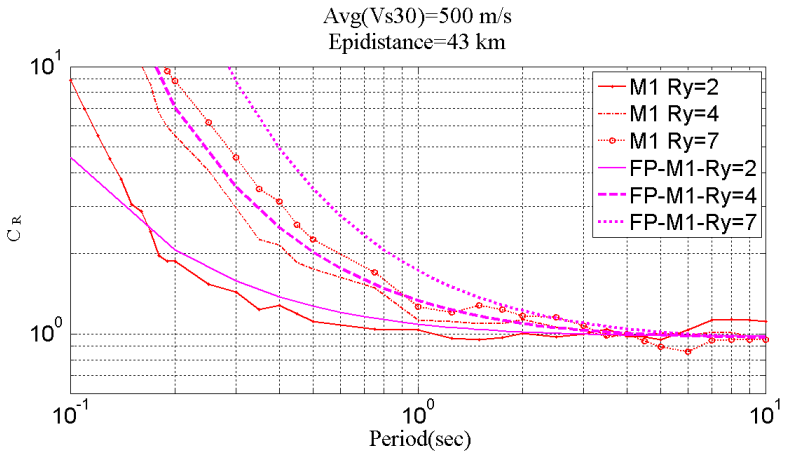

Figure 4.19. Comparison between magnitude 6.2 earthquake main stack with formulation proposed (T_B =0.4)

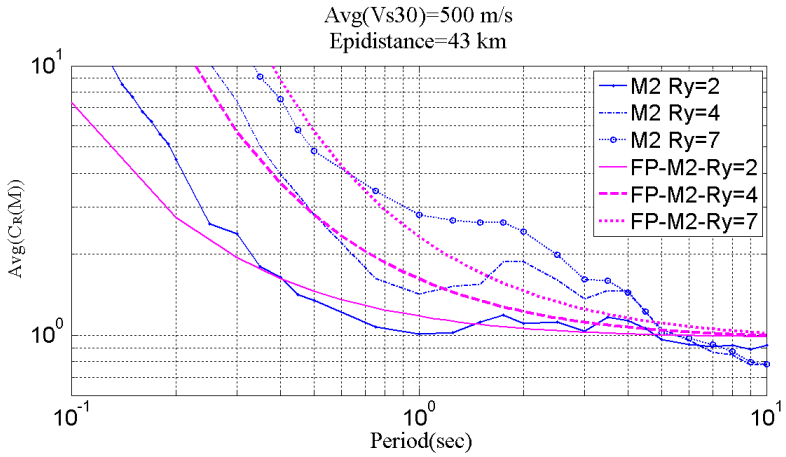

Figure 4.20. Comparison between magnitude 7.6 earthquake main stack with formulation proposed (T_B =0.4)

For soil main stack, good match is attained for inelastic displacement ratio for Chi-chi Earthquakes.

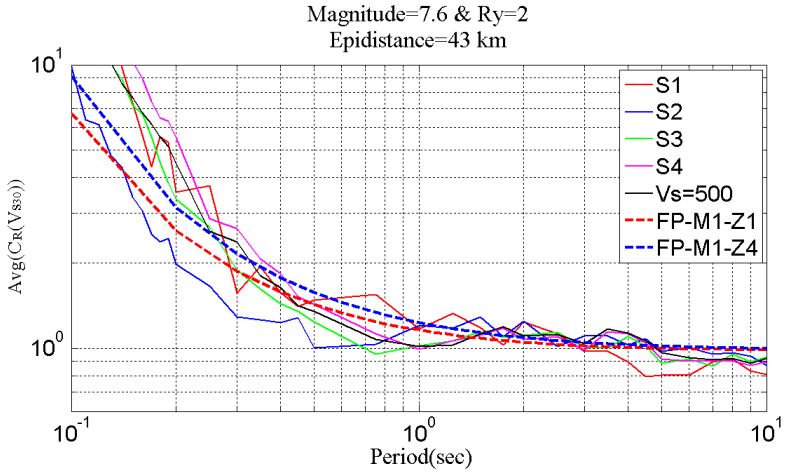

Figure 4.21. Comparison between magnitude 7.6 earthquake main stack with formulation proposed (R_y =2)

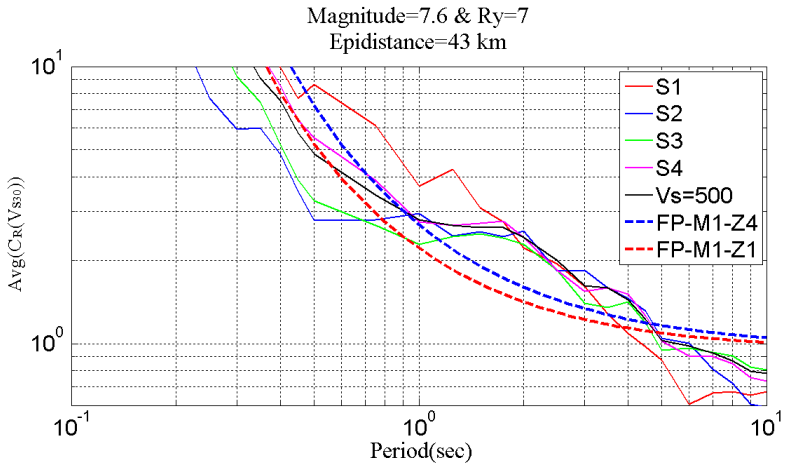

Figure 4.22. Comparison between magnitude 7.6 earthquake main stack with formulation proposed (R_y =7)

It should be noted that, maximum values for inelastic displacement ratio attained from distance to source values are used in the formulation proposed and the comparison is also made for these distance to source values. According to analysis expressed in this thesis, these distance to source values are assumed to give maximum inelastic displacement ratio for given magnitude and soil type.

5. CONCLUSIONS AND RECOMMENDATIONS

5.1. Conclusions Related with Inelastic Displacement Ratios

In this study, main aim was to control equation in the TEC (2007) Annex-7c, whether it is a good parameter to relate inelastic displacement demand with elastic displacement demand or not. In order to control it correctly, all parameters effecting inelastic and elastic displacement demand should be determined. Six parameters are assumed to affect the inelastic displacement ratio deciding from base shear formulation, attenuation relations and hysteresis models. To eliminate other parameter effects, all parameters except investigated parameter keep constant. Boundaries and their averages very sensitively selected. Used nonlinear dynamic procedures in the analysis, 34 different periods of vibration, 3 different levels of yield strength reduction factors and 555 earthquake records are analyzed. As a hysteresis model, bilinear force deformation relation is used. 7079 records are analyzed to detect the effect of post-yield stiffness on inelastic displacement ratios and correctness of TEC (2007) formulation.

As results of analysis following conclusions are drawn:

The relationship between inelastic displacement ratio boundaries and the formulations to calculate inelastic displacement ratio and TEC (2007) formulation are investigated. Chopra and Chintanapakdee (2004) formulation was the best match to inelastic displacement ratio boundaries among the previous formulations. On the other hand, it was seen that TEC (2007) formulation gives ideal results for yield strength reduction ratios as low as 2, but with the increase in the yield strength reduction ratio, the formulation results in underestimation of the inelastic displacement ratios. One of the reasons is yield strength reduction factors do not change the period where the equal displacement rule is valid and other mistake leads to such error is, periods greater than the period separating constant acceleration and velocity regions, inelastic displacement ratio is directly assumed as 1.

Effect of distance-to-source parameter is increasing with magnitude. For magnitude 6.2 earthquake, for large values of R_y, effect of distance-to-source on inelastic displacement ratios is negligible. But for magnitude 7.6 earthquake, distance-to-source parameter effect should be considered as important. However, for a design formulation, forces dependent on distance to source seems irrelevant, because the earthquake occurrence location on the fault cannot be predicted with confidence. Therefore, mutual effect of magnitude and distance-to-source effect should be considered, and maximum of two effects should be investigated.

As parallel to other studies, it is found that soil conditions have moderate effect on inelastic displacement ratio. Different from other studies, effect of soil shear wave velocity is investigated. Effect of soil shear wave velocity shows very distinctive differences inside a soil type. For example, effect of soil with 222m/sec shear wave velocity which is NEHRP-D type soil, is the maximum among all investigated soil shear wave velocities, and effect of soil with 273 m/sec shear wave velocity which is also NEHRP-D type soil, is the minimum. This finding lead in doubts about formulation proposed dependent on soil classes, and their findings related with soil conditions. How they know the investigated soil shear wave velocity, gives maximum inelastic displacement ratio.

On the most of the researches, earthquake magnitude effect was assumed as negligible or for higher yield strength reduction factor values it was assumed to have moderate effect. Because soil conditions and distance-to-source parameters are not investigated in detail, it may ended up with compensating effect of magnitude parameter. However in this research, individual effects of each parameters investigated in detail by keeping other parameters average values constant in predetermined limits. Effect of earthquake magnitude found to be highest among other parameters. Between the earthquake magnitudes of 5.9 and 7.6, it is found that there are differences up to 5 times in the inelastic displacement ratios.

Effects of critical damping, 20 per cent and 5 per cent, on inelastic displacement ratio is around 20%. While difference between 0% and 5% critical damping ratio, in short

periods up to 3.5 times were found. And for post yield stiffness (0-10) in short periods up to 2.5 times ratios were determined.

Lastly, a formulation was generated and it is a function of earthquake magnitude, soil conditions and yield strength reduction factors parameters. The previous formulations were compared with TEC (2007) formulation and inelastic displacement boundaries.

Lacking points in this study are: unable to reach Turkish soil classification values for the stations; detailed effects of Turkish soil classification on inelastic displacement ratio couldn't be analyzed. This led to use of period separating constant acceleration and velocity regions. Analysis should be done with more realistic models such as Bouc-Wen model, Modified Clough models. Degradation of material should be investigated also.

5.2. Other Conclusions

In this research, some thesis and published documents related with microzonation are investigated in order to find Turkish local site class of stations. Turkish researchers, who are surveying an area to define its approximate soil profile, prefer using NEHRP soil classification rather than TEC soil classification while calculation of both are possible and easy when the measured data are available. But after conversion of the data is made, there is no relation between them. The universities and government should encourage the use of Turkish soil classification.

Elastic design spectrum used in Turkish design and the other elastic design spectra is valid in the constant acceleration and velocity regions but not valid in constant displacement region. And because the constant displacement region changes according to soil type, its lower limit may drop as low as 1.3 seconds and this corresponds to approximately 13 storey level buildings. Because it starts to follow PGD line which is parallel to spectral accelerations in constant displacement region, elastic design spectra may not be valid in this region, and other methods should be used to determine force coefficients, or probably by overestimating force coefficient, the value corresponding to period separating the constant velocity and constant displacement should be used.

APPENDIX A: RELATED TABLES

Table A.1. Structural Behavior Factors (R_y)

BUILDING STRUCTURAL SYSTEM	Systems of Nominal Ductility Level	Systems of High Ductility Level
(1) CAST-IN-SITU REINFORCED CONCRETE BUILDINGS		
(1.1) Buildings in which seismic loads are fully resisted by frames	4	8
(1.2) Buildings in which seismic loads are fully resisted by coupled structural walls	4	7
(1.3) Buildings in which seismic loads are fully resisted by solid structural walls	4	6
(1.4) Buildings in which seismic loads are jointly resisted by frames and solid and/or coupled structural walls	4	7
(2) PREFABRICATED REINFORCED CONCRETE BUILDINGS		
(2.1) Buildings in which seismic loads are fully resisted by frames with connections capable of cyclic moment transfer	3	6
(2.2) Buildings in which seismic loads are fully resisted by single-storey hinged frames with fixed-in bases	-	5
(2.3) Buildings in which seismic loads are fully resisted by prefabricated solid structural walls	-	4
(2.4) Buildings in which seismic loads are jointly resisted by frames with connections capable of cyclic moment transfer and cast-in-situ solid and/or coupled structural walls	3	5
(3) STRUCTURAL STEEL BUILDINGS		
(3.1) Buildings in which seismic loads are fully resisted by frames	5	8
(3.2) Buildings in which seismic loads are fully resisted by single-storey hinged frames with fixed-in bases	4	6
(3.3) Buildings in which seismic loads are fully resisted by braced frames or cast-in-situ reinforced concrete structural walls		
(a) Concentrically braced frames	3	-
(b) Eccentrically braced frames	-	7
(c) Reinforced concrete structural walls	4	6
(3.4) Buildings in which seismic loads are jointly resisted by frames and braced frames or cast-in-situ reinforced concrete structural walls		
(a) Concentrically braced frames	4	-
(b) Eccentrically braced frames	-	8
(c) Reinforced concrete structural walls	4	7

Table A.2. List of ground motions in GMDS1 ensemble

#	EQ Name	YEAR	St. Name	M	EpiD (km)	Nerhp	PGA (g)	PGV (cm/sec)	PGD (cm)
1	Caldiran	1976	Maku	7.21	56	D	0.07	4.56	0.94
2	Dinar	1995	Burdur	6.4	40	D	0.04	4.65	1.15
3	Dinar	1995	Cardak	6.4	50	D	0.06	3.33	0.32
4	Dinar	1995	Denizli	6.4	95	D	0.02	2.92	1.27
5	Duzce	1999	Lamont 1058	7.14	13	C	0.09	12.64	11.57
6	Duzce	1999	Lamont 375	7.14	24	C	0.74	28.24	6.09
7	Duzce	1999	Lamont 1059	7.14	24	C	0.13	12.50	8.26
8	Duzce	1999	Lamont 531	7.14	28	C	0.14	11.93	8.13
9	Duzce	1999	Lamont 1062	7.14	29	D	0.21	13.70	9.43
10	Duzce	1999	Lamont 1061	7.14	32	C	0.12	12.85	8.10
11	Duzce	1999	Bolu	7.14	41	D	0.77	59.68	17.69
12	Duzce	1999	Mudurnu	7.14	42	C	0.09	11.07	9.37
13	Duzce	1999	Lamont 362	7.14	44	C	0.03	7.11	6.96
14	Duzce	1999	Lamont 1060	7.14	44	B	0.04	9.23	7.99
15	Duzce	1999	Sakarya	7.14	64	C	0.02	5.59	6.21
16	Duzce	1999	Yarimca	7.14	116	D	0.02	5.98	6.00
17	Duzce	1999	Aslan R.	7.14	149	D	0.01	3.47	4.27
18	Duzce	1999	Arcelik	7.14	149	C	0.01	2.41	3.37
19	Kocaeli	1999	Yarimca	7.51	19	D	0.31	60.51	54.70
20	Kocaeli	1999	Sakarya	7.51	33	C			
21	Kocaeli	1999	Iznik	7.51	40	D	0.11	23.12	12.59
22	Kocaeli	1999	Gebze	7.51	47	B	0.18	38.30	33.69
23	Kocaeli	1999	Arcelik	7.51	54	C	0.17	28.45	25.84
24	Kocaeli	1999	Goynuk	7.51	78	C	0.14	10.75	2.97
25	Kocaeli	1999	Istanbul	7.51	89	C	0.05	8.15	10.27
26	Kocaeli	1999	Mecidiyekoy	7.51	91	C	0.06	7.52	7.39
27	Kocaeli	1999	Maslak	7.51	91	C	0.04	6.56	7.49
28	Kocaeli	1999	Fatih	7.51	94	D	0.18	16.68	18.10
29	Kocaeli	1999	Zeytinburnu	7.51	95	D	0.11	16.81	15.30
30	Kocaeli	1999	Bursa Tofas	7.51	95	D	0.10	18.86	13.94
31	Kocaeli	1999	Bursa Sivil	7.51	96	C	0.06	9.02	4.40
32	Kocaeli	1999	Duzce	7.51	98	D	0.33	55.32	29.58
33	Kocaeli	1999	Atakoy	7.51	100	D	0.12	18.58	18.22
34	Kocaeli	1999	Hava Alani	7.51	102	C	0.09	20.27	22.88
35	Kocaeli	1999	Cekmece	7.51	108	D	0.16	14.64	12.41
36	Kocaeli	1999	Ambarli	7.51	112	E	0.22	37.46	27.41
37	Kocaeli	1999	Kutahya	7.51	148	D	0.05	13.89	14.13

Table A.3. List of ground motions in M1D1S5 ensemble (28 records)

#	Earthquake Name	Station Name	M	EpiD (km)	NEHRP	Vs30 (m/s)	PGA (g)	PGV (cm/sec)	PGD (cm)
1	Chi-Chi, Taiwan-03	CHY024	6.2	26	C	428	0.13	24.00	24.00
2	Chi-Chi, Taiwan-03	CHY080	6.2	29	C	553	0.33	47.27	47.27
3	Chi-Chi, Taiwan-03	TCU072	6.2	26	C	468	0.16	7.87	7.87
4	Chi-Chi, Taiwan-03	TCU074	6.2	20	C	549	0.04	3.43	3.43
5	Chi-Chi, Taiwan-03	TCU089	6.2	10	C	553	0.09	6.58	6.58
6	Chi-Chi, Taiwan-03	TCU116	6.2	28	C	493	0.13	24.16	24.16
7	Chi-Chi, Taiwan-03	TCU122	6.2	24	C	475	0.19	23.74	23.74
8	Chi-Chi, Taiwan-04	CHY024	6.2	28	C	428	0.07	11.13	11.13
9	Chi-Chi, Taiwan-04	CHY028	6.2	22	C	543	0.16	11.83	11.83
10	Chi-Chi, Taiwan-04	CHY029	6.2	30	C	545	0.06	12.69	12.69
11	Chi-Chi, Taiwan-04	CHY034	6.2	29	C	379	0.10	10.79	10.79
12	Chi-Chi, Taiwan-04	CHY035	6.2	26	C	474	0.12	12.33	12.33
13	Chi-Chi, Taiwan-04	CHY074	6.2	10	C	553	0.32	37.84	37.84
14	Chi-Chi, Taiwan-04	CHY080	6.2	15	C	553	0.12	15.86	15.86

Table A.4. List of ground motions in M1D2S5 ensemble (28 records)

#	Earthquake Name	Station Name	M	EpiD (km)	NEHRP	Vs30 (m/s)	PGA (g)	PGV (cm/sec)	PGD (cm)
1*[1]	Chi-Chi, Taiwan-03	CHY028	6.2	32	C	543	0.15	27.23	27.23
2	Chi-Chi, Taiwan-03	CHY029	6.2	39	C	545	0.07	14.43	14.43
3	Chi-Chi, Taiwan-03	CHY035	6.2	42	C	474	0.14	21.24	21.24
4	Chi-Chi, Taiwan-03	CHY041	6.2	49	C	492	0.11	7.42	7.42
5	Chi-Chi, Taiwan-03	CHY074	6.2	34	C	553	0.08	8.30	8.30
6	Chi-Chi, Taiwan-03	TCU048	6.2	49	C	551	0.03	2.45	2.45
7	Chi-Chi, Taiwan-03	TCU049	6.2	44	C	487	0.03	3.52	3.52
8	Chi-Chi, Taiwan-03	TCU052	6.2	45	C	579	0.03	3.51	3.51
9	Chi-Chi, Taiwan-03	TCU057	6.2	47	C	474	0.03	4.15	4.15
10	Chi-Chi, Taiwan-03	TCU063	6.2	41	C	476	0.04	6.73	6.73
11	Chi-Chi, Taiwan-03	TCU082	6.2	42	C	473	0.05	5.71	5.71
12	Chi-Chi, Taiwan-03	TCU100	6.2	48	C	474	0.02	5.16	5.16
13	Chi-Chi, Taiwan-03	TCU106	6.2	43	C	474	0.05	7.19	7.19
14	Chi-Chi, Taiwan-03	TCU107	6.2	43	C	474	0.07	11.23	11.23
15*	Chi-Chi, Taiwan-03	TCU109	6.2	42	C	474	0.08	7.99	7.99

[1] Record numbers with "*" mark show only one of the two hozirontal componets are used.

Table A.5. List of ground motions in M1D3S5 ensemble (28 records)

#	Earthquake Name	Station Name	M	EpiD (km)	NEHRP	Vs30 (m/s)	PGA (g)	PGV (cm/sec)	PGD (cm)
1*	Chi-Chi, Taiwan-03	CHY042	6.2	57	C	553.4	0.04	7.44	7.44
2	Chi-Chi, Taiwan-03	CHY052	6.2	68	C	473.9	0.04	4.94	4.94
3*	Chi-Chi, Taiwan-03	CHY086	6.2	57	C	553.4	0.08	9.17	9.17
4	Chi-Chi, Taiwan-03	CHY087	6.2	58	C	505.2	0.04	5.11	5.11
5	Chi-Chi, Taiwan-03	CHY102	6.2	67	C	553.4	0.02	3.74	3.74
6*	Chi-Chi, Taiwan-03	HWA024	6.2	68	C	553.4	0.01	0.48	0.48
7*	Chi-Chi, Taiwan-03	HWA031	6.2	66	C	473.9	0.01	0.48	0.48
8	Chi-Chi, Taiwan-03	HWA032	6.2	58	C	473.9	0.01	0.52	0.52
9	Chi-Chi, Taiwan-03	HWA035	6.2	60	C	473.9	0.01	0.40	0.40
10	Chi-Chi, Taiwan-03	HWA058	6.2	67	C	553.4	0.01	0.42	0.42
11	Chi-Chi, Taiwan-03	HWA059	6.2	67	C	473.9	0.01	0.52	0.52
12	Chi-Chi, Taiwan-03	KAU054	6.2	61	C	473.9	0.03	2.10	2.10
13	Chi-Chi, Taiwan-03	TCU068	6.2	53	C	487.34	0.02	3.43	3.43
14	Chi-Chi, Taiwan-03	TCU087	6.2	60	C	473.9	0.02	1.98	1.98
15	Chi-Chi, Taiwan-03	TCU103	6.2	57	C	494.1	0.02	2.11	2.11
16*	Chi-Chi, Taiwan-03	TCU104	6.2	55	C	473.9	0.02	2.50	2.50
17*	Chi-Chi, Taiwan-03	TCU136	6.2	54	C	473.9	0.02	2.63	2.63

Table A.6. List of ground motions in M1D4S5 ensemble (28 records)

#	Earthquake Name	Station Name	M	EpiD (km)	NEHRP	Vs30 (m/s)	PGA (g)	PGV (cm/sec)	PGD (cm)
1*	Chi-Chi, Taiwan-04	HWA029	6.2	85	C	614	0.01	0.61	0.61
2*	Chi-Chi, Taiwan-04	HWA058	6.2	79	C	553	0.01	0.62	0.62
3	Chi-Chi, Taiwan-04	HWA059	6.2	76	C	474	0.02	1.07	1.07
4	Chi-Chi, Taiwan-04	KAU018	6.2	86	C	474	0.01	1.12	1.12
5	Chi-Chi, Taiwan-04	KAU069	6.2	81	C	474	0.02	0.87	0.87
6	Chi-Chi, Taiwan-04	TCU068	6.2	76	C	487	0.01	2.86	2.86
7	Chi-Chi, Taiwan-04	TCU087	6.2	83	C	474	0.01	2.51	2.51
8	Chi-Chi, Taiwan-04	TCU103	6.2	80	C	494	0.01	2.22	2.22
9	Chi-Chi, Taiwan-04	TCU104	6.2	75	C	474	0.01	1.60	1.60
10	Chi-Chi, Taiwan-04	TCU105	6.2	76	C	576	0.01	2.39	2.39
11	Chi-Chi, Taiwan-04	TCU136	6.2	75	C	474	0.01	1.39	1.39
12	Chi-Chi, Taiwan-04	TTN002	6.2	85	C	474	0.01	1.14	1.14
13	Chi-Chi, Taiwan-04	TTN024	6.2	76	C	553	0.02	1.15	1.15
14	Chi-Chi, Taiwan-04	TTN026	6.2	86	C	474	0.01	1.02	1.02
15*	Chi-Chi, Taiwan-04	TTN044	6.2	75	C	474	0.04	2.57	2.57
16*	Chi-Chi, Taiwan-04	TTN046	6.2	82	C	474	0.03	1.85	1.85

Table A.7. List of ground motions in M1D5S5 ensemble (28 records)

#	Earthquake Name	Station Name	M	EpiD (km)	NEHRP	Vs30 (m/s)	PGA (g)	PGV (cm/sec)	PGD (cm)
1*	Chi-Chi, Taiwan-03	CHY022	6.2	94	C	474	0.02	1.96	1.96
2	Chi-Chi, Taiwan-03	HWA022	6.2	103	C	474	0.01	0.57	0.57
3	Chi-Chi, Taiwan-03	KAU018	6.2	109	C	474	0.01	2.29	2.29
4	Chi-Chi, Taiwan-03	KAU069	6.2	105	C	474	0.01	0.80	0.80
5	Chi-Chi, Taiwan-03	TCU015	6.2	106	C	426	0.01	1.62	1.62
6	Chi-Chi, Taiwan-03	TCU017	6.2	109	C	559	0.01	0.49	0.49
7*	Chi-Chi, Taiwan-03	TCU026	6.2	110	C	474	0.01	1.17	1.17
8	Chi-Chi, Taiwan-03	TCU033	6.2	97	C	423	0.03	1.90	1.90
9	Chi-Chi, Taiwan-03	TCU047	6.2	90	C	520	0.02	1.23	1.23
10*	Chi-Chi, Taiwan-03	TCU094	6.2	109	C	590	0.01	0.95	0.95
11	Chi-Chi, Taiwan-03	TCU095	6.2	100	C	447	0.01	1.25	1.25
12	Chi-Chi, Taiwan-03	TTN024	6.2	97	C	553	0.01	0.40	0.40
13	Chi-Chi, Taiwan-03	TTN025	6.2	103	C	705	0.01	0.43	0.43
14	Chi-Chi, Taiwan-03	TTN026	6.2	108	C	474	0.01	0.55	0.55
15	Chi-Chi, Taiwan-03	TTN044	6.2	95	C	474	0.01	0.99	0.99
16*	Chi-Chi, Taiwan-03	TTN046	6.2	102	C	474	0.01	0.66	0.66

Table A.8. List of ground motions in M1D6S5 ensemble (28 records)

#	Earthquake Name	Station Name	M	EpiD (km)	NEHRP	Vs30 (m/s)	PGA (g)	PGV (cm/sec)	PGD (cm)
1	Chi-Chi, Taiwan-03	CHY075	6.2	135	C	553	0.01	0.48	0.48
2	Chi-Chi, Taiwan-03	ILA007	6.2	134	C	474	0.01	0.54	0.54
3	Chi-Chi, Taiwan-03	KAU012	6.2	115	C	474	0.02	4.30	4.30
4	Chi-Chi, Taiwan-03	KAU077	6.2	119	C	553	0.01	0.83	0.83
5	Chi-Chi, Taiwan-03	KAU078	6.2	124	C	532	0.01	0.45	0.45
6	Chi-Chi, Taiwan-03	TCU006	6.2	126	C	474	0.00	0.30	0.30
7	Chi-Chi, Taiwan-03	TCU147	6.2	124	C	538	0.01	1.51	1.51
8	Chi-Chi, Taiwan-03	TTN018	6.2	112	C	474	0.00	0.41	0.41
9	Chi-Chi, Taiwan-03	TTN028	6.2	117	C	474	0.00	0.40	0.40
10	Chi-Chi, Taiwan-03	TTN036	6.2	118	C	474	0.00	0.82	0.82
11	Chi-Chi, Taiwan-03	TTN050	6.2	128	C	474	0.01	0.72	0.72
12	Chi-Chi, Taiwan-04	CHY075	6.2	129	C	553	0.01	1.95	1.95
13*	Chi-Chi, Taiwan-04	TCU017	6.2	133	C	559	0.01	2.02	2.02
14	Chi-Chi, Taiwan-04	TCU026	6.2	133	C	474	0.01	1.32	1.32
15*	Chi-Chi, Taiwan-04	TCU033	6.2	121	C	423	0.02	2.48	2.48

Table A.9. List of ground motions in M2D1S5 ensemble (18 records)

#	Earthquake Name	Station Name	M	EpiD (km)	NEHRP	Vs30 (m/s)	PGA (g)	PGV (cm/sec)	PGD (cm)
1	Chi-Chi, Taiwan	CHY024	7.62	24	C	428	0.23	50.15	50.15
2	Chi-Chi, Taiwan	TCU067	7.62	29	C	434	0.41	72.37	72.37
3	Chi-Chi, Taiwan	TCU072	7.62	21	C	468	0.40	60.08	60.08
4	Chi-Chi, Taiwan	TCU074	7.62	19	C	549	0.45	53.97	53.97
5	Chi-Chi, Taiwan	TCU075	7.62	21	C	573	0.30	56.69	56.69
6	Chi-Chi, Taiwan	TCU076	7.62	16	C	615	0.35	63.42	63.42
7	Chi-Chi, Taiwan	TCU116	7.62	24	C	493	0.17	47.18	47.18
8	Chi-Chi, Taiwan	TCU120	7.62	26	C	459	0.24	45.38	45.38
9	Chi-Chi, Taiwan	TCU122	7.62	22	C	475	0.24	38.82	38.82

Table A.10. List of ground motions in M2D2S5 ensemble (28 records)

#	Earthquake Name	Station Name	M	EpiD (km)	NEHRP	Vs30 (m/s)	PGA (g)	PGV (cm/sec)	PGD (cm)
1	Chi-Chi, Taiwan	CHY006	7.62	40	C	438	0.36	52.07	52.07
2	Chi-Chi, Taiwan	CHY029	7.62	40	C	545	0.26	33.11	33.11
3	Chi-Chi, Taiwan	CHY035	7.62	44	C	474	0.26	41.92	41.92
4	Chi-Chi, Taiwan	TCU048	7.62	43	C	551	0.14	39.94	39.94
5	Chi-Chi, Taiwan	TCU049	7.62	39	C	487	0.27	54.18	54.18
6	Chi-Chi, Taiwan	TCU052	7.62	40	C	579	0.35	131.95	131.95
7	Chi-Chi, Taiwan	TCU053	7.62	41	C	455	0.18	42.42	42.42
8	Chi-Chi, Taiwan	TCU057	7.62	42	C	474	0.12	38.05	38.05
9	Chi-Chi, Taiwan	TCU068	7.62	48	C	487	0.54	169.96	169.96
10	Chi-Chi, Taiwan	TCU070	7.62	48	C	401	0.21	56.45	56.45
11	Chi-Chi, Taiwan	TCU100	7.62	43	C	474	0.12	34.94	34.94
12	Chi-Chi, Taiwan	TCU102	7.62	46	C	714	0.24	93.82	93.82
13	Chi-Chi, Taiwan	TCU104	7.62	49	C	474	0.11	44.50	44.50
14	Chi-Chi, Taiwan	TCU136	7.62	49	C	474	0.17	51.68	51.68

Table A.11. List of ground motions in M2D3S5 ensemble (28 records)

#	Earthquake Name	Station Name	M	EpiD (km)	NEHRP	Vs30 (m/s)	PGA (g)	PGV (cm/sec)	PGD (cm)
1	Chi-Chi, Taiwan	CHY010	7.62	51	C	474	0.21	20.18	20.18
2	Chi-Chi, Taiwan	CHY042	7.62	60	C	553	0.08	13.71	13.71
3	Chi-Chi, Taiwan	CHY046	7.62	55	C	442	0.16	20.27	20.27
4	Chi-Chi, Taiwan	CHY086	7.62	60	C	553	0.15	15.96	15.96
5	Chi-Chi, Taiwan	CHY087	7.62	60	C	505	0.13	11.31	11.31
6	Chi-Chi, Taiwan	ESL	7.62	63	C	553	0.07	8.19	8.19
7	Chi-Chi, Taiwan	HWA020	7.62	63	C	375	0.07	7.86	7.86
8	Chi-Chi, Taiwan	HWA032	7.62	62	C	474	0.14	8.54	8.54
9	Chi-Chi, Taiwan	HWA034	7.62	63	C	379	0.14	10.82	10.82
10	Chi-Chi, Taiwan	NSY	7.62	63	C	600	0.13	47.16	47.16
11	Chi-Chi, Taiwan	TCU087	7.62	56	C	474	0.12	41.30	41.30
12	Chi-Chi, Taiwan	TCU088	7.62	58	C	553	0.52	19.06	19.06
13	Chi-Chi, Taiwan	TCU103	7.62	52	C	494	0.16	44.92	44.92
14	Chi-Chi, Taiwan	TCU128	7.62	63	C	600	0.15	70.96	70.96

Table A.12. List of ground motions in M2D4S5 ensemble (28 records)

#	Earthquake Name	Station Name	M	EpiD (km)	NEHRP	Vs30 (m/s)	PGA (g)	PGV (cm/sec)	PGD (cm)
1	Chi-Chi, Taiwan	CHY019	7.62	82	C	474	0.06	5.89	5.89
2	Chi-Chi, Taiwan	CHY050	7.62	76	C	474	0.08	9.22	9.22
3	Chi-Chi, Taiwan	CHY079	7.62	80	C	474	0.04	6.05	6.05
4	Chi-Chi, Taiwan	HWA023	7.62	83	C	553	0.04	8.93	8.93
5*	Chi-Chi, Taiwan	HWA029	7.62	77	C	614	0.08	14.48	14.48
6*	Chi-Chi, Taiwan	HWA039	7.62	75	C	375	0.08	12.06	12.06
7	Chi-Chi, Taiwan	HWA044	7.62	75	C	474	0.06	9.13	9.13
8	Chi-Chi, Taiwan	HWA056	7.62	79	C	511	0.10	9.12	9.12
9	Chi-Chi, Taiwan	HWA060	7.62	78	C	474	0.04	8.06	8.06
10	Chi-Chi, Taiwan	KAU001	7.62	79	C	474	0.03	5.58	5.58
11	Chi-Chi, Taiwan	KAU050	7.62	77	C	553	0.04	5.80	5.80
12	Chi-Chi, Taiwan	STY	7.62	77	C	553	0.04	4.40	4.40
13	Chi-Chi, Taiwan	TCU029	7.62	79	C	474	0.18	48.93	48.93
14	Chi-Chi, Taiwan	TCU031	7.62	80	C	489	0.13	52.88	52.88
15	Chi-Chi, Taiwan	TTN051	7.62	76	C	553	0.03	5.20	5.20

Table A.13. List of ground motions in M2D5S5 ensemble (28 records)

#	Earthquake Name	Station Name	M	EpiD (km)	NEHRP	Vs30 (m/s)	PGA (g)	PGV (cm/sec)	PGD (cm)
1	Chi-Chi, Taiwan	CHY022	7.62	97	C	474	0.06	5.53	5.53
2	Chi-Chi, Taiwan	CHY061	7.62	92	C	474	0.03	4.79	4.79
3	Chi-Chi, Taiwan	HWA022	7.62	104	C	474	0.11	11.38	11.38
4	Chi-Chi, Taiwan	KAU069	7.62	108	C	474	0.04	2.95	2.95
5	Chi-Chi, Taiwan	NSK	7.62	107	C	553	0.07	5.59	5.59
6	Chi-Chi, Taiwan	TCU017	7.62	105	C	559	0.10	34.58	34.58
7	Chi-Chi, Taiwan	TCU025	7.62	102	C	553	0.07	12.74	12.74
8	Chi-Chi, Taiwan	TCU026	7.62	106	C	474	0.10	31.89	31.89
9	Chi-Chi, Taiwan	TCU096	7.62	106	C	474	0.08	29.37	29.37
10	Chi-Chi, Taiwan	TTN002	7.62	109	C	474	0.03	5.17	5.17
11	Chi-Chi, Taiwan	TTN023	7.62	95	C	528	0.06	11.39	11.39
12	Chi-Chi, Taiwan	TTN024	7.62	102	C	553	0.03	3.87	3.87
13	Chi-Chi, Taiwan	TTN044	7.62	100	C	474	0.05	10.36	10.36
14	Chi-Chi, Taiwan	TTN046	7.62	107	C	474	0.09	9.05	9.05

Table A.14. List of ground motions in M3D2S5 ensemble (28 records)

#	Earthquake Name	Station Name	M	EpiD (km)	NEHRP	Vs30 (m/s)	PGA (g)	PGV (cm/sec)	PGD (cm)
1*	Chi-Chi, Taiwan-02	HWA032	5.9	48	C	474	0.04	1.61	1.61
2	Chi-Chi, Taiwan-02	HWA058	5.9	48	C	553	0.04	2.07	2.07
3	Chi-Chi, Taiwan-02	TCU052	5.9	40	C	579	0.07	5.80	5.80
4*	Chi-Chi, Taiwan-02	TCU053	5.9	45	C	455	0.03	2.97	2.97
5	Chi-Chi, Taiwan-02	TCU054	5.9	42	C	461	0.02	2.73	2.73
6	Chi-Chi, Taiwan-02	TCU063	5.9	44	C	476	0.04	4.69	4.69
7	Chi-Chi, Taiwan-02	TCU068	5.9	45	C	487	0.02	2.56	2.56
8	Chi-Chi, Taiwan-02	TCU082	5.9	41	C	473	0.03	2.63	2.63
9	Chi-Chi, Taiwan-02	TCU088	5.9	39	C	553	0.05	1.29	1.29
10	Chi-Chi, Taiwan-02	TCU100	5.9	49	C	474	0.02	2.22	2.22
11*	Chi-Chi, Taiwan-02	TCU106	5.9	49	C	474	0.05	3.36	3.36
12	Chi-Chi, Taiwan-02	TCU109	5.9	47	C	474	0.04	3.76	3.76
13	Chi-Chi, Taiwan-02	TCU116	5.9	45	C	493	0.03	3.14	3.14
14	Chi-Chi, Taiwan-02	TCU120	5.9	41	C	459	0.04	4.24	4.24
15	Chi-Chi, Taiwan-02	TCU122	5.9	43	C	475	0.07	3.17	3.17
16*	Chi-Chi, Taiwan-02	TCU138	5.9	42	C	653	0.04	3.44	3.44

Table A.15. List of ground motions in M3D5S5 ensemble (28 records)

#	Earthquake Name	Station Name	M	EpiD (km)	NEHRP	Vs30 (m/s)	PGA (g)	PGV (cm/sec)	PGD (cm)
1	Chi-Chi, Taiwan-02	CHY019	5.9	101	C	474	0.01	0.76	0.76
2*	Chi-Chi, Taiwan-02	CHY050	5.9	96	C	474	0.01	0.67	0.67
3*	Chi-Chi, Taiwan-02	CHY057	5.9	107	C	411	0.01	0.61	0.61
4	Chi-Chi, Taiwan-02	CHY061	5.9	109	C	474	0.01	0.50	0.50
5	Chi-Chi, Taiwan-02	CHY062	5.9	108	C	603	0.01	0.66	0.66
6	Chi-Chi, Taiwan-02	CHY079	5.9	97	C	474	0.01	0.46	0.46
7	Chi-Chi, Taiwan-02	ILA010	5.9	109	C	474	0.02	1.68	1.68
8	Chi-Chi, Taiwan-02	ILA021	5.9	107	C	474	0.01	1.54	1.54
9	Chi-Chi, Taiwan-02	ILA024	5.9	98	C	553	0.01	0.69	0.69
10	Chi-Chi, Taiwan-02	KAU001	5.9	95	C	474	0.00	0.34	0.34
11	Chi-Chi, Taiwan-02	TCU006	5.9	109	C	474	0.02	2.47	2.47
12	Chi-Chi, Taiwan-02	TCU026	5.9	93	C	474	0.02	2.58	2.58
13	Chi-Chi, Taiwan-02	TCU147	5.9	105	C	538	0.02	2.58	2.58
14	Chi-Chi, Taiwan-02	TTN023	5.9	100	C	528	0.01	1.60	1.60
15	Chi-Chi, Taiwan-02	TTN024	5.9	108	C	553	0.01	0.36	0.36

Table A.16. List of ground motions in M2D2S1 ensemble (24 records)

#	Earthquake Name	Station Name	M	EpiD (km)	NEHRP	Vs30 (m/s)	PGA (g)	PGV (cm/sec)	PGD (cm)
1	Chi-Chi, Taiwan	CHY002	7.62	44	D	235	0.13	49.43	49.43
2	Chi-Chi, Taiwan	CHY026	7.62	42	D	226	0.07	38.87	38.87
3	Chi-Chi, Taiwan	CHY036	7.62	44	D	233	0.26	37.24	37.24
4	Chi-Chi, Taiwan	CHY104	7.62	41	D	223	0.18	54.87	54.87
5	Chi-Chi, Taiwan	TCU111	7.62	45	D	238	0.11	43.58	43.58
6	Chi-Chi, Taiwan	TCU112	7.62	46	D	215	0.08	37.67	37.67
7	Chi-Chi, Taiwan	TCU113	7.62	44	D	230	0.07	25.86	25.86
8	Chi-Chi, Taiwan	TCU115	7.62	38	D	215	0.11	47.55	47.55
9	Chi-Chi, Taiwan	TCU117	7.62	48	D	199	0.13	63.30	63.30
10	Chi-Chi, Taiwan	TCU118	7.62	44	D	215	0.10	30.36	30.36
11	Chi-Chi, Taiwan	TCU140	7.62	48	D	215	0.06	22.20	22.20
12	Chi-Chi, Taiwan	TCU141	7.62	36	D	215	0.09	37.19	37.19

Table A.17. List of ground motions in M2D2S2 ensemble (12 records)

#	Earthquake Name	Station Name	M	EpiD (km)	NEHRP	Vs30 (m/s)	PGA (g)	PGV (cm/sec)	PGD (cm)
1	Chi-Chi, Taiwan	TCU050	7.62	41	D	273	0.14	39.56	39.56
2	Chi-Chi, Taiwan	TCU051	7.62	39	D	273	0.21	41.20	41.20
3	Chi-Chi, Taiwan	TCU056	7.62	40	D	273	0.14	41.34	41.34
4	Chi-Chi, Taiwan	TCU060	7.62	45	D	273	0.15	36.41	36.41
5	Chi-Chi, Taiwan	TCU061	7.62	42	D	273	0.14	34.73	34.73
6	Chi-Chi, Taiwan	TCU101	7.62	45	D	273	0.23	61.54	61.54

Table A.18. List of ground motions in M2D2S3 ensemble (24 records)

#	Earthquake Name	Station Name	M	EpiD (km)	NEHRP	Vs30 (m/s)	PGA (g)	PGV (cm/sec)	PGD (cm)
1	Chi-Chi, Taiwan	CHY006	7.62	40	C	438	0.36	52.07	52.07
2	Chi-Chi, Taiwan	CHY034	7.62	46	C	379	0.30	43.77	43.77
3	Chi-Chi, Taiwan	CHY035	7.62	44	C	474	0.26	41.92	41.92
4	Chi-Chi, Taiwan	TCU053	7.62	41	C	455	0.18	42.42	42.42
5	Chi-Chi, Taiwan	TCU054	7.62	38	C	461	0.18	48.89	48.89
6	Chi-Chi, Taiwan	TCU057	7.62	42	C	474	0.12	38.05	38.05
7	Chi-Chi, Taiwan	TCU070	7.62	48	C	401	0.21	56.45	56.45
8	Chi-Chi, Taiwan	TCU100	7.62	43	C	474	0.12	34.94	34.94
9	Chi-Chi, Taiwan	TCU104	7.62	49	C	474	0.11	44.50	44.50
10	Chi-Chi, Taiwan	TCU106	7.62	38	C	474	0.16	44.33	44.33
11	Chi-Chi, Taiwan	TCU107	7.62	38	C	474	0.14	42.36	42.36
12	Chi-Chi, Taiwan	TCU136	7.62	49	C	474	0.17	51.68	51.68

Table A.19. List of ground motions in M2D2S4 ensemble (12 records)

#	Earthquake Name	Station Name	M	EpiD (km)	NEHRP	Vs30 (m/s)	PGA (g)	PGV (cm/sec)	PGD (cm)
1	Chi-Chi, Taiwan	CHY029	7.62	40	C	545	0.26	33.11	33.11
2	Chi-Chi, Taiwan	TCU048	7.62	43	C	551	0.14	39.94	39.94
3	Chi-Chi, Taiwan	TCU049	7.62	39	C	487	0.27	54.18	54.18
4	Chi-Chi, Taiwan	TCU052	7.62	40	C	579	0.35	131.95	131.95
5	Chi-Chi, Taiwan	TCU068	7.62	48	C	487	0.54	169.96	169.96
6	Chi-Chi, Taiwan	TCU102	7.62	46	C	714	0.24	93.82	93.82

Table A.20. List of ground motions in M4D2SD ensemble (22 records)

#	Earthquake Name	Station Name	M	EpiD (km)	NEHRP	Vs30 (m/s)	PGA (g)	PGV (cm/sec)	PGD (cm)
1	San Fernando	LA - Hollywood Stor FF	6.61	39	D	316	0.21	18.15	18.15
2	Spitak, Armenia	Gukasian	6.77	36	D	275	0.21	21.68	21.68
3	Northridge-01	Inglewood - Union Oil	6.69	42	D	316	0.10	8.41	8.41
4	Northridge-01	LA - 116th St School	6.69	41	D	301	0.17	12.48	12.48
5	Northridge-01	LA - E Vernon Ave	6.69	37	D	309	0.15	10.03	10.03
6	Northridge-01	LA - Obregon Park	6.69	39	D	349	0.47	21.79	21.79
7	Kobe, Japan	Amagasaki	6.9	39	D	256	0.00	0.00	0.00
8	Kobe, Japan	Fukushima	6.9	44	D	256	0.00	0.00	0.00
9	Kobe, Japan	Sakai	6.9	42	D	256	0.00	0.00	0.00
10	Kobe, Japan	Tadoka	6.9	39	D	312	0.00	0.00	0.00
11	Kobe, Japan	Takarazuka	6.9	39	D	312	0.71	75.88	75.88

Table A.21. List of ground motions in M4D2SC ensemble (22 records)

#	Earthquake Name	Station Name	M	EpiD (km)	NEHRP	Vs30 (m/s)	PGA (g)	PGV (cm/sec)	PGD (cm)
1	San Fernando	Pasadena - CIT Athenaeum	6.61	43	C	415	0.10	10.94	10.94
2	Northridge-01	Alhambra - Fremont School	6.69	40	C	550	0.09	8.64	8.64
3	Northridge-01	Castaic - Old Ridge Route	6.69	40	C	450	0.49	46.51	46.51
4	Northridge-01	LA - City Terrace	6.69	39	C	365	0.27	14.07	14.07
5	Northridge-01	LA - N Figueroa St	6.69	35	C	405	0.15	9.20	9.20
6	Northridge-01	LA - Univ. Hospital	6.69	36	C	376	0.35	19.39	19.39
7	Northridge-01	Lake Hughes #12A	6.69	40	C	602	0.22	9.97	9.97
8	Northridge-01	Lawndale - Osage Ave	6.69	39	C	361	0.11	8.22	8.22
9	Northridge-01	Manhattan Beach - Manhattan	6.69	38	C	405	0.17	16.88	16.88
10	Northridge-01	San Gabriel - E Grand Ave	6.69	44	C	401	0.21	10.23	10.23
11	Northridge-01	San Marino - SW Academy	6.69	40	C	379	0.13	7.52	7.52

Table A.22. List of ground motions in M4D2SB ensemble (12 records)

#	Earthquake Name	Station Name	M	EpiD (km)	NEHRP	Vs30 (m/s)	PGA (g)	PGV (cm/sec)	PGD (cm)
1	San Fernando	Pasadena - Old Seismo Lab	6.61	39	B	969	0.14	8.88	8.88
2	Irpinia, Italy-01	Auletta	6.9	33	B	1000	0.06	6.11	6.11
3	Irpinia, Italy-01	Sturno	6.9	30	B	1000	0.29	46.86	46.86
4	Northridge-01	Lake Hughes #4 - Camp Mend	6.69	49	B	822	0.08	5.49	5.49
5	Northridge-01	Mt Wilson - CIT Seis Sta	6.69	45	B	822	0.17	6.41	6.41
6	Northridge-01	Vasquez Rocks Park	6.69	38	B	996	0.14	14.27	14.27

REFERENCES

Akgül,B. , 2007, "Comparison of Linear And Nonlinear Methods For Seismic Evaluation Of Existing Reinforced Concrete Buildings In The Turkish Earthquake Code 2007", Ms. Dissertation, Boğaziçi University

Bozorgnia Y. and Bertero V.V. (editors), 2004, Earthquake Engineering Seismology to Performance-Based Engineering, pp. 5.6-23, CRC press, Boca Raton London New York Washington

Chopra A.K. and Chintanapakdee C., 2004, "Inelastic Deformation Ratios for Design and Evaluation of Structures: Single-Degree-of-Freedom Bilinear Systems" Journal of Structural Engineering, Vol. 130, No. 9, ASCE

Federal Emergency Management Agency (FEMA). NEHRP guidelines for the seismic rehabilitation of buildings. Report no.FEMA-273 (Guidelines) and report no. FEMA-274 (Commentary), Washington, DC, 1997.

Federal Emergency Management Agency (FEMA). Prestandard and commentary for seismic rehabilitation of buildings. Report no. FEMA-356, Washington, DC, 2000.

Ruiz-Garcia J, Miranda E. Inelastic displacement ratios for evaluation of existing structures. Earthquake Eng Struct Dyn 2003;32(8): 1237–58.

Hamburger R.O., 1997, "A Framework for Performance-Based Earthquake Resistive Design", EERC-CUREe Symposium in Honor of Vitelmo V. Bertero, Berkeley, California.

Hom D. B. and Poland C. D., 2006, "ASCE 31-03: Seismic Evaluation of Existing Buildings Structures" 2004 Part of Building on the Past: Securing the Future Structures Congress 2004 George E. Blandford, Editors May 22–26, 2004, Nashville, Tennessee, USA.

Kliver, J., 2004, “Ductility Requirements for Reinforced Concrete Structures”, aspdin.wifa.uni-leipzig.de/institut/lacer/lacer09/l09_24.pdf

Krawinkler and Miranda(2004)Earthquake Engineering: From Engineering Seismology to Performance-Based Engineering, eds. Bozorgnia Y. and V.V. Bertero

Krawinkler, H., and Nassar, A. A., 1992, “Seismic design based on ductility and cumulative damage demands and capacities.”, Nonlinear Seismic Analysis and Design of Reinforced Concrete Buildings, Eds. P. Fajfar and H. Krawinkler. New York: Elsevier Applied Science.

Laue, J., Springman, S.M., & Buchheister, J. (2003b) “Site Response Analyses”, Part 2C-Case Studies, Microzonation of Pilot Areas, Adapazarı, Gölcük, İhsaniye and Değirmendere, Research Task Group Report, Chapter 6

Mehanny S.S.F., Ayoub A.S.., 2007, Variability in inelastic displacement demands: Uncertainty in system parameters versus randomness in ground records. Engineering Structures, doi:10.1016/j.engstruct.2007.06.009

Miranda, E., 1991, “Seismic upgrading and evaluation of existing buildings” PhD thesis, Dept of Civil Engineering, University of California, Berkley, California

Miranda E., 2000, “Inelastic displacement ratios for structures on firm sites.”, Journal of Structural Engineering, pp. 126:1150–1159.

Miranda E.and García J.R., 2002, “Evaluation of approximate methods to estimate maximum inelastic displacement demands”, Earthquake Engineering and Structural Dynamics Earthquake Engng Struct. Dyn.; pp.31:539–560

Newmark, N. M. and Hall, W.J., 1982, “Earthquake spectra and design”, Proceedings 7th World Conference on Earthquake Engineering, Turkish National Committee on Earthquake Engineering, Ankara, Türkiye

Otani S., 2004, “The Performance Requirements In Japanese Building Code”, International Workshop on performance-based seismic design, Concepts and implementation

Shimazaki K.and Sozen M.A., 1984, “Seismic drift of reinforced concrete structures” Res. Rep. Hazama-Gumi Ltd., Tokyo, Japan; and draft report.

Turkish Earthquake Code 1998, Specification for Structures to be Built in Disaster Areas, Ankara, 1998

Turkish Earthquake Code 2007, Specification for Buildings to be Built in Disaster Areas, Bayındırlık ve İskan Bakanlıgı, Ankara, 2007

Veletsos A.S., Newmark N.M., 1960, “Effect of inelastic behavior on the response of simple systems to earthquake motions.” Proceedings of the 2nd World Conference on Earthquake Engineering, Japan, vol. 2, pp. 895–912.

Whittaker A.S., Constantinou M., Tsopelas P., 1998, “Displacement estimates for performance-based seismic design.”, Journal of Structural Engineering (ASCE); 124(8):pp. 905–912.

Yerlici V., Luş H., “Yapı Dinamiğine Giriş”, Boğaziçi Yayın Evi, İstanbul, Türkiye, pp.143-176